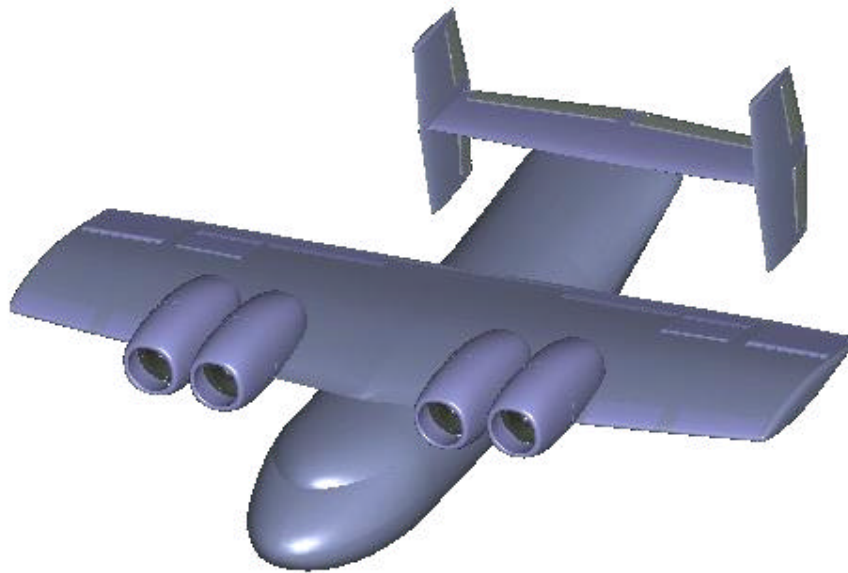




*A Graduate Team Aircraft Design*



999



*Stanford University*





## A 1999 AIAA GRADUATE TEAM AIRCRAFT PROPOSAL

### PROJECT LEADER:

**Patrick LeGresley**

AIAA Member Number 144155

MS Expected June 1999

plegresl@stanford.edu

**Jose Daniel Cornejo**

AIAA Member Number 143144

MS Expected March 2000

dcornejo@stanford.edu

**Teal Bathke**

AIAA Member Number 183891

MS Expected June 2000

teal@stanford.edu

**Jennifer Owens**

AIAA Member Number 113704

MS Expected December 1999

owensjm@stanford.edu

**Angel Carrion**

AIAA Member Number 183513

MS Expected March 2000

angelcar@stanford.edu

**Ryan Vartanian**

AIAA Member Number 154990

MS Expected June 1999

vartan@stanford.edu

### ADVISORS:

**Dr. Juan Alonso**

Assistant Professor

Stanford University Aeronautics & Astronautics

jjalonso@stanford.edu

**Dr. Ilan Kroo**

Professor

Stanford University Aeronautics & Astronautics

kroo@stanford.edu

*"When I was a student in college, just flying an airplane seemed a dream..."*  
~Charles Lindbergh

JUNE 1, 1999

## EXECUTIVE SUMMARY

Commuting from center-city to center-city is not viable with existing aircraft due to the lack of available runways in metropolitan areas for airplanes and higher expense of helicopter service. The Cardinal is a Super Short Takeoff and Landing (SSTOL) aircraft which attempts to fill this gap. The major goal of this airplane design is to fulfill the desire for center-city to center-city travel by utilizing river “barges” for short takeoffs and landings to avoid construction of new runways or heliports. In addition, the Cardinal will fulfill the needs of the U.S. Navy for a Carrier on-board delivery (COD) aircraft to replace the C-2 Greyhound. Design requirements for the Cardinal included:

- Takeoff ground roll of 300 ft
- Landing ground roll of 400 ft
- Cruise at 350 knots with a range of up to 1500 nm with reserves
- Payload
  - 24 passengers and baggage for commercial version
  - 10,000 lb payload for military version
  - Capable of carrying two GE F110 engines for the F-14D
- Spot factor requirement of 60 feet by 29 feet for military version

Many technologies for achieving the performance goals of the Cardinal were studied and two were singled out for use in preliminary designs. A preliminary design for a fixed-wing configuration with upper surface blowing (USB) and a tilt-wing configuration were completed. Upper surface blowing uses exhaust air from the engine blown over the top of the wing to achieve boundary layer control and reduce flow separation. This technology allows slower takeoff and landing speeds and hence shorter takeoff and landing ground rolls. The tilt-wing is similar to a tilt-rotor, but instead of turning only the engines, the entire wing is pivoted. Pivoting the thrust reduces the amount of lift the wing must produce and reduces the takeoff and landing speeds. Neither of these technologies has been implemented on production aircraft, but several prototype and research aircraft have been built and flight-tested for validation.

The design process for the Cardinal included initial weight and performance sizing, wing and high lift design, propulsion selection, structural layout and design, drag polar buildups, stability and performance analysis, and cost estimation. Due to the unique design and non-traditional technologies of the two designs analyzed, the Cardinal team wrote design and analysis tools for each subsystem to aid in the analysis process and allow for timely design iteration. These automated design tools allowed the team to vary different design

variables and mission requirements to design an airplane that met the mission requirements. The new design tools also allowed the team to investigate how varying the requirements changed the design point. To facilitate communication between system groups, a web page was created and maintained. The web site contained the most current results for each iteration of the design and provided access to copies of the design codes. The web site may be viewed at <http://ape.stanford.edu/cardinal/> and provides additional information about the Cardinal designs.

A collaborative optimization routine to couple the individual design analysis programs was written. A minimization of Life Cycle Cost (LCC) resulted in two potential designs that met all certification and mission requirements for the Cardinal. A comparison of the costs associated with the two designs was used to select the fixed-wing configuration (refer to Figure 1). The operating, acquisition, and LCC costs of the two resulting designs were reviewed and the fixed-wing design was selected due to its lower costs in all cost categories. Table 1 summarizes this comparison.

**Table 1: Summary of Cost Comparison Between Initial Designs**

COST METRIC	FIXED-WING	TILT-WING
Operating Cost	\$7.03/nm	\$7.82/nm
Acquisition Cost	\$17.1M	\$18.0 M
Life Cycle Cost	\$154.7B	\$172.1B

To understand how the design requirements affected the costs, several design studies were conducted. The cost associated with vertical versus short takeoff was addressed by altering the design requirements for the tilt-wing to require vertical takeoff. Acquisition cost was increased 16% to \$20.8 million and operating cost also increased 16% to \$9.06/nm. A similar study was conducted on the cost impact for a fixed-wing design by altering the ground roll constraint. This analysis showed that increasing the takeoff ground roll requirement from 300 ft to 400 ft reduced the life cycle cost by 16%. A further increase to 500 ft was estimated to reduce the life cycle cost 19% from a design with a 300 ft ground roll and 4% from the design at 400 ft. This indicates that the Cardinal requirement lies on the steep part of a curve where costs increase significantly for small changes in the requirements. Therefore, relaxing this requirement should be more thoroughly investigated.

WEIGHTS (lbs)

Maximum Takeoff Weight	46,761
Maximum Landing Weight	39,741
Design Empty Weight	22,027
Operating Empty Weight	22,678
Payload Weight	10,000

CENTER OF GRAVITY (from nose)

Empty Weight	32.61 ft
Max Takeoff Weight	31.03 ft
Most forward cg	30.13 ft
Most Aft cg	31.33

POWERPLANT

Engine Manufacturer	Avco Lycoming
Model	ALF 502
Type	Turbofan
Takeoff Uninstalled Thrust	22,875 lbs

LANDING GEAR

Tire Size (Main)	25.5 x 6.85
Tire Size (Nose)	17.8 x 5.6
Max Diameter (Main)	4.3 in
Max Diameter (Nose)	2.5 in
Total Strut Stroke (Main)	16 in
Total Strut Stroke (Nose)	6 in

WING PARAMETERS

Area	1150 sq ft
Span	64 ft
MAC	18.04 ft
Aspect Ratio	3.56 (~)
Taper Ratio	0.8 (~)
Quarter Chord Sweep	5 deg
Airfoil Section	NACA 65-214
Thickness to Chord	14%
Incidence Angle	1 deg
Dihedral Angle	0 deg

TAIL PARAMETERS

Horizontal:

Total Area	190 sq ft
Span	29 ft
Taper Ratio	0.8 (~)
Quarter Chord Sweep	0 deg
Airfoil Section	NACA 0012
Dihedral Angle	0 deg

Vertical:

Total Area	208 sq ft
Span	14 ft
Taper Ratio	0.8 (~)
Quarter Chord Sweep	0 deg
Airfoil Section	NACA 0010

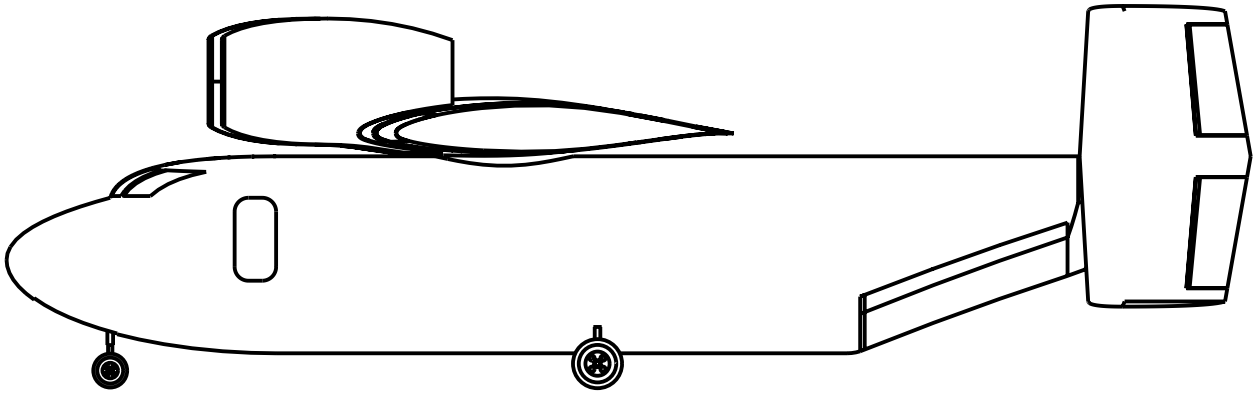
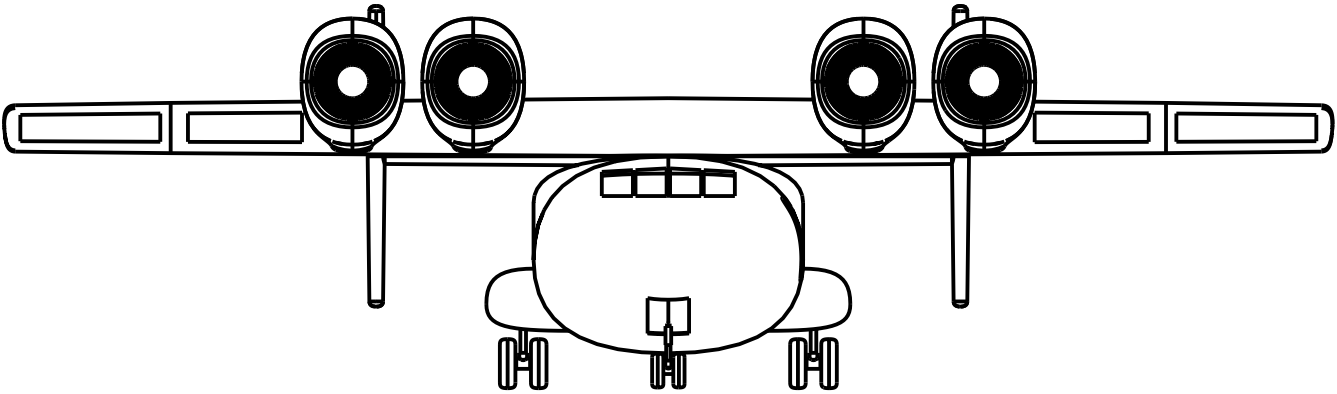
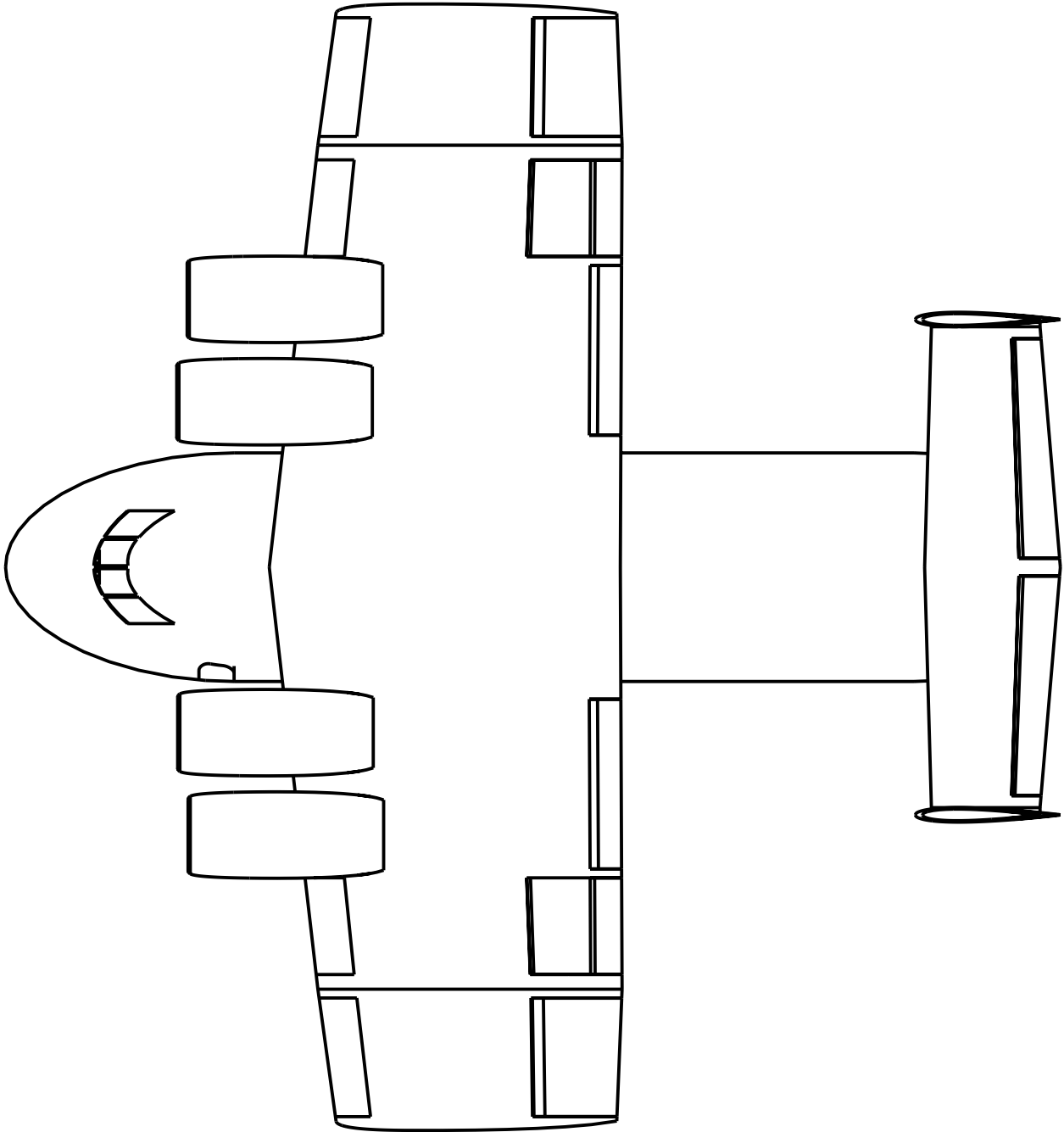


## TABLE OF CONTENTS

<b>EXECUTIVE SUMMARY .....</b>	<b>ii</b>
<b>TABLE OF CONTENTS .....</b>	<b>v</b>
<b>LIST OF FIGURES.....</b>	<b>viii</b>
<b>LIST OF TABLES.....</b>	<b>ix</b>
<b>NOMENCLATURE.....</b>	<b>x</b>
SYMBOLS .....	x
ACRONYMS.....	xiii
<b>ACKNOWLEDGEMENTS .....</b>	<b>xiv</b>
<b>1. INTRODUCTION .....</b>	<b>1</b>
1.1 MISSION OBJECTIVES <sup>2</sup> .....	1
1.2 MISSION REQUIREMENTS.....	1
<b>2. DESIGN PHILOSOPHY .....</b>	<b>3</b>
2.1 REVIEW OF EXISTING AIRCRAFT.....	3
2.2 DESIGN PROCEDURE.....	3
2.2.1 Technology Maturity Assessment <sup>33</sup> .....	5
2.3 USER PREFERENCES AND SAFETY CONSIDERATIONS FOR V/SSTOL .....	6
2.3.1 Pilot Preferences .....	7
2.3.2 Passenger Preferences .....	8
2.3.3 Aircraft Noise .....	8
2.3.3.1 Sources Of Noise.....	9
2.3.3.2 Estimates Of Noise.....	9
2.3.3.3 Fixed Wing Engine Noise.....	9
2.3.3.4 Turboprop Noise.....	9
2.3.4 Impact On Design .....	10
<b>3. INITIAL WEIGHT AND PERFORMANCE SIZING.....</b>	<b>11</b>
3.1 MISSION WEIGHT SIZING.....	11
3.2 PERFORMANCE CONSTRAINT SIZING .....	11
<b>4. CONFIGURATION SELECTION AND COMPONENT DESIGN .....</b>	<b>14</b>
4.1 FUSELAGE.....	14
4.1.1 Cockpit Layout .....	15
4.1.2 Cargo Hold.....	15
4.1.3 Passenger Cabin.....	15
4.2 WING.....	17
4.2.1 Clean Wing Design.....	17
4.2.2 High Lift and Powered Lift Design.....	19
4.2.2.1 Technology Validation and Risk Assessment .....	23
4.3 EMPENNAGE .....	23
4.4 CONTROL SURFACES .....	24
4.5 LANDING GEAR .....	24
4.5.1 Location Criteria .....	25
4.5.2 Tire Selection.....	26

4.5.3	Shock Design .....	27
4.5.4	Retraction Mechanism .....	27
<b>5.</b>	<b>PROPULSION SELECTION &amp; INSTALLATION .....</b>	<b>28</b>
5.1	ENGINE SELECTION .....	28
5.1.1	Tilt-wing Turboprop Configuration .....	28
5.1.2	Fixed-wing Turbofan Configuration.....	28
5.2	ENGINE LOCATIONS.....	29
5.3	ENGINE PERFORMANCE CHARACTERISTICS .....	30
5.3.1	Performance Data .....	30
5.3.1.1	Turboprop Performance .....	30
5.3.2	Engine Scaling .....	31
5.4	INSTALLATION LOSSES .....	31
<b>6.</b>	<b>STRUCTURAL LAYOUT AND SYSTEMS DESIGN .....</b>	<b>33</b>
6.1	MATERIALS SELECTION, STRUCTURAL DESIGN, AND LAYOUT .....	33
6.2	SYSTEMS DESIGN .....	35
<b>7.</b>	<b>WEIGHTS AND BALANCE.....</b>	<b>36</b>
7.1	V-N DIAGRAM .....	36
7.2	COMPONENT & SYSTEM WEIGHT CALCULATIONS .....	37
7.2.1	Structure and Propulsion weights <sup>42, 50</sup> .....	37
7.2.2	Fixed Equipment.....	38
7.3	CENTER OF GRAVITY EXCURSION .....	39
7.4	INERTIAS.....	40
<b>8.</b>	<b>DRAG ESTIMATION.....</b>	<b>41</b>
8.1	PARASITE DRAG .....	41
8.1.1	Fuselage, Lifting Surface, Nacelle, and Pylon Drag.....	41
8.1.1.1	Skin Friction Coefficient.....	41
8.1.1.2	Form Factor.....	41
8.1.1.3	Wetted Area.....	42
8.1.2	High Lift System Drag.....	42
8.1.3	Landing Gear Drag .....	42
8.1.4	Parasite Drag Breakdown .....	43
8.2	INDUCED DRAG .....	43
8.3	COMPRESSIBILITY DRAG .....	43
8.4	DRAG POLAR .....	44
8.5	ACCURACY/FEASIBILITY OF ESTIMATE .....	46
<b>9.</b>	<b>STABILITY AND CONTROL.....</b>	<b>47</b>
9.1	STABILITY AND CONTROL DERIVATIVES .....	47
9.2	FREQUENCIES AND DAMPING RATIOS.....	50
9.3	MINIMUM CONTROL SPEED .....	50
<b>10.</b>	<b>PERFORMANCE ANALYSIS.....</b>	<b>51</b>
10.1	TAKEOFF & LANDING DISTANCES .....	51
10.2	CLIMB PERFORMANCE.....	52
10.3	RANGE.....	54
<b>11.</b>	<b>COST ESTIMATION.....</b>	<b>56</b>
11.1	RESEARCH, DEVELOPMENT, TEST, AND ENGINEERING PHASES (RDTE) .....	57
11.2	ACQUISITION COST.....	58

11.3 OPERATING COST <sup>53</sup> .....	58
11.3.1 Direct Operating Cost (DOC) .....	59
11.3.2 Indirect Operating Cost (IOC) .....	59
11.4 DISPOSAL COST .....	60
11.5 LIFE CYCLE COST (LCC) <sup>11</sup> .....	60
11.6 ASSESSMENT OF VERTICAL TAKEOFF COST .....	61
11.7 ACCURACY/FEASIBILITY OF ESTIMATE .....	62
<b>12. DESIGN OPTIMIZATION .....</b>	<b>63</b>
12.1 DESIGN VARIABLE SELECTION .....	63
12.2 OPTIMIZATION METHODOLOGY .....	64
12.2.1 Defining a Well-Posed Problem <sup>24</sup> .....	64
12.2.2 Flow of Information .....	65
12.2.2.1 Inputs to the Optimizer .....	65
12.2.2.2 Constraints .....	67
12.2.2.3 Outputs from the Optimizer .....	67
12.2.3 Constrained Optimization <sup>13</sup> .....	68
12.3 BASELINE DESIGN OPTIONS .....	68
12.4 OPTIMIZATION RESULTS <sup>1</sup> .....	69
12.4.1 Optimized Design .....	69
12.4.2 Gradients .....	71
12.4.3 Carpet Plots <sup>41</sup> .....	71
12.4.4 Sensitivity Analyses .....	72
12.4.4.1 Takeoff/Landing Distance .....	73
12.4.4.2 Range .....	73
12.4.4.3 Payload Weight .....	74
12.5 ACCURACY/FEASIBILITY OF "SOLUTION" .....	74
<b>13. CONCLUSIONS AND RECOMMENDATIONS .....</b>	<b>76</b>
<b>14. REFERENCES .....</b>	<b>79</b>
<b>APPENDIX A .....</b>	<b>A-1</b>
<b>APPENDIX B .....</b>	<b>B-1</b>

## LIST OF FIGURES

FIGURE 1: THREE-VIEW OF THE CARDINAL.....	iv
FIGURE 2: MISSION PROFILE FOR THE CARDINAL.....	2
FIGURE 3: THREE-VIEW OF THE NASA QUIET SHORT-HAUL RESEARCH AIRCRAFT (QSRA) <sup>63</sup> .....	4
FIGURE 4: THREE-VIEW OF THE CANADAIIR CL-84 TILT-WING <sup>60</sup> .....	4
FIGURE 5: SPIRAL DEVELOPMENT MODEL <sup>12</sup> .....	5
FIGURE 6: NASA TECHNOLOGY READINESS LEVELS <sup>33</sup> .....	6
FIGURE 7: PRELIMINARY ESTIMATE OF TAKEOFF PERFORMANCE FOR THE CARDINAL.....	12
FIGURE 8: PRELIMINARY ESTIMATE OF LANDING PERFORMANCE FOR THE CARDINAL.....	12
FIGURE 9: CARGO HOLD/PASSENGER CABIN LAYOUT FOR THE CARDINAL.....	16
FIGURE 10: WING PIVOTING AND FOLDING FOR THE CARDINAL.....	18
FIGURE 11: SPANWISE LIFT DISTRIBUTION FOR THE CARDINAL.....	18
FIGURE 12: UPPER SURFACE BLOWING (USB) <sup>6</sup> .....	20
FIGURE 13: LIFT COEFFICIENT VARIATION WITH POWER SETTING FOR THE CARDINAL.....	21
FIGURE 14: TILT-WING VELOCITY COMPONENTS <sup>56</sup> .....	22
FIGURE 15: LONGITUDINAL TIP-OVER AND CLEARANCE ANGLES.....	25
FIGURE 16: LATERAL TURNOVER ANGLE.....	25
FIGURE 17: RETRACTION MECHANISM FOR THE MAIN LANDING GEAR <sup>18</sup> .....	27
FIGURE 18: AVCO LYCOMING ALF 502 TURBOFAN ENGINE <sup>61</sup> .....	29
FIGURE 19: TURBOFAN ENGINE SCHEMATIC DRAWING <sup>48</sup> .....	29
FIGURE 20: FIXED-WING INSTALLATION DRAWING.....	29
FIGURE 21: MAXIMUM CRUISE CARPET PLOT FOR CARDINAL ENGINES.....	32
FIGURE 22: INBOARD PROFILE AND STRUCTURAL ARRANGEMENT FOR THE CARDINAL.....	34
FIGURE 23: V-N GUST AND MANEUVER DIAGRAM.....	36
FIGURE 24: $X_{cc}$ EXCURSION FOR MILITARY VERSION.....	40
FIGURE 25: DRAG POLAR AND L/D VS. $C_L$ FOR TAKEOFF CONFIGURATION.....	44
FIGURE 26: DRAG POLAR AND L/D VS. $C_L$ FOR CRUISE CONFIGURATION.....	45
FIGURE 27: DRAG POLAR AND L/D VS. $C_L$ FOR LANDING CONFIGURATION.....	45
FIGURE 28: $F/S_{WET}$ FOR MANY EXISTING AIRCRAFT <sup>51</sup> .....	46
FIGURE 29: TAKEOFF AND LANDING GROUND ROLLS FOR THE CARDINAL.....	52
FIGURE 30: RATE OF CLIMB FOR THE CARDINAL AT VARYING ALTITUDES AND MACH NUMBERS.....	53
FIGURE 31: SPECIFIC RANGE FOR THE CARDINAL.....	54
FIGURE 32: PAYLOAD-RANGE DIAGRAM FOR THE MILITARY VERSION OF THE CARDINAL.....	55
FIGURE 33: LIFE CYCLE COST BREAKDOWN <sup>53</sup> .....	57
FIGURE 34: OPERATING COST BREAKDOWN <sup>1</sup> .....	60
FIGURE 35: LIFE-CYCLE COST (LCC) BREAKDOWN <sup>1</sup> .....	61
FIGURE 36: CARDINAL OPTIMIZATION FLOW CHART.....	66
FIGURE 37: CARPET PLOT FOR TAKEOFF GROUND ROLL CONSTRAINT.....	72
FIGURE 38: LIFE CYCLE COST VS. TAKEOFF GROUND ROLL.....	73
FIGURE 39: RANGE CONSTRAINT VS. CRUISE SPEED.....	B-2
FIGURE 40: LIFE CYCLE COST VS. CRUISE SPEED.....	B-2
FIGURE 41: RANGE CONSTRAINT VS. CRUISE ALTITUDE.....	B-3
FIGURE 42: LIFE CYCLE COST VS. CRUISE ALTITUDE.....	B-3

## LIST OF TABLES

TABLE 1: SUMMARY OF COST COMPARISON BETWEEN INITIAL DESIGNS .....	iii
TABLE 2: MISSION REQUIREMENTS FOR THE CARDINAL .....	2
TABLE 3: WEIGHT SIZING FOR THE CARDINAL .....	11
TABLE 4: SUMMARY OF PERFORMANCE SIZING FOR FIXED-WING .....	13
TABLE 5: SUMMARY OF PERFORMANCE SIZING FOR TILT-WING.....	13
TABLE 6: WING GEOMETRY FOR THE CARDINAL.....	19
TABLE 7: EMPENNAGE GEOMETRY PARAMETERS .....	24
TABLE 8: CONTROL SURFACES FOR THE CARDINAL .....	24
TABLE 9: LANDING GEAR TIP-OVER AND LONGITUDINAL CLEARANCE ANGLES .....	26
TABLE 10: MAIN GEAR TIRE TYPES <sup>18</sup> .....	26
TABLE 11: NOSE GEAR TIRE TYPES <sup>18</sup> .....	26
TABLE 12: STRUT DIMENSIONS FOR THE LANDING GEAR .....	27
TABLE 13: CARDINAL COMPONENT WEIGHT BREAKDOWN.....	39
TABLE 14: MOMENTS AND PRODUCTS OF INERTIA FOR MILITARY VERSION.....	40
TABLE 15: MOMENTS AND PRODUCTS OF INERTIA FOR COMMERCIAL VERSION .....	40
TABLE 16: PARASITE DRAG BREAKDOWN.....	43
TABLE 17: OSWALD EFFICIENCY FACTOR FOR SEVERAL AIRCRAFT .....	46
TABLE 18: LONGITUDINAL STABILITY DERIVATIVES FOR THE CARDINAL DESIGN .....	48
TABLE 19: LONGITUDINAL CONTROL DERIVATIVES FOR FIXED-WING CARDINAL DESIGN .....	48
TABLE 20: LATERAL-DIRECTIONAL STABILITY DERIVATIVES FOR THE FIXED-WING CARDINAL DESIGN .....	49
TABLE 21: LATERAL-DIRECTIONAL CONTROL DERIVATIVES FOR THE FIXED-WING CARDINAL DESIGN .....	49
TABLE 22: FREQUENCIES & DAMPING RATIOS FOR THE CARDINAL .....	50
TABLE 23: STALL AND MINIMUM CONTROL SPEEDS FOR THE CARDINAL .....	50
TABLE 24: FAR CLIMB GRADIENTS FOR THE MILITARY VERSION OF THE CARDINAL .....	53
TABLE 25: RANGE OF THE CARDINAL FOR MILITARY AND COMMERCIAL VERSIONS .....	55
TABLE 26: RDTE COST BREAKDOWN.....	57
TABLE 27: MANUFACTURING AND ACQUISITION COST BREAKDOWN .....	58
TABLE 28: OPERATING COST BREAKDOWN <sup>1</sup> .....	60
TABLE 29: LIFE-CYCLE COST (LCC) BREAKDOWN <sup>1</sup> .....	61
TABLE 30: ASSESSMENT OF VERTICAL TAKEOFF OPTION <sup>1</sup> .....	62
TABLE 31: EXISTING AIRCRAFT COST DATA .....	62
TABLE 32: CARDINAL DESIGN VARIABLES .....	64
TABLE 33: CARDINAL MISSION CONSTRAINTS <sup>1</sup> .....	67
TABLE 34: BASELINE DESIGN COMPARISON CHART .....	69
TABLE 35: SUMMARY OF OPTIMIZED DESIGN (MILITARY VERSION).....	70
TABLE 36: SUMMARY OF OPTIMIZED CONSTRAINT VALUES .....	70
TABLE 37: SUMMARY OF COST COMPARISON BETWEEN INITIAL DESIGNS .....	77
TABLE 38: RFP REQUIREMENTS COMPLIANCE MATRIX .....	78

## NOMENCLATURE

### SYMBOLS

SYMBOL	DEFINITION	UNITS
$\zeta$	Damping ratio	~
$\lambda_{ht}$	Horizontal Tail Taper Ratio	--
$\Lambda_{ht}$	Horizontal Tail Quarter Chord Sweep Angle	degrees
$\eta_{i \text{ flap}}$	Inboard Station of the Flaps	--
$\omega_n$	Undamped natural frequency	~
$\eta_{o \text{ flap}}$	Outboard Station of the Flaps	--
$\lambda_{vt}$	Vertical Tail Taper Ratio	--
$\Lambda_{vt}$	Vertical Tail Quarter Chord Sweep Angle	degrees
$\lambda_{wing}$	Wing Taper Ratio	--
$\Lambda_{wing}$	Wing Quarter Chord Sweep Angle	degrees
$b_{ht}$	Horizontal Tail Span	ft
$b_{vt}$	Vertical Tail Span	ft
$b_{wing}$	Wing Span	ft
$C_\mu$	Momentum Coefficient	--
$C_D$	Drag Coefficient	--
$C_{Di}$	Induced Drag Coefficient	--
$C_{Dp}$	Parasite Drag Coefficient	--
$C_{Dp, \text{ flap}}$	Parasite Drag Coefficient due to flaps	--
$C_{Dp, \text{ fuselage}}$	Parasite Drag Coefficient due to fuselage	--
$C_{Dp, \text{ gear}}$	Parasite Drag Coefficient due to landing gear	--
$C_{Dp, \text{ ht}}$	Parasite Drag Coefficient due to the horizontal tail	--
$C_{Dp, \text{ misc}}$	Parasite Drag Coefficient due to miscellaneous items	--
$C_{Dp, \text{ nacelle}}$	Parasite Drag Coefficient due to the nacelle	--
$C_{Dp, \text{ pylon}}$	Parasite Drag Coefficient due to the pylon	--
$C_{Dp, \text{ slat}}$	Parasite Drag Coefficient due to slats	--
$C_{Dp, \text{ vt}}$	Parasite Drag Coefficient due to the vertical tail	--
$C_{Dp, \text{ wing}}$	Parasite Drag Coefficient due to the wing	--
$c_f$	Skin Friction Coefficient	--
$cg_{max}$	Maximum Center of Gravity Excursion	% of wing mac
CGR	Climb Gradient	%
$C_L$	Lift Coefficient	--
$C_{Lmax}$	Maximum Lift Coefficient	--
$C_{Lmax \text{ landing}}$	Maximum Lift Coefficient, Landing Configuration	--
$C_{Lmax \text{ takeoff}}$	Maximum Lift Coefficient, Takeoff Configuration	--
$e$	Oswald Span Efficiency Factor	--
flap_angle	Flap Angle	degrees
flap_to_chord	Flap to Chord Ratio	--

$f_{\text{total}}$	Total Equivalent Parasite Drag Area	ft <sup>2</sup>
$h$	Height of Airplane Volume Envelope	ft
$I_{xx}$	Rolling Moment of Inertia	slug-ft <sup>2</sup>
$I_{xy}, I_{yz}, I_{xz}$	Products of Intertia	slug-ft <sup>2</sup>
$I_{yy}$	Pitching Moment of Inertia	slug-ft <sup>2</sup>
$I_{zz}$	Yawing Moment of Inertia	slug-ft <sup>2</sup>
$k$	Form Factor	--
$l$	Length of Airplane Volume Envelope	ft
$L/D$	Lift-to-Drag Ratio	--
$M$	Mach Number	--
$mac$	Mean Aerodynamic Chord	ft
$M_{cc}$	Crest Critical Mach Number	--
$n_{\text{ult}}$	Ultimate Load Factor	g's
$R$	Range	nm
$R_{\text{block}}$	Block Distance	nm
$RC$	Rate of Climb	ft/min
$R_{\text{cruise}}$	Cruise Distance	nm
$sfc$	Specific Fuel Consumption	lb/hr/lb or lb/hr/hp
$S_{g \text{ land}}$	Landing Ground Roll	ft
$S_{g \text{ to}}$	Takeoff Ground Roll	ft
$S_{\text{ht required}}$	Tail Reference Area Required for Takeoff Rotation	ft <sup>2</sup>
$\text{slat\_angle}$	Slat Angle	ft
$SM_{\text{min}}$	Minimum Static Margin	% of wing $mac$
$SR$	Specific Range	nm/lb
$S_{\text{ref}}$	Wing Reference Area	ft <sup>2</sup>
$S_{\text{ref, ht}}$	Horizontal Tail Reference Area	ft <sup>2</sup>
$S_{\text{ref, vt}}$	Vertical Tail Reference Area	ft <sup>2</sup>
$S_{\text{wet}}$	Wetted Area	ft <sup>2</sup>
$S_{\text{wet, total}}$	Total Airplane Wetted Area	ft <sup>2</sup>
$t/c_{\text{ht}}$	Horizontal Tail Average Thickness to Chord Ratio	--
$t/c_{\text{vt}}$	Vertical Tail Average Thickness to Chord Ratio	--
$t/c_{\text{wing}}$	Wing Average Thickness to Chord Ratio	--
$T_{\text{avail}}$	Available Thrust	lb
$t_{\text{cl}}$	Time to Climb	sec
$T_{\text{to}}$	Takeoff Thrust	lb
$T_{\text{to installed}}$	Takeoff Installed Thrust	lb
$T_{\text{to, uninstalled}}$	Takeoff Uninstalled Thrust	lb
$V$	Cruise Speed	ktas
$V_C$	Structural Design Cruise Speed	keas
$V_D$	Design Dive Speed	keas
$V_H$	Maximum Level Speed at Sea Level	keas

$V_{mc}$	Minimum Control Speed	ft/sec
$V-n$	Speed – Load Factor	keas – g's
$V_{stall, landing}$	Stall Speed in the landing configuration	ktas
$w$	Width of the Airplane Volume Envelope	ft
$W_e$	Empty Weight	lb
$W_{e, guess}$	Empty Weight, Initial Guess	lb
$W_{eng}$	Single Engine Weight	lb
$W_{fuel\ used}$	Weight of Fuel Used During Mission	lb
$W_{max\ zero\ fuel}$	Maximum Zero Fuel Weight	lb
$W_{PL}$	Payload Weight	lb
$W_{to}$	Takeoff Weight	lb
$W_{to, guess}$	Takeoff Weight, Initial Guess	lb
$x_{cg\ aft}$	Aftmost Longitudinal Center of Gravity Location	ft
$x_{cg\ forward}$	Forwardmost Longitudinal Center of Gravity Location	ft
$x_{ht}$	Longitudinal Position of the Horizontal Tail Leading Edge	ft
$x_{maingear}$	Longitudinal Position of the Main Landing Gear	ft
$x_{nosegear}$	Longitudinal Position of the Nose Landing Gear	ft
$x_{vt}$	Longitudinal Position of the Vertical Tail Leading Edge	ft
$x_{wing}$	Longitudinal Position of the Wing Leading Edge	ft
$y_{engine}$	Lateral Position of the Outboard Engine	ft
$y_{maingear}$	Lateral Position of the Main Landing Gear	ft
$z_{cg}$	Highest Center of Gravity	ft

## ACRONYMS

ACRONYM	DEFINITION
ACQ	Acquisition Phase
AEO	All Engines Operating
APU	Auxiliary Power Unit
CAD	Computer Aided Drafting
CER	Cost Estimating Relationship
CGR	Climb Gradient
DISP	Disposal Phase
DOC	Direct Operating Cost
FAR	Federal Aviation Regulations
FY	Fiscal Year
GD	General Dynamics
IOC	Indirect Operating Cost
KT	Kuhn-Tucker Equations
LCC	Life-Cycle Cost
MAC	Mean Aerodynamic Chord
MIL	Military
OEI	One Engine Inoperative
OPS	Operations Phase
QP	Quadratic Programming
RC	Rate of Climb
RDTE	Research, Development, Testing, and Engineering Phases
RFP	Request for Proposal
SQP	Sequential Quadratic Programming
SR	Specific Range
SSTOL	Super Short Takeoff and Landing
USAF	United States Air Force
USB	United States Billions
USD	United States Dollars
USM	United States Millions
USN	United States Navy
V/STOL	Vertical/Short Takeoff and Landing
VTOL	Vertical Takeoff and Landing

## ACKNOWLEDGEMENTS

*"Nor do I seek to understand that I believe, but I believe that  
I may understand. For this too I believe, that unless I first believe,  
I shall not understand."*

*St. Anselm*

The work presented here is a compilation of several months of iterative design work—throughout the process, an extended team of advisors augmented the Cardinal effort with advice, support, and constructive criticism which helped improve the final design presented herein.

It was the pleasure of the Cardinal team to meet with and learn from several men at the NASA Ames Research Center. **Dr. Yung Yu**, **Dr. Jack Franklin**, and **Larry Young** of the National Rotorcraft Technology Center and **Dr. John Davis** and **Rick Peyran** of the U.S. Army Aeroflightdynamics Directorate offered extraordinary guidance during the trade studies between initial design configurations. The team would like to especially thank **Dr. Michael Scully** and **John Preston**, also of the U.S. Army Aeroflightdynamics Directorate for access to (and navigation through) their incredible design library. Without Dr. Scully and Mr. Preston, the design would certainly have suffered. The NASA Ames team participated in two design reviews at Ames, obviously going above and beyond the call of duty to volunteer their time.

**Dennis Riddle**, former Branch Chief of Powered-Lift Flight at Ames, was an “ace in the hole.” His amazing knowledge about the QSRA was an outstanding asset to the Cardinal team. Mr. Riddle provided a wealth of flight test data from the QSRA which aided in validation of many of the Cardinal’s subsystem analyses (particularly in the areas of advanced technology).

This section would not be complete without including acknowledgement of the faculty advisors for the Cardinal project. The team is indebted to **Dr. Alonso** and **Dr. Kroo** from Stanford University. Their support as advisors of the team was an example of their dedication to students, and an asset to the project. Their expertise in aircraft design, analysis, and optimization was invaluable to the Cardinal team. It was, and continues to be, an honor to work with these professors.

*Thank You*

## **1. INTRODUCTION**

The Cardinal is an aircraft designed to fulfill the promise of center-city to center-city travel. In compliance with commercial and military requirements for such a design, the Cardinal uses a variety of innovative and proven technologies to fulfill its mission goals. There are no aircraft to date which demonstrate both the desired performance for short commutes and the economic viability of such a design. The Cardinal design presented here attempts to meet these challenges with a Super Short Takeoff and Landing (SSTOL), Carrier On-board Delivery (COD) aircraft. Designed for dual use as a passenger / military cargo aircraft, the Cardinal provides center-city to center-city travel by operating from landing "barges" on rivers. The rivers provide safe approach areas in city centers without requiring major construction within the city. A military version would replace the C-2 Greyhound for transport to aircraft carriers.

### **1.1 MISSION OBJECTIVES<sup>2</sup>**

For the past few decades, short-commute center-city to center-city travel has been a desire. This desire, however, has not yet translated into the commercial aircraft market. The complexity of this form factor, coupled with economic impact (a major driver in the aircraft design arena), makes this promise a challenging one to fulfill. Recent technology advances, and numerous attempts to produce an aircraft of this nature have once again brought the challenge to the forefront. In addition to the desires mentioned above, the severe lack of open space in center-city areas has created yet another design challenge. The military also presents a need for the SSTOL form factor. COD requirements must continue to be satisfied after disposal of the current fleet of such planes.

The Cardinal must be designed to achieve center-city to center-city travel while minimizing Life-Cycle Cost (LCC). With a design of this type, the aircraft will fulfill the promise of short commute air travel, provide a needed service to the military, and demonstrate economic success of such a mission. These performance and cost objectives form the foundation for the Cardinal design. Throughout the design process, these major mission goals were addressed. The final design represents an airplane compliant with the desired mission.

### **1.2 MISSION REQUIREMENTS**

The mission requirements for a Super Short Takeoff and Landing (SSTOL) transport aircraft were provided in the American Institute of Aeronautics and Astronautics (AIAA) Graduate Team Aircraft Design Competition

Request for Proposal (RFP): SSTOL Carrier On-board Delivery (COD) Aircraft<sup>2</sup> A summary of the mission requirements for the Cardinal is provided in Table 2 and the mission profile is shown in Figure 2.

**Table 2: Mission Requirements for the Cardinal<sup>2</sup>**

DESIGN MISSION PROFILE
Warm up and taxi for 10 minutes, Sea Level (SL), Standard Atmosphere (SA) +27°F day with full passenger and baggage load
Take off within a ground roll of 300 ft, SL, SA+27°F with full passenger and baggage load
Climb at best rate of climb to best cruising altitude
Cruise at best cruise speed (at least 350 knots) for 1500 nm
Descend to SL (no credit for range)
Land with domestic fuel reserves within ground roll of 400 ft
Taxi to gate for 5 minutes
SPECIAL COMMERCIAL DESIGN REQUIREMENTS
Passenger Capacity – 24 passengers (commercial) and baggage
Overhead stowage space shall be provided
Weight of passenger and baggage – 200 lbs
SPECIAL MILITARY DESIGN REQUIREMENTS
Can accommodate priority cargo, passengers or both
Must be capable of carrying two GE F110 engines (for F-14D)
Wing folding allowed to meet spot factor requirements of 60 ft by 29 ft
Maximum payload is 10000 lbs
Arresting hooks for landing or catapult devices for launch not allowed
ADDITIONAL REQUIREMENTS AND CONSTRAINTS
Shall conform to all applicable FAR
All performance requirements shall be standard day unless otherwise noted: $T_{SL} = 58.69^{\circ}\text{F}$ , $P_{SL} = 2116 \text{ lb/ft}^2$
Technology availability date is 2005

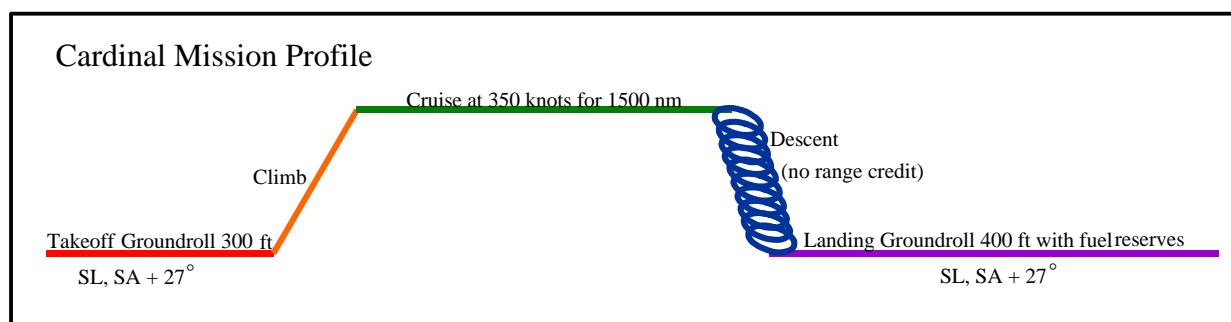


**Figure 2: Mission Profile for the Cardinal**

## **2. DESIGN PHILOSOPHY**

As stated in the Request For Proposal (RFP),<sup>2</sup> new technologies offer the opportunity for center-city to center-city travel. While many existing aircraft have incorporated some of these technologies, none of them as a whole have proven to be economically viable. To produce an economically viable design for the Cardinal, it was of primary importance to understand and avoid past mistakes in similar designs, capitalize on design elements that proved successful, and include new technologies that would further the favorable performance of the final design. This section highlights the design philosophy of the Cardinal team—from an early review of existing aircraft to technology maturity issues, it is a comprehensive outline to the methodology followed throughout the design process.

### **2.1 REVIEW OF EXISTING AIRCRAFT**

The mission requirements for the Cardinal required takeoff and landing ground rolls approaching the limits of fixed-wing aircraft. A review of past and current aircraft found two that were similar in size to that expected for the Cardinal and had similar ground roll performance capabilities. The first is the NASA Quiet Short-haul Research Aircraft (QSRA) shown in Figure 3. The QSRA utilizes Upper Surface Blowing (USB) flaps to achieve spectacular short field performance for a fixed-wing aircraft. A second aircraft with similar performance is the Canadair CL-84 Tilt-wing. Tilt-wing aircraft are similar to tilt-rotors except that instead of only tilting the engine/rotor rotating, the entire wing is rotated. The QSRA and CL-84 were prototype/research aircraft and never entered production. However, the flight test programs of these aircraft provided a significant amount of data for validating potential approaches to short takeoff and landing for the Cardinal. In addition, data on these aircraft was used to validate the assumptions and calculations made for the Cardinal.

### **2.2 DESIGN PROCEDURE**

From the review of the mission requirements and aircraft with similar performance the Cardinal team chose to investigate two designs: a tilt-wing aircraft and a fixed-wing aircraft with upper surface blowing (USB) flaps. A complete analysis, design, and optimization of the two aircraft was conducted to develop the ‘best’ design for each aircraft. Cost comparisons between the two concepts were used to select the final design.



optimize performance, trades must be done for every requirement change. Therefore, as illustrated by the spiral development model, trade and risk analyses must be a continuing part of the complete design process. On the Cardinal project, system level trades were done early on in the design, and relevant subsystem trades were done continually as the design matured.

To accommodate concurrent engineering, preliminary sizing estimates were made during the first iteration. These estimates provided approximate weights, wing and tail sizing, and propulsion selection. Optimization occurred after subsystem analyses and design tools were created, and the final design point was selected after sensitivity analysis was completed. Because of the unique requirements of the Cardinal and the desire to have total control and understanding of the design and analysis tools, the Cardinal design team wrote all of the programs used in the design process. To provide a common environment for all design tools the team chose to do all analysis work in Matlab,<sup>34</sup> a technical computing program that includes a programming language with built-in tools for plotting, interpolation, and optimization.

To ensure a quality design, periodic reviews were included at the end of each iteration to facilitate feedback from advisors, industry professionals, and faculty. The final spiral culminated with the delivery of this proposal.

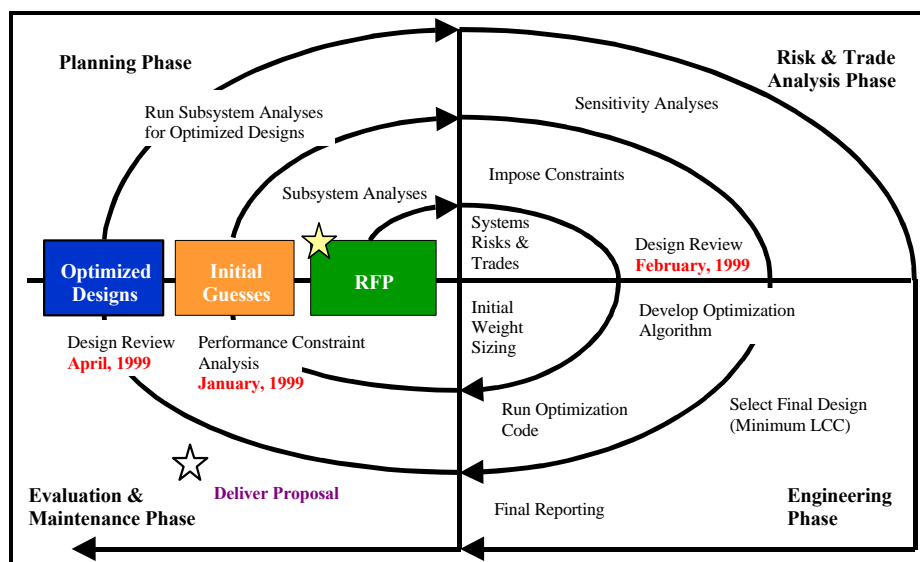


Figure 5: Spiral Development Model<sup>12</sup>

### 2.2.1 TECHNOLOGY MATURITY ASSESSMENT<sup>33</sup>

Technology Readiness Levels (TRLs) are a systematic metric/measurement system that supports assessments of the maturity of a particular technology and the consistent comparison of maturity between

different types of technology. The TRL approach has been used on-and-off in NASA space technology planning for many years—the Cardinal team chose to take advantage of this system to evaluate prospective technologies. The RFP<sup>2</sup> states a technology readiness date of 2005. To comply with this restriction, the Cardinal design implements technologies currently at a TRL of Level 5 or higher. While components/technologies of this nature have not been “flight-qualified” or “flight-proven” as of the submittal of this proposal, each of these technologies is predicted to reach TRL Level 9 by 2005. By limiting the range of new technology, the Cardinal implicitly reduces the risk of its design. Figure 5 illustrates the NASA TRL Levels. Note the shaded region that indicates technology levels deemed acceptable for the Cardinal design. Technology assessment and risk analysis for the Cardinal design are provided throughout the summary of the subsystems (see sections 4.2.2 and 5.3.2).

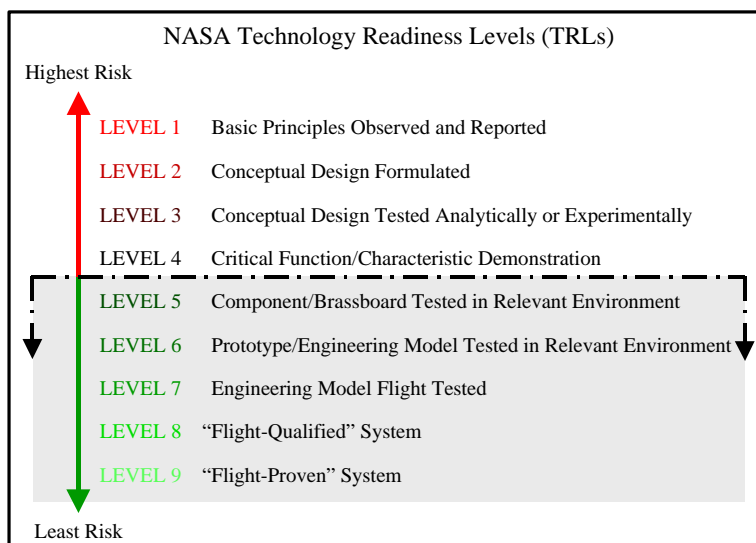


Figure 6: NASA Technology Readiness Levels<sup>33</sup>

## 2.3 USER PREFERENCES AND SAFETY CONSIDERATIONS FOR V/SSTOL

This section describes the pilot and passenger preferences between SSTOL and VTOL. Passenger preferences are mainly based on noise, vibration and perceived safety, while user preferences are generally based on control authority. Safety, however, is of primary importance to the user, and thus this section also addresses the safety issues involved in VTOL and SSTOL operations for the same mission. The importance of each of these factors is discussed with respect to V/STOL aircraft and the Cardinal design.

### **2.3.1 PILOT PREFERENCES**

Any aspect of aircraft performance that lowers the level of confidence during takeoff or landing is considered an inherent safety issue. With that in mind, reference data from flight tests was the primary source of information in the determination of pilot preferences. An evaluation of the Canadair CL-84 tilt-wing aircraft was performed to analyze user preferences between VTOL and STOL scenarios.<sup>7</sup> The scenarios covered in the evaluation included takeoff, hover (for VTOL), climb, and landing. A fixed-wing STOL scenario was also analyzed, which was mainly based on the QSRA flight test data.<sup>44,45,16</sup> SSTOL pilot preferences and safety issues were then inferred from the STOL data.

When the CL-84 was operated in STOL configuration, the takeoff and landing behavior was similar to conventional aircraft. As the vehicle accelerated for takeoff, the rotor configuration produced a downwash effect on the aerodynamic surfaces, causing the nose to pitch down. Pilot interaction was required to maintain a level fuselage for takeoff. This nose-down pitch reaction was also observed during landing, accompanied by buffeting and vibration attributed to ground effects. Since these behaviors are effects of the aircraft's dynamic characteristics, it is likely that similar vehicles would experience similar behavior. Such behavior, which requires continuous pilot interaction to maintain a level attitude, constitutes a safety issue in both takeoff and landing.

For the fixed-wing design, STOL scenarios demanded no unusual piloting techniques, even in an "OEI<sup>44</sup> and stability augmentation systems turned off"<sup>16</sup> scenario. Only minor nose wheel steering inputs, for example, were required to maintain a straight takeoff path. Tests on an aircraft carrier of the QSRA resulted in approaches to touch-down with extreme precision, thus requiring minimal pilot authority. An SSTOL configuration would require greater pilot authority than an STOL design, but since the STOL scenarios demanded no unusual pilot techniques, a fixed-wing SSTOL design would not require a significant increase in pilot interaction. A fixed-wing SSTOL design, therefore, does not constitute a safety issue in both takeoff and landing.

Safety issues in the VTOL mode appeared primarily in the transition between hover and aerodynamic flight. In the transition to aerodynamic flight after takeoff, testers observed an altitude loss of 50 feet before sufficient forward velocity to produce lift was acquired. The reverse transition, from aerodynamic flight to hover, was even more complicated. Gradually tilting the wing upward raised the angle of attack, causing the

aircraft to rise and lose speed until wing stall resulted in a sudden loss of altitude. During both transitions, the pilot was required to make continual adjustment to maintain pitch trim. These modes of irregular behavior lowered the confidence level, therefore presenting safety issues. Vertical touchdown also presented difficulties. Within a few feet of touchdown, ground effects disturbed the vehicle's motion about all axes, requiring pilot control and making it difficult for the pilots to find the ground. These problems associated with VTOL designs were drawbacks compared to a fixed-wing SSTOL design, similar to that chosen for the Cardinal.

Noise is another factor taken into account in pilot preferences. VTOL designs tend to have larger engines, which generate more noise. Generally, VTOL aircraft are all tilt-wing, tilt-rotor, or thrust vectored designs, while SSTOL can be either tilt-wing or fixed-wing designs. Pilots enjoy the benefits of a smaller engine design because it permits the ability to communicate without the use of microphone equipment; thus the crew does not have to speak above a conversational level.<sup>37</sup> This feature enhances the communication effectiveness between pilot and copilot. Hence, for VTOL designs, the noise generated by the engines is not preferred by pilots over the SSTOL design.

### **2.3.2 PASSENGER PREFERENCES**

Though the data from the evaluations was primarily based on pilot preferences, passenger preferences can be inferred from the flight performance information. Based on the evaluation<sup>7,16,44,45</sup> of the tilt-wing and fixed-wing aircraft, the fixed-wing SSTOL design would be preferred by passengers over a VTOL design. The main drawback of a VTOL design is the reconversion from forward flight to hover. Since deceleration would be difficult for the pilot to control, the aircraft would tend to experience oscillatory movements, which could result in vibration. Since vibration motion in an aircraft is perceived by passengers to be a dangerous mode in flight, the VTOL reconversion would not be desired by passengers, compared to the slow, steady descent of an SSTOL. As mentioned in Section 2.3.1, tilt-wing designs have higher associated noise than their fixed-wing counterparts. Like users, passengers also generally prefer a quiet cabin; passengers perceive a quiet environment as a safe one.

### **2.3.3 AIRCRAFT NOISE**

Aircraft noise is subject to certification requirements, community acceptance of aircraft and airports, and has a significant effect on passenger comfort. There are many sources of aircraft noise, the largest of which is

due to the propulsion system. Presented in the following sections are comparisons of noise characteristics for turbofan and turboprop engines and the impacts of these characteristics on the Cardinal design.

#### **2.3.3.1 SOURCES OF NOISE**

The noise produced by aircraft is transient and can vary greatly in spectral character, making it different from many other types of noise which people cope with daily. These properties come from the high number of noise sources, including the engine exhaust, fuselage boundary layer, wake vorticity from the airframe, and landing gear vorticities. During flight, however, the aircraft noise is dominated by that created by the engine. This is comprised of noise from the mixing of jet exhaust gases with the surrounding atmosphere, as well as noise created by the engine components, turbine and compressor, individually.

#### **2.3.3.2 ESTIMATES OF NOISE**

Although the noise created by the aircraft includes airframe noise, these are small effects in comparison to those of the engine. A good approximation of the noise generated by the aircraft, can be formulated by examining the noise characteristics of the engines alone. While this value is generally near 90 dB, the highest contribution from other factors will be from high lift devices at landing which contribute nearly 10 dB.

#### **2.3.3.3 FIXED WING ENGINE NOISE**

The fixed-wing configuration uses high bypass-ratio turbofan engines, which contribute the largest component of noise generated by this aircraft. The combined polar sound pressure levels produced by a typical high bypass-ratio turbofan range from 70 to 100 dB for frequencies from 20 to 20,000 Hz.<sup>31</sup> Additionally, the upper surface blowing reduces the sound levels - “the noise impact area for upper surface blown aircraft is small compared to a conventional jet transport having the same size engines.”<sup>5</sup> The noise levels can be further reduced by acoustically treating the flaps, and adding noise-suppressing materials to the inlet and exhaust ducts.

#### **2.3.3.4 TURBOPROP NOISE**

Turboprop noise is very different from turbofan noise generation. The primary source of noise is attributed to air-volume displacement effects, which come from the regular pressure pulse created by the blade. The rotation of the propeller also leads to upwash at the blade leading edge and blade/wake interaction. The combination of all these effects results in a noise level which is generally higher than that of aircraft with turbofan propulsion.

#### **2.3.4 IMPACT ON DESIGN**

The fixed-wing SSTOL design does not pose safety issues in any flight mission. Both pilot and passenger preferences also favor the fixed-wing SSTOL design. These factors are important for the commercial design because the passenger is the customer. For the military version, the user preferences are important because the pilot is the user of the aircraft. For the military design, of primary importance is the success of the mission, which is highly dependent on the pilot operating the aircraft effectively. Noise considerations also favor the fixed-wing design due to its lower noise levels than that of the tilt-wing. Though the final determining factor between the fixed-wing and tilt-wing design was a minimization of life-cycle cost (see section 12), the importance of passenger and user preferences was not overlooked. Mathematical optimization works well for choosing the “best” numeric parameters but doesn’t consider the intangible issues that are important for a practical design. The Cardinal team was cognizant of this fact, and chose to include human factors in the final design selection process.

### 3. INITIAL WEIGHT AND PERFORMANCE SIZING

Initial weight and performance sizing was performed to estimate the weight, wing area, and installed thrust/power for both a fixed-wing and a tilt-wing design. The results became initial guesses for the optimization routine described in section 12. The methods were incorporated into a Matlab code available on the Cardinal web site.<sup>1</sup>

#### 3.1 MISSION WEIGHT SIZING

The weights of both the fixed-wing aircraft and the tilt-wing aircraft were estimated based on the known mission profile and regression coefficients that relate the empty weight and takeoff weight for a given type of aircraft. The mission profile used for the weight sizing was obtained from the RFP<sup>1</sup> and shown in Figure 2. The profile requires a minimum cruise speed of 350 knots with a maximum 10,000 lb payload for a 1500 nm range with reserves. Regression coefficients for military transport aircraft<sup>46</sup> and the Breguet range equations can be used iteratively to find the empty, takeoff, and fuel weights expected for the aircraft. This requires the assumption of lift-to-drag ratios, specific fuel consumptions, and propeller efficiencies—typical values from Reference 46 were assumed. The mission weight sizing method computes fuel weights for start, warmup, taxi, takeoff, landing, and shutdown using statistical approximations to existing aircraft data. The Breguet range equations are used to compute the fuel weight used during cruise.

Table 3 summarizes the initial weight estimates for the Cardinal.

**Table 3: Weight Sizing for the Cardinal**

WEIGHT	FIXED-WING	TILT-WING
Takeoff Weight	48,635 lb	59,922 lb
Empty Weight	25,487 lb	34,588 lb
Fuel Weight	12,504 lb	14,635 lb

#### 3.2 PERFORMANCE CONSTRAINT SIZING

The required landing and takeoff distances were the only constraints considered in the initial performance constraint sizing. Typical statistical relations for takeoff and landing distances<sup>46</sup> do not account for SSTOL or VTOL capabilities, hence approximate models of the full equations of motion for takeoff and landing distance were used for the initial estimates.<sup>30</sup>

Sizing for the fixed-wing aircraft was used to find ranges of the thrust-to-weight ratio and the wing-loading that met both the takeoff and landing requirements. An initial value for wing loading was chosen, and iterations

on the thrust-to-weight ratio were conducted until the takeoff distance requirement was met. The wing-loading value from the takeoff distance computation was used to calculate the landing ground roll, which is approximately independent of the thrust-to-weight ratio.<sup>30</sup> The assumed maximum lift coefficients were based on a review of upper surface blowing (USB) data from the YC-14.<sup>63</sup> Figure 7 and Figure 8 show the constraint lines for takeoff and landing (selected design points are denoted by stars). Table 4 summarizes the design point for the fixed-wing version of the Cardinal.

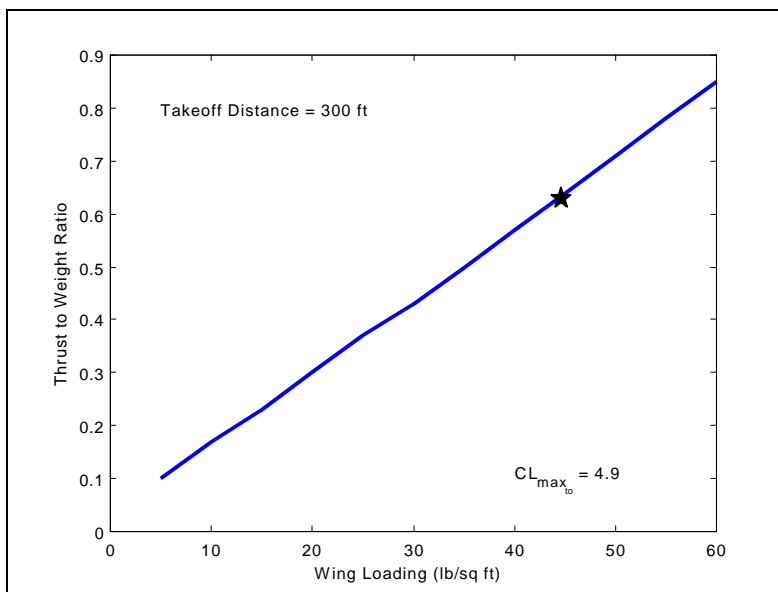


Figure 7: Preliminary Estimate of Takeoff Performance for the Cardinal

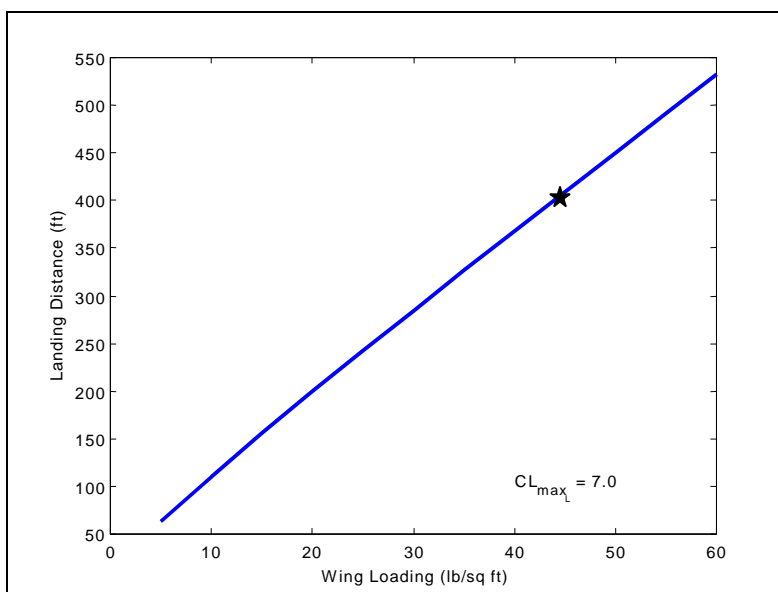


Figure 8: Preliminary Estimate of Landing Performance for the Cardinal

**Table 4: Summary of Performance Sizing for Fixed-Wing**

PARAMETER	VALUE
Wing Loading	47 lb/ft <sup>2</sup>
Thrust-to-Weight Ratio	0.6
Wing Area	1,000 ft <sup>2</sup>
Installed Thrust	30,000 lb

The goal of the tilt-wing analysis was to find values for wing loading and power loading which satisfied both the takeoff and landing ground roll constraints. Using ‘rule-of-thumb’ design guidelines for tilt-wing design and NASA windtunnel test data, stable conversion profiles and takeoff/landing speeds were estimated for a tilt-wing configuration. The speeds were then used in the same performance sizing used for the fixed-wing configuration. Table 5 summarizes the sizing for the tilt-wing configuration.

**Table 5: Summary of Performance Sizing for Tilt-Wing**

PARAMETER	VALUE
Wing Loading	86 lb/ft <sup>2</sup>
Power Loading	5.7 lb/hp
Wing Area	700 ft <sup>2</sup>
Installed Power	10,500 hp

#### **4. CONFIGURATION SELECTION AND COMPONENT DESIGN**

The performance constraints on the aircraft as well as structural and aerodynamic considerations dominated selection of the final configuration. The driving parameter in layout of the fuselage was the size of the cargo and cargo containers. The resulting space available in the passenger configuration makes for a more generous seating layout than available in most existing aircraft. Cockpit layout and accommodations for crew were designed to meet both the required FAR and MIL specifications.

The requirement for structural continuity in the fuselage dictated the placement of the wing. A low-wing design would not allow for structural support of the tail in an efficient manner, thus a high-wing was chosen. The wingspan in both designs exceeded the spot area requirement of 29 feet (the fixed-wing had a 64 foot wingspan, while the tilt-wing had a 48 foot wingspan). This violation of the spot area requirement was remedied by including complicated folding and pivoting systems to allow the stowed aircraft to fit within the spot area requirements. The chosen high lift system was upper surface blowing, similar to the system used on the Boeing YC-14.<sup>63</sup>

The empennage design involves an H-tail consisting of a horizontal tail resting on the upper surface of the fuselage with two vertical tail endplates. Endplates were chosen to allow large vertical tail areas required for OEI operation without violating the height constraint of the folded aircraft.

The nose gear consists of a single strut design in which the tires retract to a position forward of the attachment point. This design facilitates extension of the gear after hydraulic power failure without the need for backup actuators. The main gear configuration was based on the retraction mechanisms of similar cargo aircraft (i.e. the C-130, C-141, and the C-5).<sup>18</sup> The main gear is contained in blister fairings on the side of the fuselage.

##### **4.1 FUSELAGE**

The overall length of the fuselage was 60 feet and the maximum height and width were 9.5 feet and 13 feet respectively. The forward-most section was 13 feet and consisted of the cockpit and crew area along with the lavatory and main entrance to the aircraft. The cargo bay is immediately aft of the main entrance and is 27 feet in total length. Aft of the cargo bay are the empennage section and the cargo bay door. The entire fuselage is pressurized in both modes of operation. The cargo bay area is easily convertible to passenger transport mode that includes the insertion of seats, baggage stowage, and a galley system.

#### **4.1.1 COCKPIT LAYOUT**

The cockpit was laid out for a two-crewmember configuration. The seating and window layouts were arranged to meet all applicable FAR and MIL specifications on visibility and component travel for use by a wide variety of crewmember sizes. The Cardinal design meets the requirements for cockpit visibility angles.<sup>48</sup>

The center panel of both sides of the cockpit consists of the primary flight display, navigation display, and a full set of electronic flight instruments. A center-mounted autopilot and autothrottle panel is located atop the instrument panel. Beneath the autopilot and autothrottle are the warning display and the system display. The console between the captain and the flight officer consists of a warning display for each crewmember along with the power quadrant and the aircraft central computer for system monitoring.

#### **4.1.2 CARGO HOLD**

The cargo hold was laid out by considering the military application cargo. Several initial layouts of the cargo were considered, but the geometric constraints on the size of the aircraft limited the size of the cargo bay and the arrangement of the cargo. The resulting layout (Figure 9) was a two-by-two arrangement of two containers forward, each side-by side, and two containers aft, also side-by-side. This configuration results in a well-balanced and space efficient cargo bay. Note that due to the large size of the cargo bay, ample amounts of other cargo may be transported when not in use for engine transport.

Considerations for loading and unloading the cargo bay have been considered. A 6" clearance has been provided between the cargo wall and the cargo at all locations, and ample vertical clearance has been included to allow ceiling clearances during loading and unloading. Methods for cargo tie-down are included on the cargo bay floor throughout the cargo hold.

#### **4.1.3 PASSENGER CABIN**

The passenger cabin (Figure 9) consists of accommodations for 24 passengers. The seating arrangement is single aisle, with two seats on each side of the aisle, resulting in 12 rows of seats. The seat pitch is 32 inches and the seat width is 19 inches. In the passenger version of the aircraft, windows have been installed in the fuselage for passenger comfort.

The passenger cabin is closed off from the aft section of the airplane to allow for baggage and cargo storage. Overhead storage bins for carry-on luggage have been included. The forward-most section of the fuselage includes a wardrobe for hanging clothes and jackets and a galley for meal and drink service.

## CARDINAL CARGO BAY AND PASSENGER CABIN LAYOUT

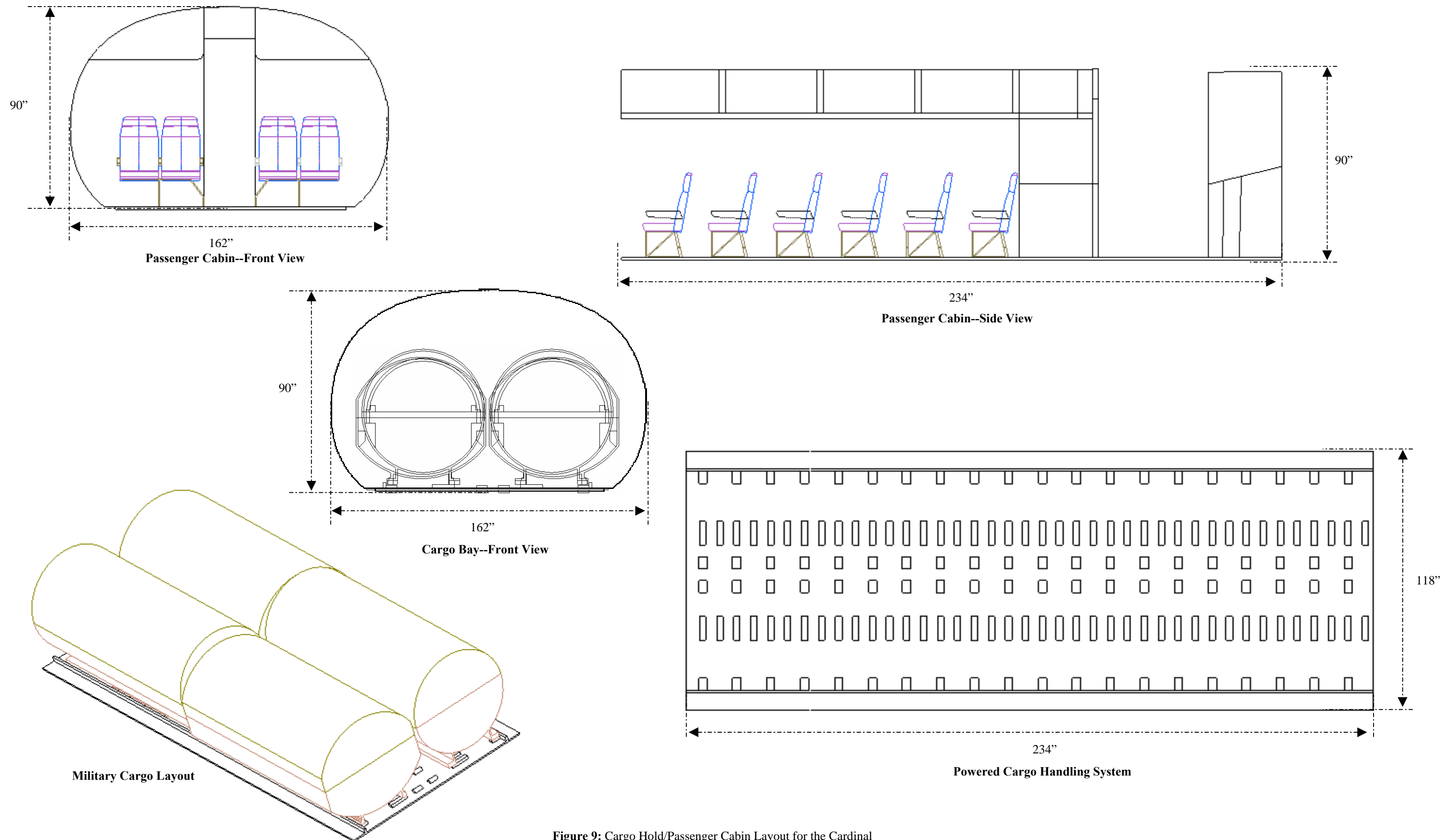


Figure 9: Cargo Hold/Passenger Cabin Layout for the Cardinal

## **4.2 WING**

The wing designs for both the fixed-wing and tilt-wing configurations were severely restricted by geometric constraints. The RFP specified a 29 ft by 60 ft storage requirement for the military version of the aircraft.<sup>2</sup> U.S. Navy geometric constraints include a desire for a maximum wingspan of 64 ft, a storage height requirement of 18.5 ft, and, if wing folding is used, a maximum height of 24.5 ft while folding.<sup>43</sup> This section describes the preliminary design and analysis process for the clean wing layout and high lift design.

### **4.2.1 CLEAN WING DESIGN**

The performance constraint analysis described in section 3.2 provided an initial value for the wing reference area. The configuration selection (described in section 4) of both aircraft necessitated a high wing design. The high wing design was desirable for the tilt-wing because a tilting wing would be very difficult to place in a low- or mid- configuration without interfering with the passenger cabin or cargo hold. The high wing design for the fixed-wing stemmed mainly from the structural considerations for the aft fuselage and cargo door, described in section 4.1.

Due to the relatively large wing areas and restrictions on wingspan, both the tilt-wing and fixed-wing designs had low aspect ratios. Low aspect ratios increase the size of the chord relative to the wing span--thus a high taper ratio was used to keep the root chord length reasonable. The calculation of the wing span considered all geometric constraints imposed by the RFP<sup>2</sup> and Navy specifications,<sup>43</sup> as well as techniques for wing folding and pivoting.<sup>42</sup> These calculations were incorporated into a Matlab code (available on the Cardinal web site<sup>1</sup>) for use in the optimization routine described in section 12.

The fixed-wing configuration utilized both pivoting and wing folding to comply with the geometric constraints. Due to the rotation of the wing, the wing tips had to be folded upward to avoid interference with the fuselage. Using this storage method permitted the Navy's maximum desirable wingspan of 64 ft while still meeting all geometric constraints. The tilt-wing configuration also utilized wing pivoting and folding devices. Figure 10 (dimensions are in inches) displays the wing pivoting and folding concept for the final Cardinal design.

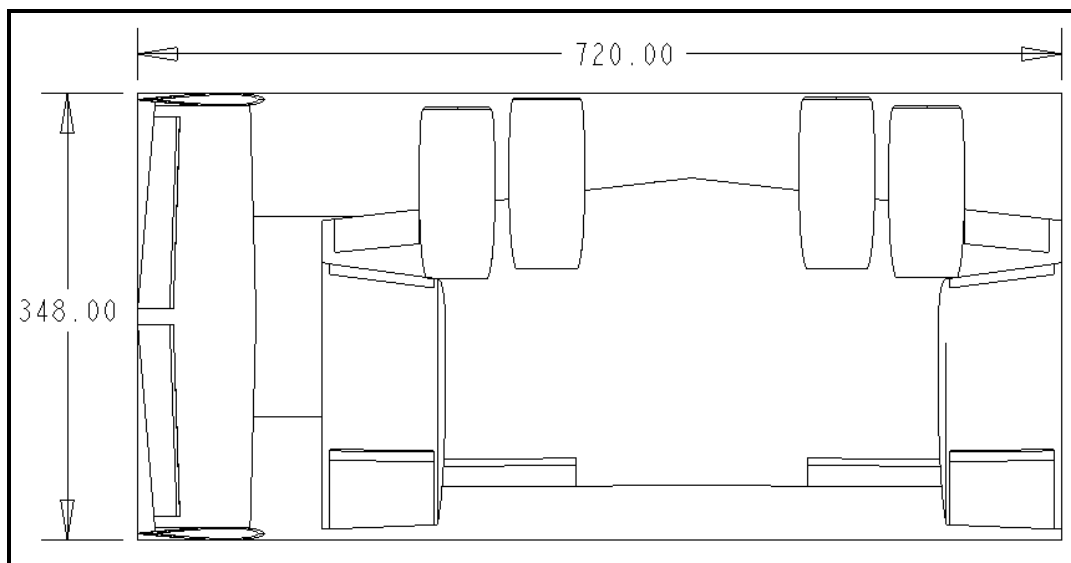


Figure 10: Wing Pivoting and Folding for the Cardinal

The average thickness-to-chord ratio for the wing was selected to avoid compressibility drag at the design lift coefficient and cruise Mach number.<sup>28</sup> Airfoil selection was based on the desired thickness-to-chord ratio, the design cruise lift coefficient, and the desire to operate within the airfoil drag “bucket.” The drag bucket is a range of lift coefficients over which the drag coefficient is a minimum. The NACA 63<sub>2</sub>-214 airfoil<sup>3</sup> best met all of the requirements. Though the exact airfoil was not available, the airfoil minimum drag coefficient was scaled<sup>3</sup> from the NACA 63<sub>2</sub>-215. To maintain a level cabin floor at cruise, the necessary incidence angle was computed to be 1°. The twist angle distribution was selected to maximize the span efficiency factor and avoid tip stall. Figure 11 contains the corresponding lift distribution.

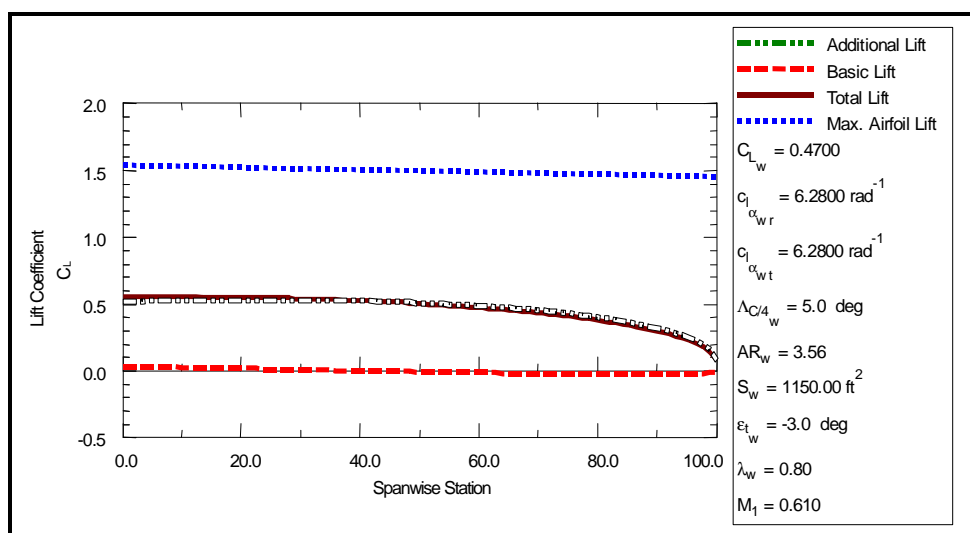


Figure 11: Spanwise Lift Distribution for the Cardinal

All relevant wing geometry for both the fixed-wing and tilt-wing configurations was calculated based on the wing area and the relevant wingspan constraints. The fuel volume of the integral wing tanks was computed in the CAD model to be 360 ft<sup>3</sup> which corresponds to approximately 17,505 lb of fuel. The maximum fuel (including reserves) needed for the Cardinal to meet the design mission range is 14,483 lbs; hence, no fuselage or empennage tanks were necessary. Table 6 summarizes the relevant wing geometry for the final version of the Cardinal.

**Table 6: Wing Geometry for the Cardinal**

WING GEOMETRY PARAMETERS	FIXED-WING
Wing Area, $S_{ref}$	1150 ft <sup>2</sup>
Span, $b$	64 ft
Aspect Ratio, $AR$	3.56
Taper Ratio, $\lambda$	0.8
Quarter Chord Sweep, $\Lambda_{c/4}$	5°
Root Chord, $c_{root}$	19.97 ft
Tip Chord, $c_{tip}$	15.97 ft
Mean Aerodynamic Chord, $MAC$	18.04 ft
Average thickness to chord ratio, $(t/c)_{avg}$	14 %
Dihedral, $\Gamma$	0°
Incidence Angle, $i_w$	1°
Twist Angle, $\epsilon_t$	-3°
Fuel Volume	17,505 lb

#### 4.2.2 HIGH LIFT AND POWERED LIFT DESIGN

Two different approaches to achieving low takeoff and landing speeds and the associated short takeoff and landing distances were considered for the Cardinal design: (a) Upper Surface Blowing (USB) flaps, and (b) a tilt-wing configuration. In this section, a review of the principles, methodology for analysis, and a risk assessment for using these technologies is presented. All calculations were incorporated into a code (available on the Cardinal web site<sup>1</sup>) for use in the optimization routine described in section 12.

There are many ways to achieve high lift coefficients using methods such as: upper surface blowing (USB), leading edge blowing, jet flaps, and circulation control wings (CCW). Leading edge blowing, jet flaps, and circulation control wings require significant amounts of bleed air from the engine which reduces propulsive efficiency and sometimes leads to the need for dedicated engines simply to provide sufficient mass flow for the high lift system. Ducts, valves, and associated controls are also required to transport and distribute the bleed air from the engines to its desired location in the leading and trailing edges.

The concept of USB is illustrated in Figure 12. By placing the engines in a way that the exhaust is directed over the upper surface of the wing, the system provides boundary layer control (BLC) for the aft part of the wing which is prone to separation. The flaps also deflect the engine exhaust, providing a vectored thrust component. A review of past aircraft designs utilizing upper surface blowing, such as the Boeing YC-14<sup>63</sup> and the NASA Quiet, Short-Haul Research Aircraft (QSRA)<sup>5,19</sup> described in section 2.1, indicate that ‘equivalent’ lift coefficients of 8 to 12 are possible. This equivalent lift coefficient consists of three parts: the lift coefficient of the wing itself, an increase in wing lift coefficient due to ‘super’ circulation, and the vertical component of thrust due to the jet deflection.<sup>35</sup>

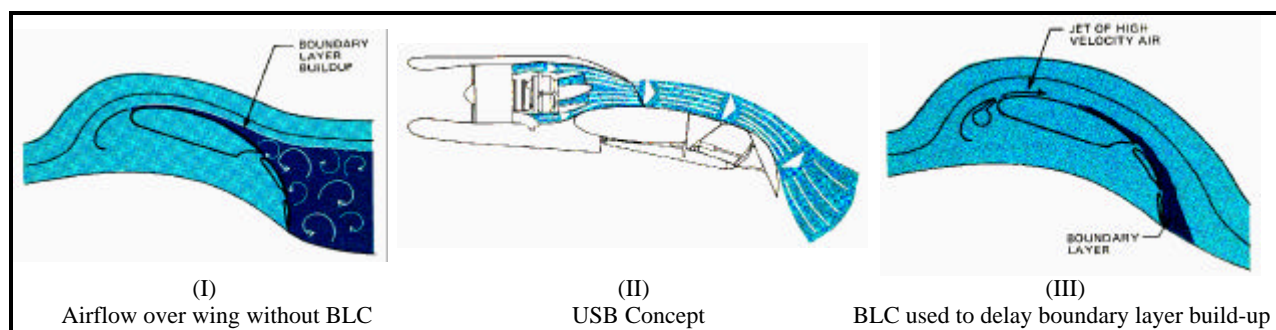
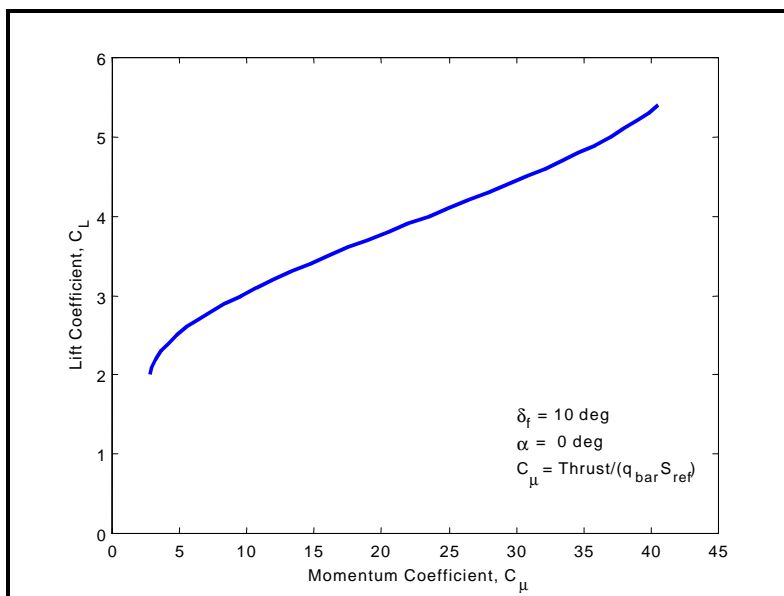


Figure 12: Upper Surface Blowing (USB)<sup>6</sup>

The major difficulty in a USB design is analyzing the magnitude of lift coefficients achievable. For the Cardinal design, the high lift system was analyzed using the method presented in Aerodynamics of V/STOL Flight by McCormick.<sup>35</sup> This method uses a combination of theoretical calculations and correlation to experimental results to estimate the lift coefficient for a given angle of attack, flap deflection, and power setting. This methodology was incorporated into a Matlab code, available on the Cardinal web site,<sup>1</sup> for use in the optimization described in section 12. Figure 13 shows an example of a calculation for the Cardinal in the takeoff configuration. It should be noted that it is difficult to define a maximum lift coefficient, as the lift coefficient varies not only with flap deflection and angle of attack, but also with the momentum coefficient.



**Figure 13: Lift Coefficient Variation with Power Setting for the Cardinal**

To validate the calculations for the blown flaps, the results were compared to data from the QSRA. Flight test data from the QSRA (available in References 16, 17, 44, and 45) were used to compare the lift coefficients achieved by the QSRA and those computed for the Cardinal. Maximum lift coefficients for the Cardinal were 4-5 in the takeoff configuration and 10-12 in the landing configuration. The lift coefficients achieved by the QSRA and Cardinal for similar flight conditions were within approximately  $\pm 20\%$ .<sup>44</sup> The calculated lift coefficients for the Cardinal seem reasonable compared to those measured for the QSRA. For preliminary design the method used is acceptable, but as discussed in section 4.2.2.1, this is a critical technology for the Cardinal and more detailed calculations will certainly be needed before proceeding beyond preliminary design.

An alternate configuration considered for the Cardinal was a tilt-wing aircraft. The tilt-wing offers several advantages over a tilt-rotor, such as the Bell/Boeing V-22. Some of these advantages include less download<sup>15</sup> and better short takeoff performance.<sup>56</sup> While the hover characteristics of the tilt-rotor are superior to those of the tilt-wing, the mission requirements of the Cardinal do not require significant amounts of hover such as might be necessary for search and rescue. The short rather than vertical takeoff requirements of the Cardinal also pushed the design team towards a tilt-wing design.

The tilt-wing aircraft relies on a vertical component of thrust and some boundary layer control from the propeller/wing interaction to achieve its short or vertical takeoff and landing characteristics. Although no production aircraft have been built using a tilt-wing configuration, there have been several prototype aircraft

built and flight-tested. Some of these include the Change Vought XC-142A and the Canadair CL-84, described in section 2.1. In addition, there have been many windtunnel tests made on tilt-wing configurations.<sup>20,22</sup> Like USB, it is difficult to make a 'simple' analysis for a tilt-wing configuration. Many papers and reports have been written on this subject and offer rules of thumb and guidelines which greatly aided in the tilt-wing design analyzed for this proposal.<sup>38,56</sup>

For the Cardinal, the method of analysis was based on the method for propeller/wing interaction described by McCormick.<sup>35</sup> This method considers the airflow velocities seen by the wing as a combination of the velocity due to flight and that produced by the propeller, as shown in Figure 14. Aerodynamic calculations can then be conducted in the usual fashion, but using the local velocity and angle of attack of the wing. All computations were incorporated into an analysis code for the optimization described in section 12. A copy of the computational code is available on the Cardinal web site.<sup>1</sup>

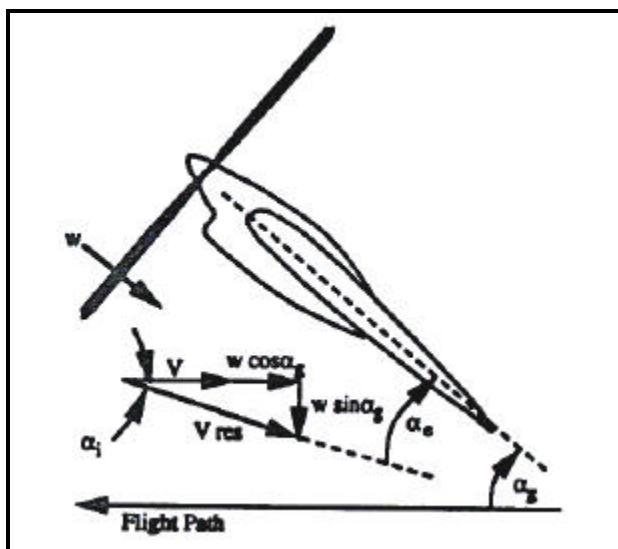


Figure 14: Tilt-wing Velocity Components<sup>56</sup>

Due to the unconventional nature of this analysis method, it was desirable to validate it with experimental or flight test results. Data from windtunnel tests<sup>20,22</sup> and flight tests<sup>8,10,39,59</sup> were compared to the computational results for the Cardinal. In general, the results showed all of the same trends. One discrepancy, however, was that the maximum allowable wing angle occurring before stall was consistently underpredicted in the computational results for the Cardinal. The consequences of this are discussed further in Section 4.2.2.1 where technology validation and risk for a tilt-wing are discussed.

#### 4.2.2.1 TECHNOLOGY VALIDATION AND RISK ASSESSMENT

The use of new and emerging technology to achieve better performance and lower costs must be weighed against the risks of using unproven technologies. In section 2 a summary of the design philosophy for the Cardinal was presented. The selection of a high- or powered-lift methodology is the highest risk aspect of the Cardinal design. Although there have been a significant number of tests of USB and tilt-wings, no production aircraft have implemented either of these technologies. Based on the Technology Readiness Levels (TRLs) presented in section 2.2.1, both USB and the tilt-wing configuration are a Level 7 technology. This means that an engineering model has been flight tested, but has not been "flight-qualified" or "flight-proven" in everyday operations.

#### 4.3 EMPENNAGE

The geometric constraints of the RFP require the aircraft be stored in a 60 foot by 29 foot box,<sup>2</sup> while U.S. Navy height constraints restrict the height of the aircraft to 18.5 ft stored and 24.5 feet while folding.<sup>43</sup> These requirements had to be considered when sizing the empennage surfaces. No folding of the vertical tails was required to accommodate the wing while pivoted for storage (see Figure 10).

Preliminary tail sizes were initially estimated using the volume coefficient method.<sup>28</sup> The volume coefficient sizing method relies on the fact that similar aircraft tend to have similar volume coefficients. However, the unconventional design of the Cardinal (large wing chords and relatively low wingspan) made it difficult to obtain reasonable results from this method. Instead of volume coefficients, the horizontal tail sizing used a longitudinal X-plot or scissors plot.<sup>28</sup> An X-plot shows how the static margin varies with the position and size of the horizontal tail.

The U.S. Navy carrier height requirement coupled with the required upsweep angle required for takeoff rotation constrained the span of the vertical tail. The vertical tail area was sized to meet One Engine Inoperative (OEI) minimum control speed requirements. A balancing moment due to the asymmetric thrust and the windmilling drag of the inoperative engine must be generated at 1.2 times the landing stall speed without stalling the vertical tail. Due to the large vertical tail reference area and the height constraint, twin vertical tails placed as end plates on the horizontal tail were used.

A more complete discussion of the Cardinal compliance with stability and control requirements may be found in section 9. Table 7 summarizes the relevant horizontal and vertical tail geometry parameters.

**Table 7: Empennage Geometry Parameters**

Parameter	Horizontal Tail	Vertical Tails
Reference Area, $S_{ref}$	190 ft <sup>2</sup>	208 ft <sup>2</sup>
Span, $b$	29 ft	14 ft
Aspect Ratio, $AR$	4.43	1.88
Taper Ratio, $\lambda$	0.8	0.8
Quarter Chord Sweep, $\Lambda_{c/4}$	5°	5°
Root Chord, $c_{root}$	7.28 ft	8.25 ft
Tip Chord, $c_{tip}$	5.82 ft	6.60 ft
Mean Aerodynamic Chord, $MAC$	6.58 ft	7.46 ft
Average thickness to chord ratio, $(t/c)_{avg}$	12 %	10 %
Dihedral, $\Gamma$	0°	N/A
Volume Coefficient, $V_{h/v}$	0.2068	0.0617

#### 4.4 CONTROL SURFACES

Control surfaces were initially sized using statistical methods<sup>81</sup> based on similar aircraft. Trim requirements and FAR 25 / MIL-F-8785C specifications were then used to verify that the control surfaces provided acceptable levels of control power (see section 9 for the complete stability and control analysis). Data from the C-141B and YC-14 aircraft<sup>63</sup> were averaged to size the control surface ratios for the ailerons, rudder, spoilers and elevators. Control surfaces were sized to be 30% of the chord so that they could easily be attached to the rear spar located at 70% chord. The maximum throw angle of all control surfaces was limited to  $\pm 25^\circ$  to prevent flow separation at full deflection. Table 8 summarizes the control surface geometry for the Cardinal.

**Table 8: Control Surfaces for the Cardinal**

CONTROL SURFACE	PERCENTAGE CHORD (%)	INBOARD LOCATION (FT)	OUTBOARD LOCATION (FT)
Rudder	30	1.36	6.48
Aileron	30	24.54	31.42
Elevator	30	0.48	20.32
Flaps	30	7.43	23.11
Spoilers	20	15.75	23.11

#### 4.5 LANDING GEAR

The following section describes the methods used to determine the most important aspects of the landing gear design. Gear location criteria, strut loads, tire selection, and shock design are among the topics covered. All calculations were incorporated into a landing gear code (available from the Cardinal web site<sup>1</sup>) for use in the optimization routine described in section 12. The data for the final design is shown below.

#### 4.5.1 LOCATION CRITERIA

To allow the aircraft to take off and land without problems, the longitudinal location of the main landing gear is driven by aerodynamic requirements. The Cardinal's upsweep clearance angle was designed to comply with the pitch angle necessary for takeoff and landing. Furthermore, the tip-over angle<sup>18</sup> between the aft limit for the center of gravity and the bottom of the main tires should be greater than the upsweep clearance angle to prevent the center of gravity of the aircraft from traveling aft of the main gear pivot point during takeoff rotation. Figure 15 illustrates the upsweep clearance angle and longitudinal tip-over angles for the Cardinal.

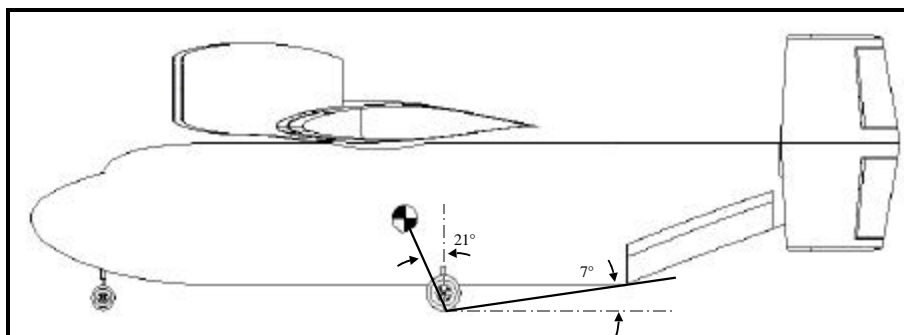


Figure 15: Longitudinal Tip-over and Clearance Angles

The nose gear must carry enough loads for the aircraft to be able to steer while maneuvering on the ground. Therefore, a load percentage for the nose gear of 8%-20% of the airplane weight is required, with values closer to 8% preferred.<sup>18</sup> The nose gear load percentage for the Cardinal was 9% for the military version and 15% for the commercial version. The landing gear could not interfere with the cargo space; therefore, it was decided to place the gear in blister fairings on the sides of the fuselage. Furthermore, the turnover angle should be less than  $54^\circ$  for aircraft-carrier-based vehicles, and less than  $63^\circ$  for land-based vehicles.<sup>18</sup>

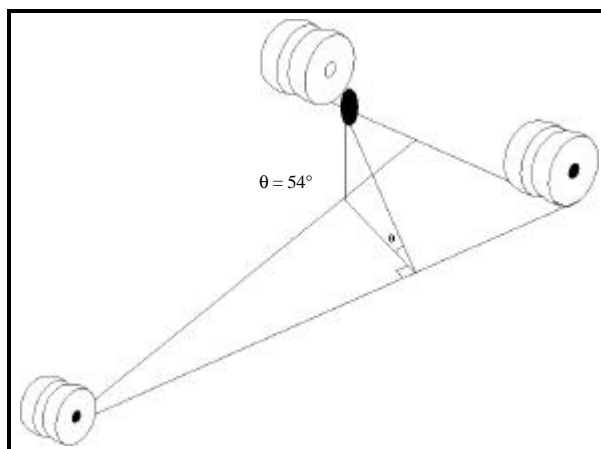


Figure 16: Lateral Turnover Angle

The vertical position was determined by the geometric constraints outlined in the RFP.<sup>2</sup> Therefore, a maximum distance of 2 feet was allowed between the ground and the bottom of the fuselage. This affected the upsweep angle, and was taken into account when considering the longitudinal position. To meet the turnover angle requirement, the clearance between the fuselage and the ground must be reduced by one foot. The Cardinal achieved this clearance with the implementation of kneeling landing gear. Table 9 presents a summary of the design angles for the Cardinal.

**Table 9: Landing Gear Tip-over and Longitudinal Clearance Angles**

CARDINAL VERSION	TIP-OVER ANGLE (DEGREES)	TURNOVER (DEGREES)	UPSWEPT CLEARANCE (DEGREES)
Military	10.7	53.7	9.9
Commercial	18.0	56.7	9.9

#### 4.5.2 TIRE SELECTION

The number of tires per strut was determined according to loads estimated for each strut. Two tires per strut sufficiently met the loading requirements. Data for similar aircraft supported this design decision.<sup>18</sup> The type of tire to be used is based on load and speed ratings, size, and weight. A safety margin of 7% was used on the strut loads for choosing the tires.

**Table 10: Main Gear Tire Types<sup>18</sup>**

TYPE	MAXIMUM LOAD (LBS)	PRESSURE (PSI)	SPEED (MPH)	DIAMETER (INCHES)	WIDTH (INCHES)	WEIGHT (LBS)
VII	12,950	320	225	30.12	6.50	38.0
VII <sup>+</sup>	13,000	300	275	25.50	6.85	35.5
VII	13,800	230	200	28.40	7.85	41.5
VIII	12,700	235	275	26.00	8.00	38.0
ND	15,500	155	200	34.00	9.25	55.5

<sup>+</sup> Tire used on the Cardinal

**Table 11: Nose Gear Tire Types<sup>18</sup>**

TYPE	MAXIMUM LOAD (LBS)	PRESSURE (PSI)	SPEED (MPH)	DIAMETER (INCHES)	WIDTH (INCHES)	WEIGHT (LBS)
VII	7725	275	200	20.00	4.45	14.5
VII	9300	215	275	17.90	5.70	14.6
VII <sup>+</sup>	9300	215	230	17.80	5.60	13.7
VII	7950	120	200	25.75	6.65	27.2

<sup>+</sup> Tire used on the Cardinal

#### 4.5.3 SHOCK DESIGN

Based on a review of similar aircraft an oleo-pneumatic shock was selected. These shocks absorb energy by compression of a chamber of oil against a chamber of dry air. The stroke lengths for the main and nose gear were computed using an energy conservation method.<sup>18</sup> A margin of 1 inch was added to the calculated strokes. The dual use nature of the Cardinal requires aircraft carrier based operations. Therefore, in compliance with aircraft carrier requirements, the sink speeds used were 10 ft/sec for the nose gear and 15 ft/sec for the main gear.<sup>18</sup> The resulting strokes for the nose and main struts were 6 and 16 inches, respectively.

The strut area was determined by assuming a shock pressure of 1500 psi when the strut is compressed. The diameter was computed using this value. To determine the length of the strut, a minimum permissible overlap of 2.75 times the shock diameter was added to the stroke length. For each strut the resulting length was determined as a sum of overlap plus stroke length plus margin.

**Table 12: Strut Dimensions for the Landing Gear**

GEAR COMPONENT	STROKE (INCHES)	STRUT DIAMETER (INCHES)	STRUT LENGTH (INCHES)
Main	16	4.3	27.7
Nose	6	2.5	12.7

#### 4.5.4 RETRACTION MECHANISM

The retraction mechanism was designed to be as space-saving as possible to minimize the size of the blister fairings which enclose the main gear. The positions of the extended and retracted gear are shown in Figure 17.

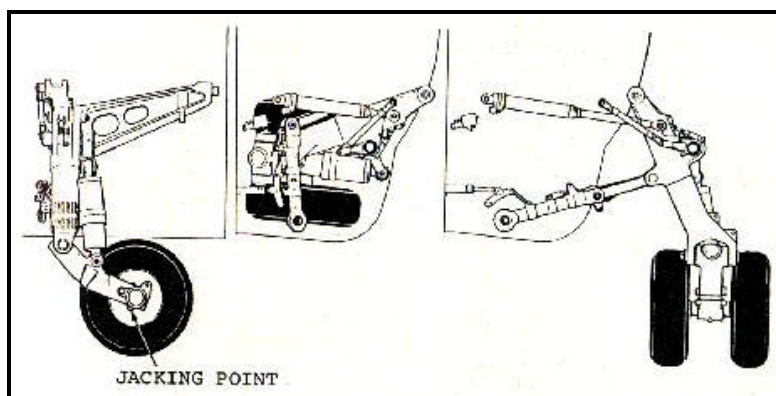


**Figure 17: Retraction Mechanism for the Main Landing Gear<sup>18</sup>**

## **5. PROPULSION SELECTION & INSTALLATION**

The following sections describe the methods used for propulsion selection, the engine scaling methodology, and installation losses. All calculations were incorporated into a Matlab code (available on the Cardinal web site<sup>1</sup>) for use in the optimization routine described in section 12.

### **5.1 ENGINE SELECTION**

Propulsion systems were selected for two configurations: the tilt-wing with four turboprop engines, and the fixed-wing with four turbofan engines. The tilt-wing design uses turboprop engines and the fixed-wing design uses turbofan engines. Preliminary engine size was based on the results from the performance sizing described in section 3. Because complete performance information is often proprietary and not publicly available, there were a limited number of engines for which data was available.

#### **5.1.1 TILT-WING TURBOPROP CONFIGURATION**

For the tilt-wing design, the engine described in “1989 AIAA/United Technologies-Pratt & Whitney Engine and Propeller Data Package”<sup>4</sup> was selected. The engine was chosen mainly because its specifications and available data met the design specifications and were publicly available. Four turboprop engines geared to two propellers comprise the propulsion installation for the tilt-wing. This configuration eliminates the need for cross-shafting between the engines for engine out control in a two-engine configuration.

The geometric constraints limit the span of the wing so it must be folded or pivoted. Folding alone did not work for the four-engine configuration because the engines could not fit on the unfolded section of the wing. Instead, the more costly and heavier pivoting wing and wing folding were necessary for the four-engine configuration. The pivoting wing allows the wing span to be nearly the fuselage length, and thus there was enough space to arrange all four engines.

#### **5.1.2 FIXED-WING TURBOFAN CONFIGURATION**

Two-engine configurations have the advantage of requiring fewer maintenance hours and slightly higher efficiency compared to the smaller engines that would be used in a four-engine configuration. However, the FAR minimum climb gradients for engine out would require severe oversizing of the engines for the Cardinal. Also, the USB flaps depend on engine flow and cross-shafting of the engines (as done in the YC-14<sup>63</sup>) would be

necessary if there was only a single engine on each wing. This would make the engines ‘custom’ built and relatively expensive.

The ALF502 turbofan engine (Figure 18) was selected as representative of a high bypass-ratio turbofan engine for the four-engine fixed-wing configuration. The ALF502 was chosen primarily because it has similar thrust and complete performance data was available.<sup>31</sup> The data allowed for a complete analysis and scaling of the engine thrust and specific fuel consumption data, which was required to perform the optimization described in section 12.

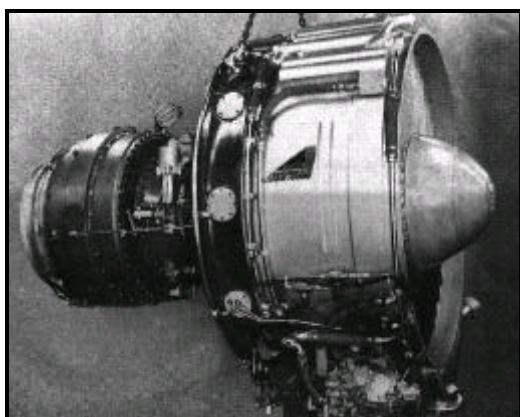


**Figure 18: Avco Lycoming ALF 502 Turboprop Engine<sup>61</sup>**

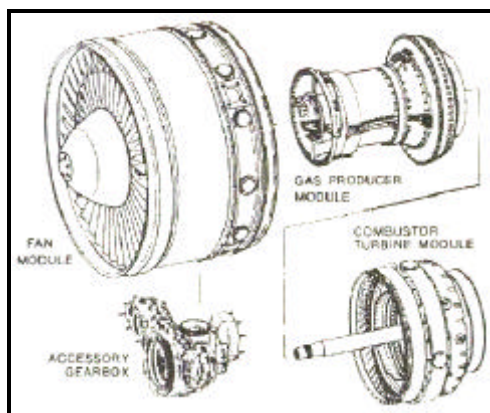


**Figure 19: Turboprop Engine Schematic Drawing<sup>48</sup>**

## 5.2 ENGINE LOCATIONS

The engines for the fixed-wing design were placed far forward of the wing (see Figure 20) for upper surface blowing over the wing. For the tilt-wing design, the engines were placed slightly forward of the wing to maximize the propeller slipstream effect on the wing and provide proper spacing between the propeller and the wing.

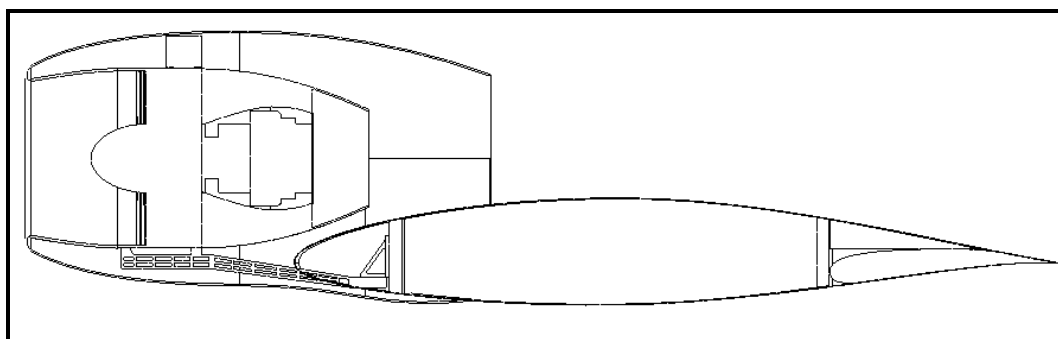


**Figure 20: Fixed-Wing Installation Drawing**

Since both the tilt-wing and fixed-wing include the pivoting wing device, the location of the engine along the wingspan was not highly constrained. The engines for the fixed-wing were placed inboard to satisfy OEI requirements and to provide upper surface blowing of the inboard flaps.

Foreign Object Damage (FOD) requirements<sup>49</sup> were reviewed to verify that the engines on the Cardinal were placed in such a way that the likelihood of FOD is minimized. In both the fixed-wing and the tilt-wing the engines were located ahead of the main gear so no objects could be thrown by the main gear and damage the engine or propellers. However, the nose gear could pose a problem because it is mounted forward of the engines. The relatively wide fuselage should deflect debris away from the engines and chined tires or a splash guard should not be necessary.

### **5.3 ENGINE PERFORMANCE CHARACTERISTICS**

Engine performance data is provided by the manufacturer for a range of altitudes and speeds or Mach numbers. The data is normally 'uninstalled' data and must be corrected for losses from installing them on the aircraft. A summary of the performance data for the engines used, a scaling methodology for altering the thrust or power of an engine for which performance data is available, and a method for estimating installation losses is presented. All calculations were incorporated into a Matlab code (available on the Cardinal web site<sup>1</sup>) for use in the optimization routine described in section 12.

#### **5.3.1 PERFORMANCE DATA**

All data used for turboprop calculations was obtained from Reference 4. This included values for power and fuel flow at varying altitudes and speeds for several flight conditions. The engine was scaled to meet the desired uninstalled thrust requirements. Installation losses were then calculated as described in section 5.4. Data was provided for take-off, maximum cruise, and several intermediate cruise settings. Where necessary the data was interpolated settings.

Data for the turbofan included graphs and charts relating the engine performance, thrust and fuel flow to altitude and Mach number for many flight conditions.<sup>31</sup> Seven cruise conditions were given in the data package. Interpolation between cruise settings was done where necessary.

##### **5.3.1.1 TURBOPROP PERFORMANCE**

To prevent wing stall of the tilt-wing design, the entire wing span must be immersed in the propeller slipstream. Preliminary sizing was done using guidelines for typical ratios of wing chord to blade diameter.<sup>38,56</sup>

In the optimization code the requirement for stable descent meant that the optimizer was free to alter the chord to diameter ratio as long as the resulting configuration had a stable descent configuration. To provide a minimum one foot clearance between the ground and propeller blade, the tilt-wing was found to require a minimum  $15^\circ$  wing angle during takeoff and landing.

### **5.3.2 ENGINE SCALING**

The optimization routine used for the Cardinal and described in section 12 required varying the thrust/power. Because data for only one engine was available, a scaling methodology was applied to the baseline engine data.<sup>28</sup> An engine scaling factor, ESF, was used to scale the baseline engine (i.e. dimensions, thrust, fuel flow) to create new performance data for a scaled engine with the same technology level.

In addition to scaling at constant technology level, a technology scaling factor was applied. The RFP<sup>2</sup> allows for a technology availability date of 2005. The maximum cruise specific fuel consumption (sfc) of the baseline engine was compared to the maximum efficiency of modern high bypass engines at transonic cruise which have maximum efficiencies between 34% - 38%.<sup>28</sup> The baseline engine data was scaled to account for the actual sfc of the baseline engine and the predicted sfc of engines predicted to be available in 2005.

## **5.4 INSTALLATION LOSSES**

Installation losses were computed to correct the uninstalled engine data available from the manufacturer to the performance of the engine installed on the aircraft. The air induction system of the installed engine changed both the pressure recovery and drag, which in turn affected engine performance. The manufacturer tests are made using a bell-mouth inlet system to determine engine characteristic data. These values could vary from the installed values because of a difference in the induction system. Power extraction is necessary to run essential airplane services, such as lights, also changed the engine performance. This factor was normally included in the manufacturer's data. A third important consideration of losses was from a difference between the exhaust nozzle used for manufacturer testing and that used on the installed engine.

To calculate the installation losses, a turboprop performance method and a turbofan performance method were used.<sup>51</sup> The inlet efficiency, accounting for inlet pressure losses for both the turboprop and the fixed-wing engines, was assumed to be 99%. The remnant thrust for the turboprop in cruise was neglected.

Power extraction was divided into three categories of losses: electrical, mechanical, and pneumatic. The electrical and mechanical losses were assumed to be proportional to the takeoff weight for both the turboprop and fixed-wing engine configurations.<sup>51</sup> The pneumatic losses were assumed to be proportional to the engine mass flow. These loss relationships were then used to calculate the installed power from the uninstalled data. Exact values of power and fuel flow were then found for a specific flight condition by interpolating the scaled, installed engine data. Figure 21 contains the installed cruise carpet plot for the turbofan engines used on the final version of the Cardinal.

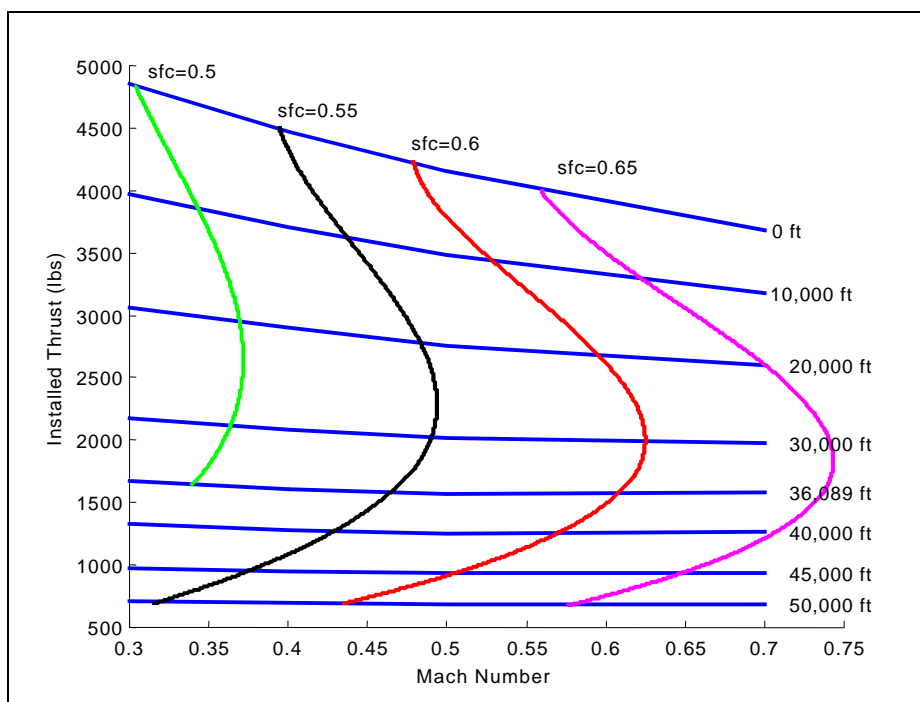


Figure 21: Maximum Cruise Carpet Plot for Cardinal Engines

## **6. STRUCTURAL LAYOUT AND SYSTEMS DESIGN**

The structural layout was based on structural configurations of existing cargo aircraft such as the C-130.<sup>48</sup> The layout consists of standard frames, longerons, ribs, and spars along with the specialized structural components for lifting surface integration and cargo floors and doors. Efforts to make use of advanced materials where useful and cost effective have been made. Systems design was based on standard systems layout of passenger and military aircraft with attention to applicable FAR and MIL specifications.<sup>52</sup>

### **6.1 MATERIALS SELECTION, STRUCTURAL DESIGN, AND LAYOUT**

Materials selection is based on strength-to-weight ratio, fatigue characteristics, dominant failure modes, familiarity and experience, cost, and existing manufacturing facilities for a given material. Aluminum and composites are the most common materials in transport aircraft similar to the Cardinal. Composites have the advantage of often being lighter in weight and easier to form into aerodynamic shapes. However, experience with composites is not always available, and poorly designed composite structures usually weigh more than conventional aluminum structures. Composites also have the disadvantage of being difficult to repair. Experience with aluminum structures is almost universal among aerospace companies and modern finite element models allow for very efficient structures. The cost of aluminum compared to composites is quite favorable to aluminum as well. Cargo aircraft often receive minor damage in the process of loading and unloading cargo, and repair of aluminum structures is well understood. Based on these characteristics, an aluminum structure was selected for the Cardinal. However, some components, such as aerodynamic fairings would be more easily manufactured using composites. To reduce the weight needed to balance the control surfaces, they will also be constructed of composites.

The structural arrangement of the Cardinal was based on typical structural spacing and example structural arrangements presented in Reference 48. The Cardinal wing structure is a conventional rib and spar arrangement. The wing spars are located at 25% and 70% of chord which allows the 30% chord flaps and ailerons to be attached directly to the rear spar. For the empennage surfaces, spars are located at 25% and 75% chord with 25% chord rudders and elevators attached to the rear spars. Rib spacing for the wing and empennage surfaces is 24 inches. The fuselage frame depth is 3 inches with a spacing of 24 inches. Fuselage longerons are spaced every 12 inches. The structural arrangement is shown in Figure 22.

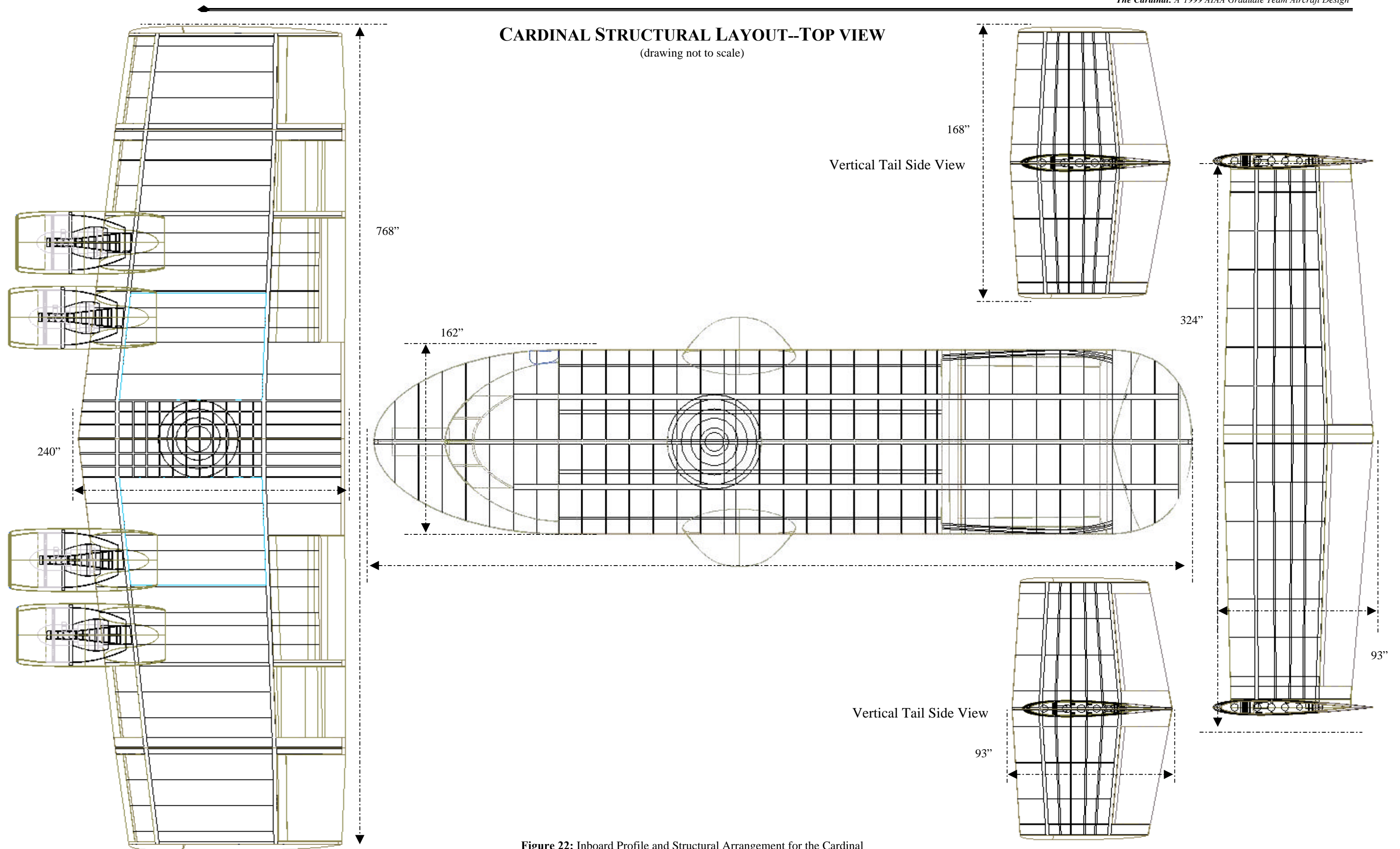


Figure 22: Inboard Profile and Structural Arrangement for the Cardinal

## **6.2 SYSTEMS DESIGN**

Both versions of the aircraft have the need for sophisticated on-board systems. Such systems include auxiliary power units (APUs), flight control systems, fuel systems, hydraulic systems for folding and doors, braking and anti-skid systems, electrical systems, and environmental control systems.

Auxiliary power units have been installed to supply the necessary airflow in the engines for engine startup. This allows engine startup to be independent of ground crew, allowing access to remote airfields.

The aircraft active control system consists of a control system computer along with electrohydraulic actuators. This system includes trim control and high lift-system for control for all modes of aircraft operation. Considerations for control feel and control system redundancy has been considered and will be included in the production design.

The fuel systems consists of fuel pressurization, engine feed, fuel transfer, refuel and defuel, venting systems, and fuel jettison systems. The fuel transfer system will be used for maintaining balance during flight and the jettison system has been included for fuel dumping in case of emergency.

The hydraulic system consists of a substantial number of hydraulic actuators along with two reservoirs and three hydraulic pumps for redundancy. The hydraulic fluid used will be MIL-H-83282, which is entirely synthetic and has reduced flammability compared with MIL-H-5606. Hydraulic fluid cooling and cleaning systems will also be included. Emergency power will be supplied to the hydraulic system using an accumulator system. Coupled with the hydraulic system, an electronically controlled automatic braking system that includes anti-skid has been included to aid in aircraft deceleration during short landing situations.

The aircraft electrical system contains both AC and DC components along with a battery storage system for ground operation. A ram air turbine has been included for emergency power that allows an ample power supply for aircraft operation. A switching computer allows for disconnection of the non-essential consumers during emergency or power conserving operations.

Environmental control systems, anti-icing and cabin pressurization systems are included. Pressurization will be accomplished using bleed air from the propulsion system. A full array of emergency systems including fire detection and suppression has also been included. Emergency oxygen and evacuation systems along with in-flight data recorders will come with all aircraft.

## 7. WEIGHTS AND BALANCE

The following section describes the method used to determine the weight and center of gravity locations for the Cardinal. Component weights were estimated by averaging the component weight estimates from several weight estimation methods. Estimates of component center of gravity locations were used to determine the airplane center of gravity and how it moves for various loading scenarios. This methodology was incorporated into a Matlab code (available on the Cardinal web site<sup>1</sup>) for use during optimization (see section 12).

### 7.1 V-N DIAGRAM

An estimate of the vehicle loads is the first step in the process of aircraft weight estimation. A speed - load factor (V-n) diagram represents the maximum load factor the airplane would be expected to experience as a function of speed. The maneuver diagram represents the maximum load factor the plane can achieve aerodynamically. Atmospheric disturbances also exert loads on the airframe. The magnitude of these loads is represented by the gust diagram. The limit load factor may be read from the plot as the maximum load factor experienced by the airplane and may occur on either the gust or the maneuver line. The ultimate load factor is then 1.5 times the limit load factor as determined from the V-n diagram. The V-n diagram, shown in Figure 23, for the Cardinal was constructed using the methods in References 50 and 28.

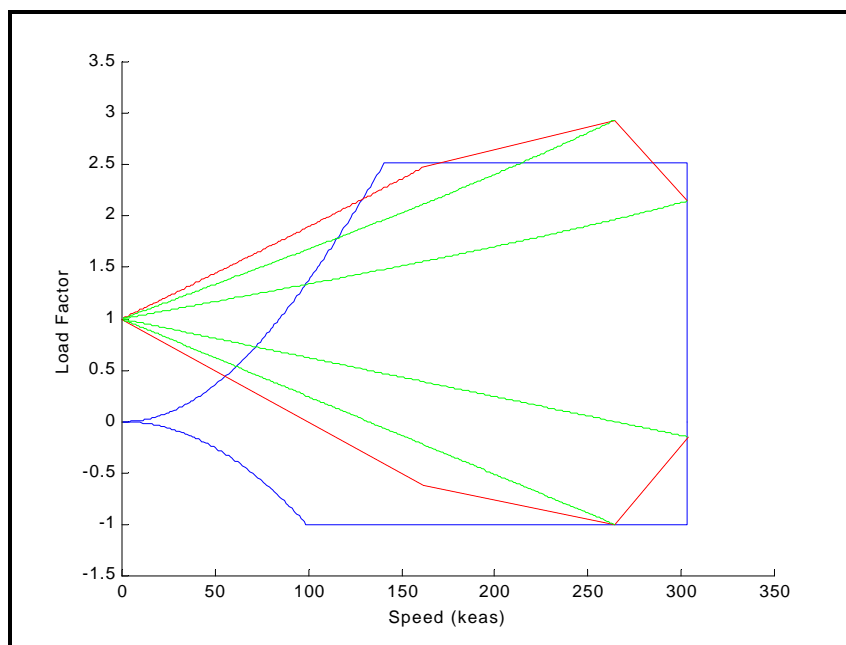


Figure 23: V-n Gust and Maneuver Diagram

## 7.2 COMPONENT & SYSTEM WEIGHT CALCULATIONS

The component weights for structural components and systems for the Cardinal were estimated using equations based on statistical correlation of existing aircraft. These relations included methods from the US Air Force (USAF), US Navy (USN), Torenbeek, and General Dynamics (GD) as discussed in References 50 and 62. Where multiple methods were available, the component or system weight computed by each method was used to compute an average weight. Many of the component weights are functions of the takeoff weight, therefore it was necessary to make an initial guess for the takeoff weight. After computation of the component weights using this initial guess, a takeoff weight can be calculated. If the calculated takeoff weight differs from the initial guess, the calculated takeoff weight is used to recompute the component weights. This process continues until the takeoff weight converges. Convergence usually takes 3-4 iterations. A Matlab code (available on the Cardinal web site<sup>1</sup>) was written to implement this weight estimation method for use in the optimization routine described in Section 12. This section presents a summary of the methods used for component weight estimation for the Cardinal.

### 7.2.1 STRUCTURE AND PROPULSION WEIGHTS<sup>42, 50</sup>

Methods from the USAF and Torenbeek were used to compute the basic wing weight. To account for the weight of wing folding mechanisms the basic wing weight was increased by 12%. For the weight of the wing pivoting mechanism, an additional 15% was added. The weight of the tilting mechanism for the tilt-wing design was estimated as 15% of the wing weight. The horizontal and vertical tail weights were determined by averaging the weight estimates from the USAF, Torenbeek, and GD methods. These methods accounted for the twin vertical tails and variable incidence stabilizer. Fuselage weight was estimated from the average of the weights computed using the USN, USAF, GD, and Torenbeek methods. These methods accounted for fuselage pressurization, the location of main gear attachments, and the weight of the cargo floor. Landing gear weights were estimated using the Torenbeek, GD, USAF, and USN methods. The landing gear weight includes struts and wheels, the retraction mechanism, and the steering system.

The propulsion weights were broken into three parts: (a) engines, (b) fuel systems, and (c) propulsion systems. Engine weights were computed from statistical correlations relating takeoff power or thrust to the dry weight of the engine. The number of blades, blade diameter, and power input determined the propeller weights. Fuel and propulsion system weights include the weight of the fuel tanks, fuel pumps, and the engine controls.

These system weights depended on the engine location, type of starting system, and the type of fuel tank. Nacelle weights were computed using the Torenbeek and GD methods.

### **7.2.2 FIXED EQUIPMENT**

Fixed equipment includes such things as flight controls, the hydraulic and electrical system, and furnishings. Like the structure and propulsion weights in Section 7.2.1, where multiple methods were available for weight estimation, the weight was computed as the average of the weights computed using the available methods.

The flight controls weight was estimated using the Torenbeek and GD methods. The weights of the hydraulic system, Auxiliary Power Unit (APU), and exterior paint were calculated as a percentage of the takeoff weight using percentages recommended in Airplane Design Part V by Roskam.<sup>50</sup> Component weight estimates for instrumentation, air conditioning, the electrical system, and the oxygen system were made by averaging the weights from the Torenbeek and GD methods.<sup>50</sup> The weight of furnishings was estimated using the Torenbeek and GD methods.<sup>50</sup> The military and commercial version have substantially different furnishing weights and separate calculations were made for each version. Baggage and cargo handling equipment weight was calculated as a function of the number of passengers.<sup>50</sup>

The last element considered in the weight calculations was the payload weight. The RFP specified the payload weights for the military and commercial versions of the Cardinal to be 10,000 and 4,920 lbs respectively.<sup>2</sup> Documentation for the engine shipping containers<sup>25</sup> indicates that the weight of the containers is approximately 5000 lbs which corresponds to a 15000 payload weight for the military version of the Cardinal. An attempt to clarify the design payload weight for the military version was made<sup>9</sup>, but lacking clarification the Cardinal was designed using the 10,000 lb payload specified in the RFP.<sup>2</sup>

The component center of gravity locations were placed using guidelines in References 28 and 50. Table 13 summarizes the component weight breakdown and component center of gravity locations for the final design of the military and commercial versions of the Cardinal.

**Table 13: Cardinal Component Weight Breakdown**

CARDINAL COMPONENT	COMPONENT WEIGHTS (LBS)		CENTER OF GRAVITY LOCATIONS		
	MILITARY VERSION	COMMERCIAL VERSION	X <sub>CG</sub> (FT)	Y <sub>CG</sub> (FT)	Z <sub>CG</sub> (FT)
Wing	3322	2966	32.44	0	12.9
Horizontal Tail	509	509	52.75	0	11.5
Vertical Tail	438	438	54.73	0	11.5
Fuselage	3457	3457	35	0	6.75
Nacelles	1125	1125	55.53	0	13.13
Nose Gear	274	274	5	0	1.5
Main Gear	1232	1232	35	0	1.5
Engines	4334	4334	30.33	0	13.13
Fuel System	676	676	38.51	0	12.9
Propulsion	374	374	30.33	0	13.13
Flight Controls	669	669	34.25	0	12.9
Hydraulic	501	501	37.52	0	12.55
Inst. & Avionics	853	853	5.2	0	8
A/C & Pressurization	1283	1283	13	0	8
Electrical System	1741	1741	33.83	0	8.35
Oxygen	65	65	30	0	8
APU	401	401	35	0	8
Furnishings	223	2056	35	0	6
Baggage Handling	26	26	35	0	6
Auxiliary	255	255	30	0	8
Paint	226	226	30	0	9
<b>EMPTY</b>	<b>22027</b>	<b>23460</b>	<b>32.61</b>	<b>0</b>	<b>10.03</b>
Trapped Fuel & Oil	251	251	32.44	0	12.9
Crew	400	600	5.85	0	6.75
Fuel	14483	13883	32.44	0	12.9
Payload	10000	4920	35	0	6.75
<b>TAKEOFF</b>	<b>46761</b>	<b>43114</b>	<b>31.03</b>	<b>0</b>	<b>10.2</b>

### 7.3 CENTER OF GRAVITY EXCURSION

The airplane center of gravity location (and how it moves as the plane is loaded and unloaded) affects landing gear placement, the ability of the aircraft to rotate during takeoff, and stability/control. The following configurations were analyzed to determine the range over which the center of gravity would be expected to vary: (a) full fuel with military payload, (b) full fuel with commercial payload, (c) no fuel with military cargo, and (d) no fuel with commercial cargo. Figure 24 illustrates center of gravity movement with respect to both the airplane Mean Aerodynamic Chord (MAC) and the main landing gear as fuel and cargo are loaded/unloaded. The center of gravity excursion was found to be approximately 5% of the wing MAC; the center of gravity never moves aft of the main gear. A verification of the Cardinal landing gear location criteria may be found in section 4.5.1. Stability and control issues are addressed in section 9.

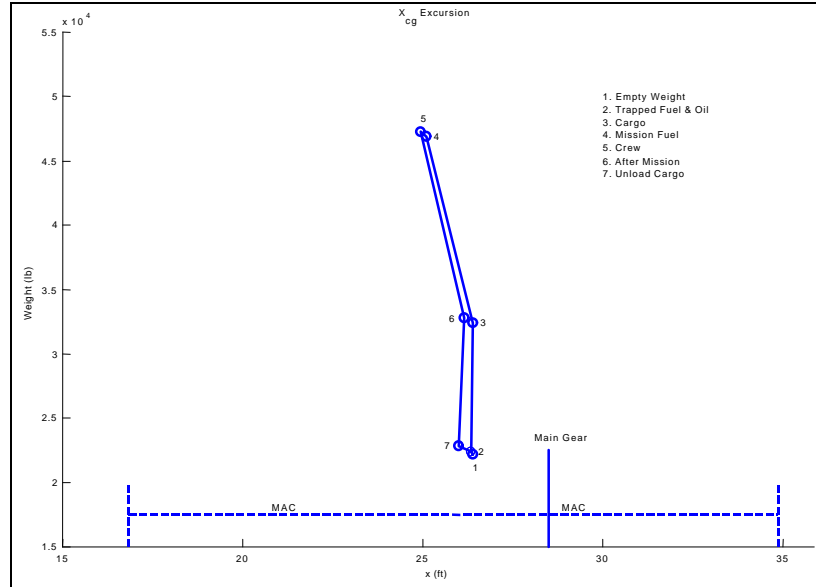


Figure 24:  $X_{cg}$  Excursion for Military Version

#### 7.4 INERTIAS

The aircraft moments and products of inertia are needed for a stability and control analysis of the aircraft. Assuming a breakdown of component weights is available (such as the one in Table 13) the aircraft inertias can be computed about the center of gravity. The principal moments of inertia of the components can be assumed to be negligible.<sup>50</sup> The aircraft weight is assumed to be symmetric about the xz plane, hence the products of inertia  $I_{xy}$ , and  $I_{yz}$  are zero. The moments and products of inertia for the takeoff, cruise, and landing configurations for both versions of the Cardinal are presented in Table 14 and Table 15. The Cardinal moments of inertia were compared to existing aircraft data<sup>50</sup> showing good correlation.

Table 14: Moments and Products of Inertia for Military Version

MOMENT/PRODUCT OF INERTIA	TAKEOFF	CRUISE	LANDING
$I_{xx}$ (slug ft <sup>2</sup> )	244,500	176,816	131,498
$I_{yy}$ (slug ft <sup>2</sup> )	8,977	6,300	2,300
$I_{zz}$ (slug ft <sup>2</sup> )	302,443	233,760	187,757
$I_{xz}$ (slug ft <sup>2</sup> )	16,856	14,770	12,508

Table 15: Moments and Products of Inertia for Commercial Version

MOMENT/PRODUCT OF INERTIA	TAKEOFF	CRUISE	LANDING
$I_{xx}$ (slug ft <sup>2</sup> )	244,276	176,802	131,752
$I_{yy}$ (slug ft <sup>2</sup> )	6,810	5,112	2,289
$I_{zz}$ (slug ft <sup>2</sup> )	300,538	231,854	185,769
$I_{xz}$ (slug ft <sup>2</sup> )	14,970	13,427	11,686

## **8. DRAG ESTIMATION**

For the Cardinal design, a standard drag build-up approach was used to estimate the drag polar. Drag for each major airplane component was calculated according to guidelines outlined in “Aircraft Design: Synthesis and Analysis.”<sup>28</sup> Total drag was estimated from three sources: parasite drag, induced drag, and compressibility drag. Each of these drag items is discussed in the following sections. For the detailed drag computations, refer to the Cardinal web site.<sup>1</sup>

### **8.1 PARASITE DRAG**

Parasite drag accounts for skin friction, roughness, and pressure drag associated with each airplane component. Parasite drag of the following components was taken into consideration: fuselage, lifting surfaces, nacelle & pylon, high-lift systems, and landing gear. In addition to these components, corrections were made for miscellaneous items (antennas, door handles, etc.), interference between components, and roughness via guidelines in reference 28.

#### **8.1.1 FUSELAGE, LIFTING SURFACE, NACELLE, AND PYLON DRAG**

The equivalent parasite area of the body and airfoil components was calculated as the product of the skin friction coefficient, a form factor, and the wetted area of the specified component. The skin friction coefficient,  $c_f$ , accounts for the relative skin friction drag of each component. The form factor,  $k$ , accounts for pressure drag and the increased surface velocity due to thickness. The wetted area,  $S_{wet}$ , accounts for the exposed area that actually contributes to the parasite drag. The parasite drag coefficient was then calculated by non-dimensionalizing the parasite area for each component by the wing reference area.

##### **8.1.1.1 SKIN FRICTION COEFFICIENT**

The value of the skin friction coefficient for each component was found by comparing to experimental data<sup>28</sup> for turbulent flat plates that was fitted to theoretical laminar boundary layer data, and plotted against Reynolds Number for ease of selection. All transition locations were assumed to be at the leading edge. Aerodynamic heating due to Mach number effects was also taken into account for the parasite drag estimate.

##### **8.1.1.2 FORM FACTOR**

The form factor, as noted above, accounts for the change in surface velocity due to thickness. For the fuselage and nacelle, simple bodies of revolution, effective fineness ratios (length of the respective section divided by the effective diameter) were calculated and compared to data from reference 28.

For aerodynamic surfaces, a similar approach was followed. Instead of using the fineness ratio, however, the thickness-to-chord ratio was used to determine the form factor for the wing, empennage, and pylon.

#### **8.1.1.3 WETTED AREA**

Wetted areas were calculated for the fuselage, empennage, wing, nacelle, and pylon following guidelines in reference 28. For aerodynamic surfaces, the wetted area was estimated to be a bit more than twice the exposed area (due to curvature of their respective surfaces). For the fuselage and nacelle, the wetted area was obtained from the CAD model. Details of these calculations can be seen in the drag computations on the Cardinal web site.<sup>1</sup>

#### **8.1.2 HIGH LIFT SYSTEM DRAG**

Parasite drag due to the double-slotted flaps was calculated following guidelines in reference 51. For the Cardinal drag calculations, a look-up table of data from reference 51 was used to compute the profile drag increment due to flaps which was corrected for the non-zero sweep of the Cardinal wings.

Parasite drag due to slats was calculated following the methodology in reference 51. The value was estimated using the ratio of wing chord with slats extended to that of slats stowed. The drag increment was calculated as the product of the wing parasite drag times this ratio. As with the flap drag, this value was modified to account for the sweep angle of the wing quarter-chord. For the calculation of the total parasite drag coefficient, both flap and slat profile drag increments were non-dimensionalized by the wing reference area.

#### **8.1.3 LANDING GEAR DRAG**

Reference 51 outlines the approach used for landing gear parasite drag estimation. The Cardinal uses retractable landing gear, and took advantage of data shown in this reference to estimate the profile drag increment for both the nose gear and main gear. This data was gathered for several existing aircraft, and included the effects of interference.

Calculations for the nose gear were made using nose gear frontal area. To calculate the total parasite drag area, it was necessary to non-dimensionalize this value by the wing reference area instead of the nose gear frontal area. Main gear calculations were conducted in a similar manner, including interference effects and non-dimensionalization by the wing reference area. All landing gear calculations were made assuming a closed landing gear cavity. This is consistent with the Cardinal design. Details of these calculations can be found in reference 1.

#### 8.1.4 PARASITE DRAG BREAKDOWN

Table 16 shows the component breakdown for the Cardinal parasite drag calculations. All values were obtained from the optimal configuration, as selected by the constrained optimization problem discussed in section 12. Reference 1 shows the Matlab code used to obtain these values.

**Table 16: Parasite Drag Breakdown**

COMPONENT		CRUISE	TAKEOFF	LANDING
Fuselage	$C_{Dp, fuselage}$	0.0075	0.0086	0.0087
Wing	$C_{Dp, wing}$	0.0074	0.0078	0.0082
Vertical Tail	$C_{Dp, vt}$	0.0016	0.0021	0.0021
Horizontal Tail	$C_{Dp, ht}$	0.0016	0.0020	0.0021
Nacelle	$C_{Dp, nacelle}$	0.0004	0.0004	0.0005
Pylon	$C_{Dp, pylon}$	0.0001	0.0001	0.0001
Flaps	$C_{Dp, flap}$	0	0.0038	0.0190
Slats	$C_{Dp, slat}$	0	0.0003	0.0006
Landing Gear	$C_{Dp, gear}$	0	0.0007	0.0007
Miscellaneous Items	$C_{Dp, misc}$	0.0190	0.0259	0.0413
<b>TOTAL PARASITE DRAG</b>	<b><math>C_{Dp}</math></b>	<b>0.0195</b>	<b>0.0267</b>	<b>0.0426</b>

#### 8.2 INDUCED DRAG

The induced drag for the Cardinal in cruise was estimated using the standard equation for drag due to lift. As outlined in reference 28, this method took into account fuselage interference effects, wing twist effects, and viscosity effects. For the wing/body, the induced drag was calculated as a function of the wing/body lift coefficient. For the horizontal tail, the trim drag term was calculated as a function of the lift coefficient for the horizontal tail.

For takeoff and landing segments of the flight profile, effects due to the blown flaps were taken into consideration<sup>35</sup>. As outlined in reference 28, a correction to the wing/body lift coefficient was calculated using data gathered from blown flap operations on existing aircraft. This effectively increased the induced drag, which was as expected for the blown flap configuration.

#### 8.3 COMPRESSIBILITY DRAG

The final component of the Cardinal drag estimate was compressibility drag. This drag contribution takes into account the effects of Mach number. For the takeoff and landing configurations, this is obviously not an issue, as the Mach number is low. During the cruise segment, however, the compressibility drag cannot be ignored. As outlined in reference 28, the compressibility drag is related to the crest critical Mach number,  $M_{cc}$

(a function of the quarter-chord wing sweep angle). After finding the value of  $M_{cc}$ , the compressibility drag increment could be found based on data in reference 28.

#### 8.4 DRAG POLAR

The drag polar shows the total airplane drag coefficient for a range of airplane lift coefficients. This graph was used to verify that the Cardinal design fell within the range of reasonable airplane designs (see section 8.5 for more in-depth discussion). Data from the drag polar, specifically  $C_D/C_L$  was used in subsequent subsystem calculations to evaluate the performance of the Cardinal aircraft.

Figure 25, Figure 26, and Figure 27 show drag polars as well as Lift-to-Drag Ratio (L/D) vs. Lift Coefficient ( $C_L$ ) for takeoff, cruise, and landing respectively. Note that stars on these figures indicate the operating ranges for the Cardinal (specifically the beginning and ending of the cruise segment).

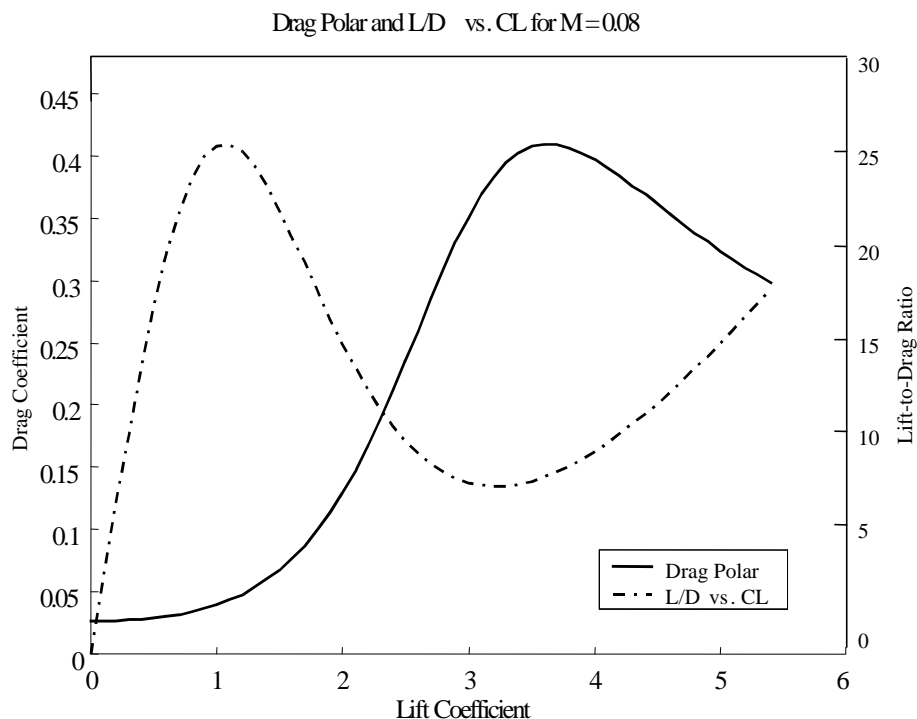


Figure 25: Drag Polar and L/D vs.  $C_L$  for Takeoff Configuration

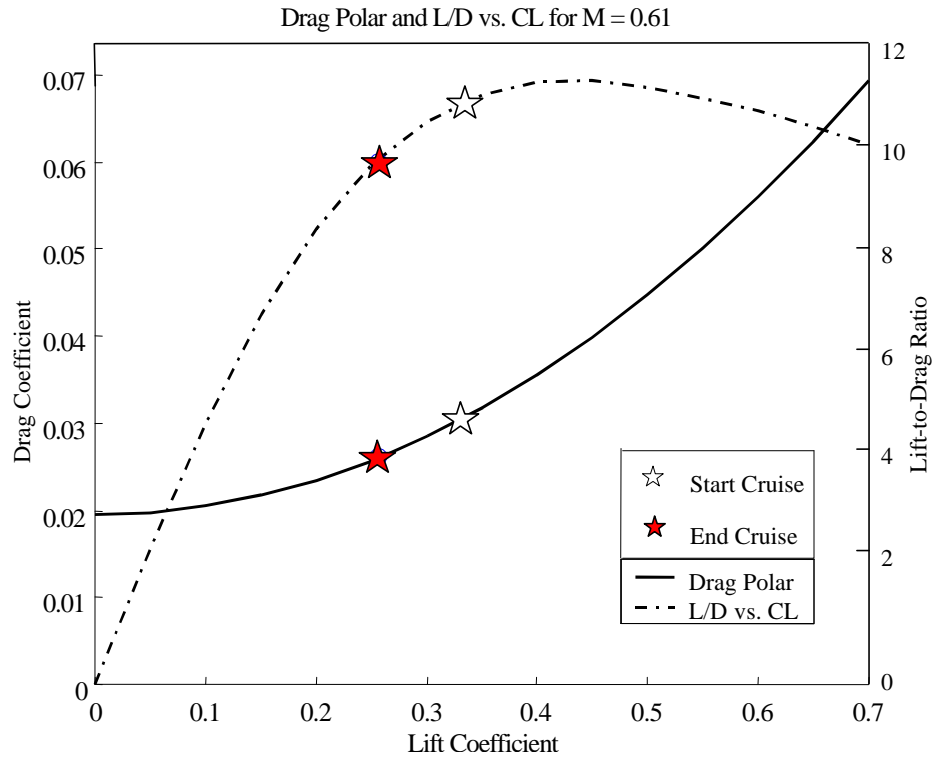


Figure 26: Drag Polar and L/D vs. CL for Cruise Configuration

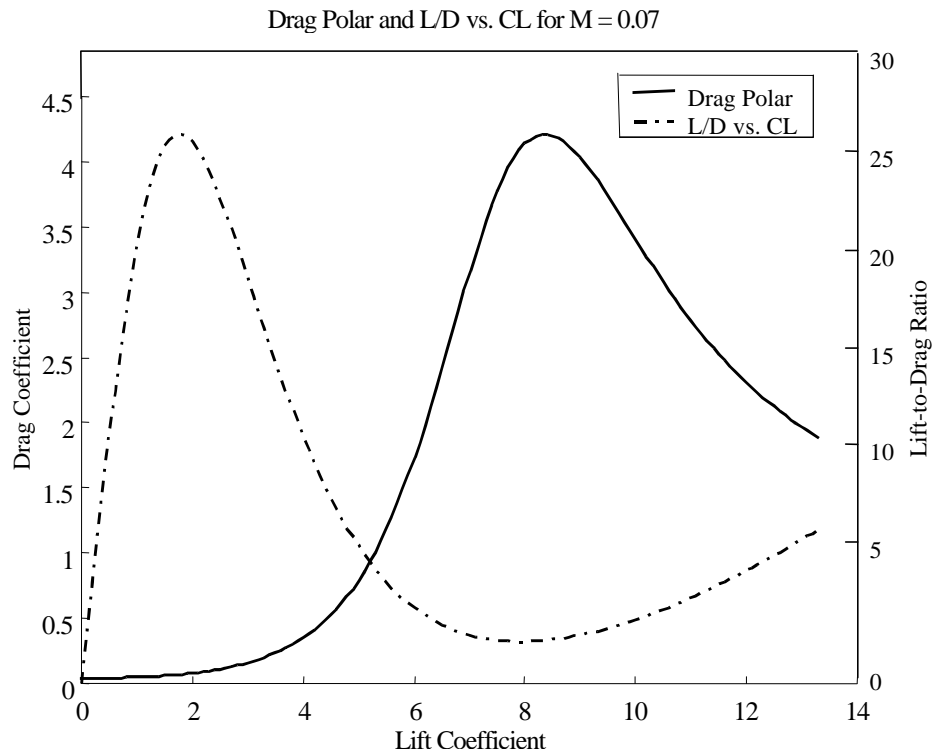


Figure 27: Drag Polar and L/D vs. CL for Landing Configuration

## 8.5 ACCURACY/FEASIBILITY OF ESTIMATE

The drag estimate for Cardinal was based on methodology predominantly used for conventional aircraft. While this method seemed adequate, and gave a final drag estimate that looked reasonable, it was important to correlate the results to similar, existing aircraft. Three parameters were used to compare<sup>51</sup> the Cardinal data with existing data: the total equivalent parasite area ( $f_{\text{total}}$ ), the total wetted area ( $S_{\text{wet total}}$ ), and the airplane span efficiency factor ( $e$ ).

Figure 28 shows a chart from reference 51 with  $f/S_{\text{wet}}$  for approximately 50 existing aircraft. As shown in the plot, all 50 aircraft lie along the same band, showing the range of reasonable values expected for the Cardinal design. The star on Figure 28 shows where the Cardinal lies with respect to existing aircraft. The values of  $f_{\text{total}}$  and  $S_{\text{wet}}$  for the Cardinal seem quite reasonable, at 23 ft<sup>2</sup> and 4970 ft<sup>2</sup> respectively.

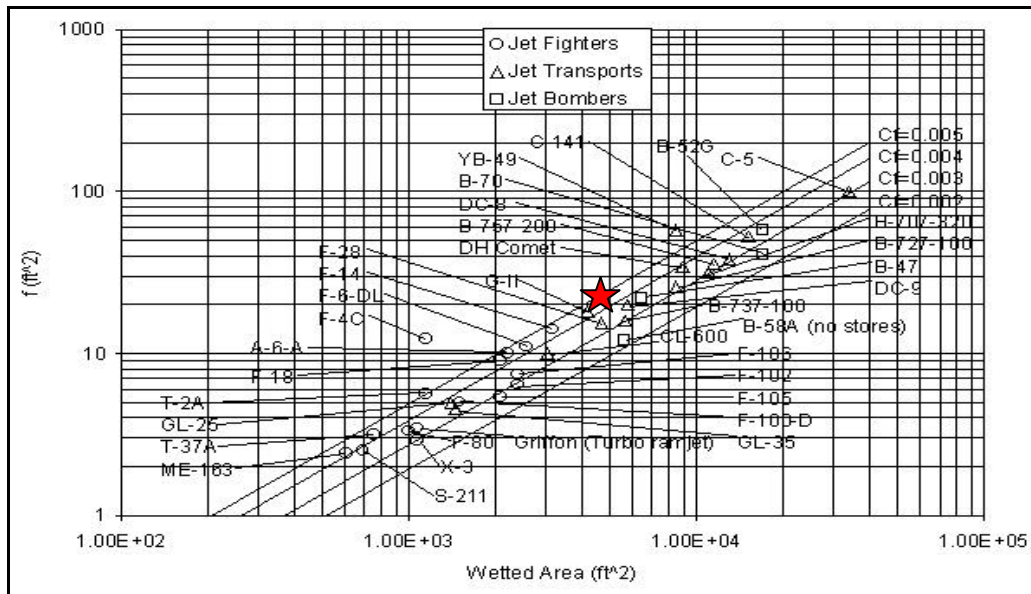


Figure 28:  $f/S_{\text{wet}}$  for Many Existing Aircraft<sup>51</sup>

From the induced drag term,  $C_{Di}$ , the value of the Oswald efficiency factor,  $e$ , was extracted. This value was compared with data from reference 51. The airplane efficiency factor,  $e$ , seemed appropriate given the Cardinal design. A summary of the results is presented in Table 17.

Table 17: Oswald Efficiency Factor for Several Aircraft

AIRCRAFT	OSWALD EFFICIENCY FACTOR <sup>51</sup>	AIRCRAFT	OSWALD EFFICIENCY FACTOR <sup>51</sup>
Cardinal Design	0.84	XB-19	0.76
C-54A	0.81	B-24D	0.78
C-60A	0.63	B-24G	0.84
C-69	0.82		

## **9. STABILITY AND CONTROL**

The stability and control characteristics of the Cardinal must comply with the Part 25 Federal Aviation Regulations (FAR 25) for the commercial version and MIL-8785C for the military version.<sup>2</sup> These regulations place restrictions on the allowable range of frequencies and damping ratios for the airplane. Roll control and engine out control are also regulated. In this section, the longitudinal and lateral-directional stability and control derivatives for the Cardinal are presented for the takeoff, landing, and cruise flight conditions. A summary of the longitudinal & lateral-directional modes is provided.

### **9.1 STABILITY AND CONTROL DERIVATIVES**

All stability and control calculations were made using the Advanced Aircraft Analysis (AAA) software which is based on the methods described in References 51, 54, and 55. Because the optimization routine described in section 12 only had basic stability and control constraints (minimum allowable static margin and minimum control speed) it was necessary to do a post-optimization analysis of the design to verify that the stability and control characteristics were acceptable.

Table 18 summarizes the longitudinal stability derivatives for takeoff, landing, and cruise, along with typical ranges. Longitudinal control derivatives are contained in Table 19, again with the corresponding typical ranges. For the lateral-directional derivatives, the stability derivatives are summarized in Table 20 and the control derivatives in Table 21. Again, ranges of typical values are provided.

**Table 18: Longitudinal Stability Derivatives for the Cardinal Design**

	TAKEOFF CONFIGURATION (0 ft, 65 knots, 46761 lbs)		LANDING CONFIGURATION (0 ft, 55 knots, 33860 lbs)		CRUISE CONFIGURATION (37000 ft, 350 knots, 41000 lbs)	
DERIVATIVE	CARDINAL	TYPICAL RANGES <sup>54</sup>	CARDINAL	TYPICAL RANGES <sup>54</sup>	CARDINAL	TYPICAL RANGES <sup>54</sup>
$C_{D_u}$ (~)	0	-0.010 to 0.300	0	-0.010 to 0.300	0	-0.010 to 0.300
$C_{L_u}$ (~)	0.0275	-0.20 to 0.60	0.0274	-0.20 to 0.60	0.1766	-0.20 to 0.60
$C_{m_u}$ (~)	0.0041	-0.400 to 0.600	0.0029	-0.400 to 0.600	0.0281	-0.400 to 0.600
$C_{D_a}$ (rad <sup>-1</sup> )	2.34	0 to 2.00	2.37	0 to 2.00	0.2731	0 to 2.00
$C_{L_a}$ (rad <sup>-1</sup> )	3.92	1.00 to 8.00	3.92	1.00 to 8.00	4.3147	1.00 to 8.00
$C_{m_a}$ (rad <sup>-1</sup> )	-0.56	-4.00 to 1.00	-0.56	-4.00 to 1.00	-0.4716	-4.00 to 1.00
$C_{D_q}$ (rad <sup>-1</sup> )	0	0	0	0	0	0
$C_{L_q}$ (rad <sup>-1</sup> )	1.61	-5.0 to 15.0	1.61	-5.0 to 15.0	2.0240	-5.0 to 15.0
$C_{m_q}$ (rad <sup>-1</sup> )	-3.17	0 to -20.0	-3.16	0 to -20.0	-3.9668	0 to -20.0
$C_{D_p}$ (rad <sup>-1</sup> )	0	0	0	0	0	0
$C_{L_p}$ (rad <sup>-1</sup> )	5.15	0 to 30.0	5.15	0 to 30.0	6.19	0 to 30.0
$C_{m_p}$ (rad <sup>-1</sup> )	-5.91	0 to -90.0	-5.90	0 to -90.0	-6.7478	0 to -90.0

**Table 19: Longitudinal Control Derivatives for Fixed-Wing Cardinal Design**

	TAKEOFF CONFIGURATION (0 ft, 65 knots, 46761 lbs)		LANDING CONFIGURATION (0 ft, 55 knots, 33860 lbs)		CRUISE CONFIGURATION (37000 ft, 350 knots, 41000 lbs)	
DERIVATIVE	CARDINAL	TYPICAL RANGES <sup>54</sup>	CARDINAL	TYPICAL RANGES <sup>54</sup>	CARDINAL	TYPICAL RANGES <sup>54</sup>
$C_{D_{\delta_h}}$ (rad <sup>-1</sup> )	0.4003	0	0.6701	0	0.0480	0
$C_{L_{\delta_h}}$ (rad <sup>-1</sup> )	0.6706	0 to 1.20	0.4046	0 to 1.20	0.7592	0 to 1.20
$C_{m_{\delta_h}}$ (rad <sup>-1</sup> )	-1.3179	0 to -8.0	-1.3168	0 to -8.0	-1.4880	0 to -8.0
$C_{D_{\delta_e}}$ (rad <sup>-1</sup> )	0.1448	0	0.1465	0	0.0138	0
$C_{L_{\delta_e}}$ (rad <sup>-1</sup> )	0.2425	0 to 0.60	0.2427	0 to 0.60	0.2186	0 to 0.60
$C_{m_{\delta_e}}$ (rad <sup>-1</sup> )	-0.4766	0 to -4.0	-0.4769	0 to -4.0	-0.4284	0 to -4.0

**Table 20: Lateral-Directional Stability Derivatives for the Fixed-Wing Cardinal Design**

	TAKEOFF CONFIGURATION (0 ft, 65 knots, 46761 lbs)		LANDING CONFIGURATION (0 ft, 55 knots, 33860 lbs)		CRUISE CONFIGURATION (370000 ft, 350 knots, 41000 lbs)	
DERIVATIVE	CARDINAL	TYPICAL RANGES <sup>54</sup>	CARDINAL	TYPICAL RANGES <sup>54</sup>	CARDINAL	TYPICAL RANGES <sup>54</sup>
$C_{Y_b}$ (rad <sup>-1</sup> )	-0.7366	-0.100 to -2.00	-0.7366	-0.100 to -2.00	-0.7366	-0.100 to -2.00
$C_{l_b}$ (rad <sup>-1</sup> )	-0.2147	0.100 to -0.400	-0.1858	0.100 to -0.400	-0.2148	0.100 to -0.400
$C_{n_b}$ (rad <sup>-1</sup> )	0.2007	0 to 0.400	0.2027	0 to 0.400	0.1973	0 to 0.400
$C_{Y_{\dot{b}}}$ (rad <sup>-1</sup> )	-0.0186	-	-0.0452	-	-0.0201	-
$C_{l_{\dot{b}}}$ (rad <sup>-1</sup> )	-0.0057	-	-0.0110	-	-0.0062	-
$C_{n_{\dot{b}}}$ (rad <sup>-1</sup> )	-0.0197	-	-0.0250	-	-0.0105	-
$C_{Y_p}$ (rad <sup>-1</sup> )	0.0412	-0.300 to 0.800	0.0578	-0.300 to 0.800	0	-0.300 to 0.800
$C_{l_p}$ (rad <sup>-1</sup> )	-0.3914	-0.100 to -0.800	-0.4504	-0.100 to -0.800	-0.3698	-0.100 to -0.800
$C_{n_p}$ (rad <sup>-1</sup> )	-0.2638	-0.500 to 0.100	-0.2730	-0.500 to 0.100	-0.0316	-0.500 to 0.100
$C_{Y_r}$ (rad <sup>-1</sup> )	0.4737	0 to 1.2	0.4737	0 to 1.2	0.4695	0 to 1.2
$C_{l_r}$ (rad <sup>-1</sup> )	0.8187	0 to 0.600	0.8089	0 to 0.600	0.2025	0 to 0.600
$C_{n_r}$ (rad <sup>-1</sup> )	-0.5552	0 to -1.00	-0.5553	0 to -1.00	-0.2635	0 to -1.00

**Table 21: Lateral-Directional Control Derivatives for the Fixed-Wing Cardinal Design**

	TAKEOFF CONFIGURATION (0 ft, 65 knots, 46761 lbs)		LANDING CONFIGURATION (0 ft, 55 knots, 33860 lbs)		CRUISE CONFIGURATION (37000 ft, 350 knots, 41000 lbs)	
DERIVATIVE	CARDINAL	TYPICAL RANGES <sup>54</sup>	CARDINAL	TYPICAL RANGES <sup>54</sup>	CARDINAL	TYPICAL RANGES <sup>54</sup>
$C_{Y_{\delta_a}}$ (rad <sup>-1</sup> )	0	0	0	0	0	0
$C_{l_{\delta_a}}$ (rad <sup>-1</sup> )	0.0566	0 to 0.400	0.0566	0 to 0.400	0.0588	0 to 0.400
$C_{n_{\delta_a}}$ (rad <sup>-1</sup> )	-0.0567	-0.080 to 0.080	-0.0566	-0.080 to 0.080	-0.0092	-0.080 to 0.080
$C_{Y_{\delta_r}}$ (rad <sup>-1</sup> )	0.1418	0 to 0.500	0.1420	0 to 0.500	0.1191	0 to 0.500
$C_{l_{\delta_r}}$ (rad <sup>-1</sup> )	0.0015	-0.040 to 0.040	-0.0012	-0.040 to 0.040	0.0069	-0.040 to 0.040
$C_{n_{\delta_r}}$ (rad <sup>-1</sup> )	-0.0779	0 to -0.150	-0.0780	0 to -0.150	-0.0649	0 to -0.150
$C_{Y_{\delta_{sp}}}$ (rad <sup>-1</sup> )	0	-	0	-	0	-
$C_{l_{\delta_{sp}}}$ (rad <sup>-1</sup> )	0.0057	-	0.0057	-	0.0059	-
$C_{n_{\delta_{sp}}}$ (rad <sup>-1</sup> )	1.1080	-	1.1080	-	1.1080	-

## 9.2 FREQUENCIES AND DAMPING RATIOS

The FAR and MIL regulations place constraints not on the derivatives but on the various modes. Using the same software used to compute the derivatives, the frequencies, damping ratios, and time constants were computed and compared against the applicable certification requirements. For the many cases when FAR 25 does not provide quantitative requirements, the MIL-F-8785C specifications were used.<sup>54</sup> Table 22 summarizes the frequencies, damping ratios, and time constants which complied with all FAR 25 and MIL requirements.

**Table 22: Frequencies & Damping Ratios for the Cardinal**

	TAKEOFF CONFIGURATION (0 ft, 65 knots, 46761 lbs)	LANDING CONFIGURATION (0 ft, 55 knots, 33860 lbs)	CRUISE CONFIGURATION (37000 ft, 350 knots, 41000 lbs)
<b>LONGITUDINAL MODES<sup>54</sup></b>			
Short Period	$W_{n_{SP}} = 2.3 \text{ rad/sec}$ $Z_{SP} = 0.37 (\sim)$	$W_{n_{SP}} = 2.2 \text{ rad/sec}$ $Z_{SP} = 0.35 (\sim)$	$W_{n_{SP}} = 4.61 \text{ rad/sec}$ $Z_{SP} = 0.74 (\sim)$
Phugoid	$W_{n_P} = 0.032 \text{ rad/sec}$ $Z_P = 0.043 (\sim)$	$W_{n_P} = 0.031 \text{ rad/sec}$ $Z_P = 0.041 (\sim)$	$W_{n_P} = 0.134 \text{ rad/sec}$ $Z_P = 0.05 (\sim)$
<b>LATERAL-DIRECTIONAL MODES<sup>54</sup></b>			
Spiral Time Constant	$T_s = 153.2 \text{ sec}$	$T_s = 150.5 \text{ sec}$	$T_s = 94.6 \text{ sec}$
Roll Time Constant	$T_r = 0.953 \text{ sec}$	$T_r = 1.02 \text{ sec}$	$T_r = 0.82 \text{ sec}$
Dutch Roll	$W_{n_D} = 1.2416 \text{ rad/sec}$ $Z_D = 0.1869 (\sim)$	$W_{n_D} = 1.08 \text{ rad/sec}$ $Z_D = 0.21 (\sim)$	$W_{n_D} = 2.63 \text{ rad/sec}$ $Z_D = 0.0803 (\sim)$

## 9.3 MINIMUM CONTROL SPEED

The minimum control speed is the minimum speed at which the yawing moment due to an inoperative engine can be balanced by the vertical tail without stalling. FAR 25 requires that the minimum control speed be less than or equal to 1.2 times the stall speed in the landing configuration.<sup>54</sup> MIL-F-8785C requires the minimum control speed to be less than or equal to the highest of: (a) 1.1 times the stall speed, or (b) the stall speed plus 10 knots.<sup>54</sup> The minimum control speed computation took into account the thrust loss of an inoperative engine and the windmilling drag.<sup>54</sup> This computation was incorporated into a Matlab code (available on the Cardinal web site<sup>1</sup>) for use in the optimization routine described in section 12. Table 23 summarizes the results for the Cardinal. Comparison of the speeds in Table 23 with the regulatory requirements indicates that the Cardinal exactly meets the FAR requirements and exceeds the minimum MIL requirement.

**Table 23: Stall and Minimum Control Speeds for the Cardinal**

SPEED	CARDINAL DESIGN
Stall speed, $V_s$	75 ft/sec
$1.2 V_s$	90 ft/sec
Minimum Control Speed, $V_{mc}$	90 ft/sec

## 10. PERFORMANCE ANALYSIS

Many of the design requirements for the Cardinal involve minimum performance requirements; for example, range, cruise speed, and takeoff/landing ground roll requirements were all defined in the RFP.<sup>2</sup> In this section, the methodologies used in the analysis of takeoff and landing distances, climb performance, and cruise speed and range are presented, as well as compliances with applicable FAR/MIL requirements. Details of the calculations (and copies of the codes written to implement them) may be found on the Cardinal web site.<sup>1</sup>

### 10.1 TAKEOFF & LANDING DISTANCES

The RFP<sup>2</sup> requires that the Cardinal have a maximum takeoff ground roll of 300 feet and a maximum landing ground roll of 400 ft. There are many statistical and approximate methods available for estimating takeoff and landing distances, either through statistical correlation with existing aircraft or simplifications of the equations of motion.<sup>30</sup> Due to the stringent takeoff and landing distance requirements for the Cardinal, the statistical methods are not applicable. Therefore, the takeoff and landing distance computations were made by numerical integration of the equations of motion.

Using integral equations for the takeoff and landing distances<sup>30</sup> (modified to account for the vertical component of thrust in the case of the tilt-wing) a simple Euler integration was used to compute the ground rolls. For both the takeoff and landing analysis the runway was assumed to be level zero wind speed. Constant weight and attitude on the landing gear (constant lift and drag coefficients are constant) were assumed. A typical rolling ground friction coefficient,  $\mu_g$ , of 0.025 was used throughout the calculations.<sup>30</sup>

For the variation of thrust with speed for turbofan engines, the performance code implemented a simple correlation between Mach number and the ratio of actual to static thrust.<sup>28</sup> The variation of thrust with speed and rotor angle for the tilt-wing aircraft was computed from data in Aerodynamics of V/STOL Flight by McCormick.<sup>35</sup> FAR regulations do not allow for any engine-dependent means of slowing down during landing (e.g. thrust reversers) to be used for certification;<sup>30</sup> the analysis for the Cardinal assumes no use of such devices.

For the fixed-wing design takeoff rotation was assumed to occur at a speed of 1.1 times the stalling speed in the takeoff configuration with liftoff occurring at 1.15 times the stall speed. During landing, the approach speed for the fixed-wing design is 1.3 times the stalling speed in the landing configuration with touchdown assumed to be at 1.15 times the landing stall speed. Because the lift coefficient of a wing with blown flaps is a

function of throttle setting, with the thrust being a function of speed and drag coefficient, the stall speeds in both the takeoff and landing configurations were determined iteratively.

For the tilt-wing configuration, a force balance was done at each step in the integration to determine whether the plane had taken off. Landing speeds for the tilt-wing were computed by iterating to find a stable unaccelerated descent profile with a flight path angle of no more than  $-7^\circ$ . Once the touchdown speed was established, the same method of integration was used to determine the landing ground roll.

The computations of takeoff and landing ground roll were incorporated into a Matlab code for use in the optimization described in Section 12 (a copy is available on the Cardinal web site<sup>1</sup>). A summary of the takeoff and landing ground rolls as a function of weight is shown in Figure 29 for the final Cardinal design. The maximum takeoff weight of the Cardinal is 46,761 lb -- Figure 29 shows that at this weight the takeoff ground roll is 289 ft. The landing ground roll constraint was imposed at the maximum landing weight which was assumed to be 85% of the maximum takeoff weight (39,747 lb). Results of this calculation showed a ground roll of 273 ft.

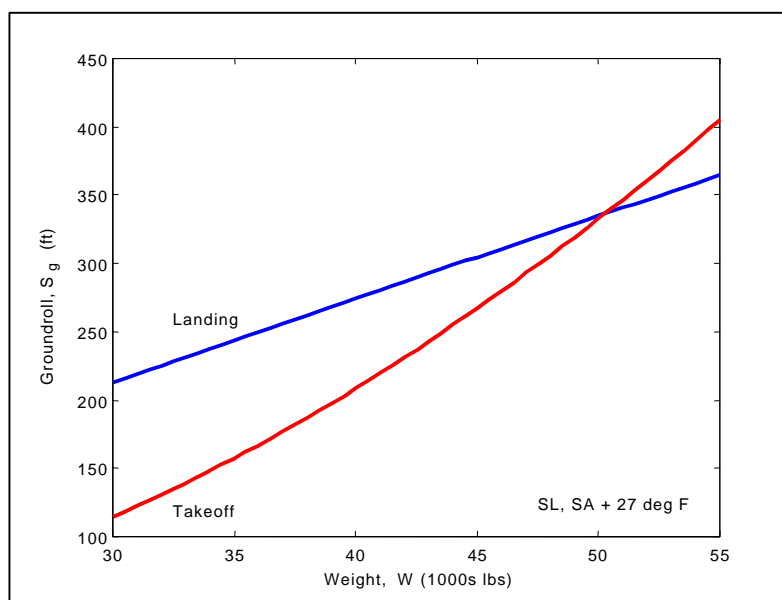


Figure 29: Takeoff and Landing Ground Rolls for the Cardinal

## 10.2 CLIMB PERFORMANCE

Climb performance must be computed to compute the time required to climb to altitude, compute range credits for climb, and verify that applicable FAR and MIL specifications for climb gradients are met with both

All Engines Operating (AEO) and One Engine Inoperative (OEI). A summary of the method used in computing the climb performance and verifying compliance with the FAR and MIL specifications is presented below.

Using the method outlined in Airplane Aerodynamics & Performance by Roskam & Lan,<sup>30</sup> the climb rate was computed from drag, weight, and propulsion data. This data was then used passed to the optimization code, described in Section 12, to compute time to climb and range covered during climb. The AEO climb performance for various altitudes and Mach numbers is summarized in Figure 30.

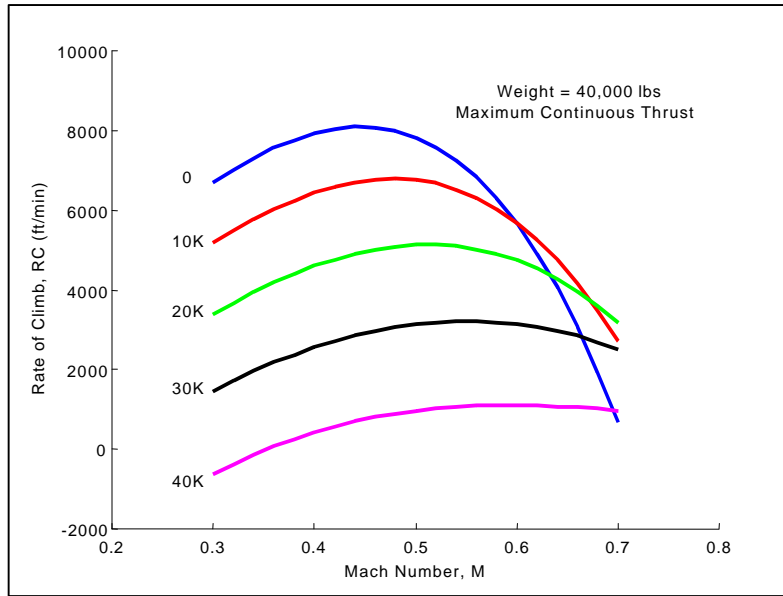


Figure 30: Rate of Climb for the Cardinal at Varying Altitudes and Mach Numbers

The FAR 25 climb performance requirements set minimum allowable climb gradients (CGR) for the aircraft in different configurations and speeds with OEI. This analysis included the effects of windmilling drag on the stopped engine and the additional rudder drag for trim. The climb gradients were computed for the various flight phases using a Matlab code available on the Cardinal web site.<sup>1</sup> Table 1 summarizes the results for the Cardinal and the applicable FAR requirement. Because the FAR requirements are more stringent than the USN requirements, satisfying the FAR requirement means that the USN requirements are also met.

Table 24: FAR Climb Gradients for the Military Version of the Cardinal

FAR Part	Flight Phase	FAR Minimum CGR <sup>30</sup>	CGR for Cardinal
FAR 25.121a	First Segment Climb	0.5	0.53
FAR 25.121b	Second Segment Climb	3.0	3.19
FAR 25.121c	Third Segment Climb	1.7	2.35
FAR 25.121d	Go-around (Approach)	2.7	3.19
FAR 25.119	Go-around (Landing)	3.2	3.80

### 10.3 RANGE

The range of the Cardinal was specified by the RFP to be 1500 nm with full payload.<sup>2</sup> Range was computed by numerical integration of the specific range from begin cruise weight to end cruise weight. The specific range, or range factor, is defined as the number of nautical miles which can be flown per pound of fuel. This value was computed for a range of airplane weights, speeds, and altitudes.

Section 10.2 discussed the climb calculations which provide the begin cruise weight and the distance traveled during climb. These values can be applied to the 1500 nm range requirement required by the RFP.<sup>2</sup> The range specified does not allow a range credit for descent, and requires adequate remaining fuel reserves after landing. For the case of USN cargo and transport aircraft, which was the critical version of the Cardinal for sizing purposes, the fuel reserve requirement is the greater of (a) 10% of mission fuel (including one approach, a wave-off, a go-around, a second approach, and trap) or (b) fuel equal to 30 minutes of loiter at sea-level speeds plus 5% of mission fuel.<sup>30</sup> The end cruise weight was iterated to provide adequate reserves, and the resulting range was computed from the known beginning and ending cruise weights. A Matlab code was written to incorporate this method into the optimization routine described in Section 12. A copy of the code is available on the Cardinal web site.<sup>1</sup> Figure 31 contains a plot of the specific range for the Cardinal over a range of weights at an altitude of 37,000 feet.

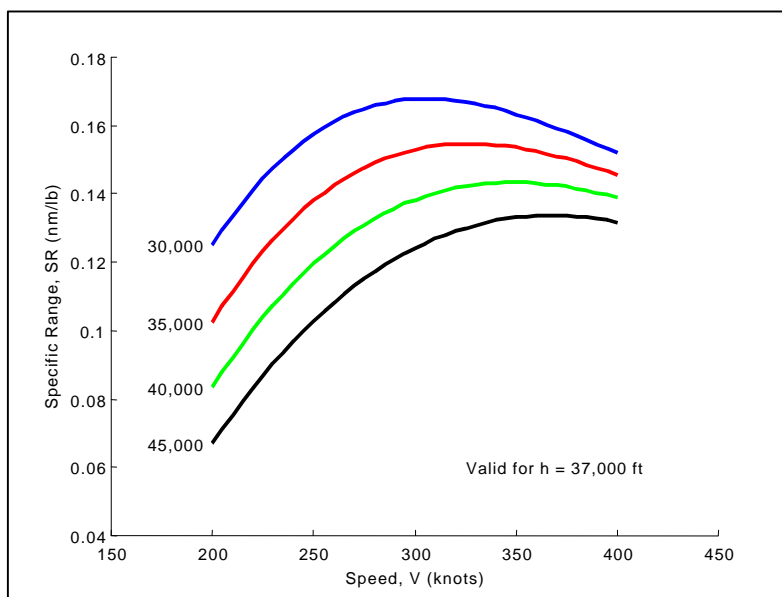


Figure 31: Specific Range for the Cardinal

A payload-range diagram was constructed to show the effects of various combinations of payload and fuel loading. Figure 32 shows that at the design payload of 10,000 lbs, the military version of the Cardinal has a range of 1,500 nm. The ferry range, representing the maximum range of the aircraft, was calculated to be 2,968 nm. Table 25 summarizes the range for various configurations of the Cardinal. The first listing for the commercial version represents the range with the design payload and maximum volumetric fuel, while the second listing corresponds to the configuration with a 1500 nm range and a design payload of 24 passengers & baggage.

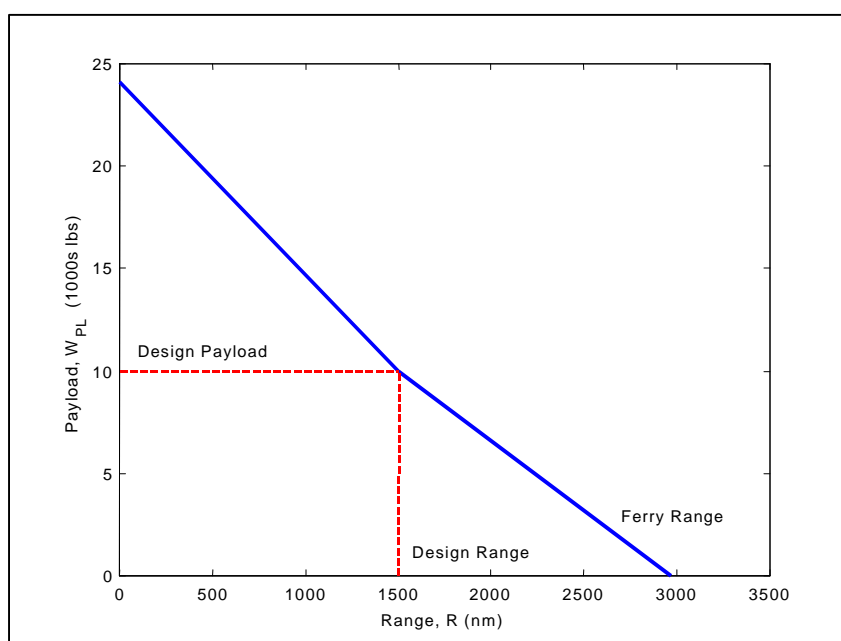


Figure 32: Payload-Range Diagram for the Military Version of the Cardinal

Table 25: Range of the Cardinal for Military and Commercial Versions

VERSION	TAKEOFF WEIGHT (LBS)	PAYLOAD (LBS)	RANGE (NM) (WITH RESERVES)
Military	46,761	10,000	1500
Commercial	43,114	4,920	1988
Commercial	42,608	4,920	1500

## 11. COST ESTIMATION

During the Cardinal design process, it was imperative to choose a figure of merit to compare prospective designs. While elements of the system such as weight, field length, or wing area may highlight a specific performance objective, cost is a more universal way to compare two designs. The following sections detail the methodology used to estimate the cost of the Cardinal design—a technique outlined in Airplane Design Volume VIII by Roskam.<sup>53</sup> The basic approach consists of a simple cost breakdown—estimating the cost for several airplane program phases, and then summing the estimates to compute life-cycle cost.

Included in this analysis were (a) Research, Development, Test, and Engineering (RDTE), (b) Acquisition, (c) Operating, (d) Disposal, and (e) Life Cycle. Each of these costs represents a significant portion of the total cost estimate. As illustrated in Figure 33, the RDTE phases comprise about ten percent of the Acquisition phase, which comprises about ten percent of the Operations phase. All detailed cost calculations can be found on the Cardinal web site.<sup>1</sup> Please note that all cost calculations were conducted for **fiscal year 1999**.

The RFP<sup>2</sup> requires a dual-use aircraft. The Cardinal aircraft was designed with both commercial and military configurations to comply with this requirement. In the cost analysis, the number of airplanes played a significant role—many cost numbers, particularly operating cost and life-cycle cost, depend heavily on the production run. For the analysis discussed herein, a production run of 750 airplanes, of **one version** (commercial or military), was assumed. For actual operation of this aircraft, the production run will be 750 airplanes. However, they will not all be of the same version. To simplify the design, and make it possible to account for any number of commercial vs. military versions, the cost calculations were done assuming all one configuration. To find the cost associated with a mixed production run, a simple percentage of each type can be used. If, for example, there were 375 of each type, the cost would be half that of the commercial run, and half that of the military run. For clarity, results from the single version production run only are presented in the following sections.

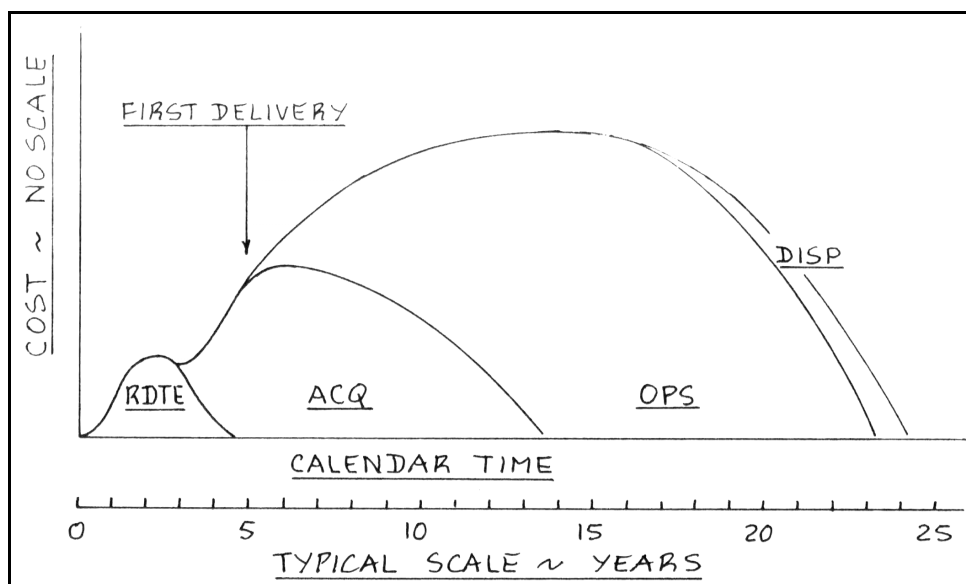


Figure 33: Life Cycle Cost Breakdown<sup>53</sup>

### 11.1 RESEARCH, DEVELOPMENT, TEST, AND ENGINEERING PHASES (RDTE)

The RDTE phases span the initial part of the airplane program. The RDTE phases begin with mission definition and conceptual design, move through trade studies and preliminary design, and conclude with detailed design and flight test. For the RDTE cost estimate, seven factors were considered: Airframe Engineering and Design, Development Support and Testing, Flight Test Airplanes, Flight Test Operations, Test and Simulation Facilities, RDTE Profit, and Financing the RDTE phases. Each of these factors had associated Cost Estimating Relationships (CERs) that took into account labor rates, manhours, materials selection, mission profile, interest rates, etc. All CERs were based on statistical data gathered for many existing aircraft.<sup>53</sup> Table 26 shows a breakdown of the RDTE costs for the Cardinal design.

Table 26: RDTE Cost Breakdown

RDTE COST ELEMENT	CARDINAL RESULTS (in FY99 \$USMillion)
Airframe Engineering & Design:	78.2
Development Support & Testing:	22.4
Flight Test Airplanes:	365.6
Flight Test Operations:	4.6
Test & Simulation Facilities:	67.2
RDTE Profit:	67.2
RDTE Financing:	67.2
<b>TOTAL RDTE COSTS:</b>	<b>672.5</b>

## 11.2 ACQUISITION COST

Acquisition consists of airplane manufacturing and delivery to the customer. As noted in Figure 33, this phase represents a significantly larger portion of the cost than the RDTE phases. The Cardinal design calls for a production run of 750 airplanes—a figure represented in the calculations of this section. The total cost of acquisition is estimated as the sum of the manufacturer's cost plus the manufacturer's profit. This sum, shown in Table 27, is broken down into Airframe Engineering and Design, Airplane Production, Production Flight Test Operations, Financing the Manufacturing Phase, and Profit. Similar to calculations in the RDTE phases, these estimates take many factors (such as tooling, quality and control, avionics, etc.) into consideration.<sup>53</sup> Details can be found in the cost calculations.<sup>1</sup>

**Table 27: Manufacturing and Acquisition Cost Breakdown**

MANUFACTURING & ACQUISITION COST ELEMENT	CARDINAL RESULTS (in FY99 \$USMillion)
Airframe Engineering & Design:	125.8
Airplane Program Production:	9,741.3
Production Flight Test Operations:	72.0
Financing the Manufacturing Phase:	1,104.3
Profit Made by Manufacturer:	1,104.3
<b>TOTAL MANUFACTURING &amp; ACQUISITION COSTS:</b>	<b>12,147.8</b>

The Airplane Estimated Price was also calculated as part of the acquisition cost. For the selected design, the Airplane Estimated Price was \$17.1M. This value not only served as an important factor in choosing the overall design, but also gave an additional figure of merit for comparing the Cardinal design to existing aircraft. While life-cycle cost numbers for existing aircraft are rarely provided to the public, the airplane price is usually available. A discussion of how the Cardinal design compared to other aircraft can be found in section 11.7.

## 11.3 OPERATING COST<sup>53</sup>

Program operating cost is the cost associated with operation of the airplane. This cost, as noted in Figure 33, accounts for the largest fraction of the life-cycle cost. This estimate is calculated in two segments: Direct Operating Cost, and Indirect Operating Cost. The operating cost is based on statistical data gathered for many existing aircraft.<sup>32</sup> The estimate for this major cost factor takes into account many parameters associated with aircraft operations such as mission range, number of years of operation, and number of airplanes acquired by the customer.

Operating cost is an important figure of merit for validation of the cost estimate. Similar to the Airplane Estimated Price, the operating cost is an excellent way to compare the Cardinal design to existing aircraft. Section 11.7 discusses this in more detail. In addition to comparison with existing aircraft, the operating cost was a major factor in choosing the final Cardinal design.

Figure 34 shows the operating cost breakdown for both versions of the Cardinal. The dual-use nature of this aircraft required analyses for two rather different designs. The commercial version, without the large payload, was much lighter. The figure also highlights the impact of weight reduction for the commercial version. All operating cost calculations were done with a block distance of 1500 nm as specified by the RFP<sup>2</sup>. Note that Figure 34 includes the Direct Operating Cost breakdown, as well as the Indirect Operating Cost (17% of the total Operating Cost), as shown.

#### **11.3.1 DIRECT OPERATING COST (DOC)**

The direct operating cost was further broken down into the following direct costs: (a) Flying, (b) Maintenance, (c) Depreciation, Landing, Navigation, and (d) Registry, and Financing. Included in this estimate were values for the crew costs, fuel and oil, insurance, etc. The final figure was calculated in terms of U.S. dollars per nautical mile. Details of this calculation can be found on the Cardinal web site.<sup>1</sup>

#### **11.3.2 INDIRECT OPERATING COST (IOC)**

The indirect operating cost is difficult to estimate, as it varies considerably depending on the operator. The method outlined in reference 53 suggests estimating Indirect Operating Cost as a simple fraction of the Direct Operating Cost. This was the approach taken for the Cardinal design--Figure 34 shows the IOC as 17% percent of the DOC. While the costs associated with indirect operations do not comprise the largest portion of the total Program Operating Costs, they could not be ignored. Costs associated with indirect operations include food service, ticketing agents, ground equipment, administration, etc.

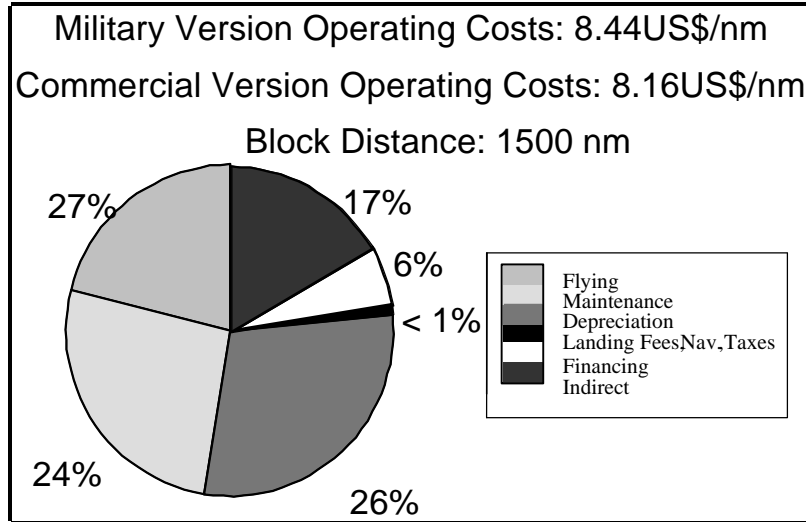


Figure 34: Operating Cost Breakdown<sup>1</sup>

Table 28: Operating Cost Breakdown<sup>1</sup>

OPERATING COST ELEMENT Production run of 750 airplanes	MILITARY VERSION (in FY99 \$USBillion)	COMMERCIAL VERSION (in FY99 \$USBillion)
Flying:	37.4	35.8
Maintenance:	33.8	33.4
Depreciation:	36.3	34.4
Landing Fees, Navigation, and Registry Taxes:	1.2	1.1
Financing:	8.2	7.9
Indirect Operating Costs:	23.4	22.5
<b>TOTAL OPERATING COSTS:</b>	<b>140.3</b>	<b>135.2</b>

#### 11.4 DISPOSAL COST

Disposal cost accounts for the disposal of the airplane at end-of-life. This cost usually consists of (a) temporary storage, (b) draining of liquids and disposal thereof, (c) dissassembly of engines and instruments, and (d) dismantling of the airframe and disposal of the resulting materials.<sup>53</sup> This cost is very difficult to estimate. Following guidelines in reference 53, the disposal cost was estimated to be one percent of the Life-Cycle Cost.

#### 11.5 LIFE CYCLE COST (LCC)<sup>11</sup>

The Life-Cycle cost of the Cardinal airplane program was estimated as the sum of the aforementioned parts: RDTE Phases, Acquisition, Operating Cost, and Disposal. This cost was calculated over an estimated lifetime of 20 years, for a production run of 750 airplanes. Figure 35 shows the allocation of cost for each program phase. As predicted (see Figure 33), the operating costs are by far the major contributor to the Life-Cycle Cost.

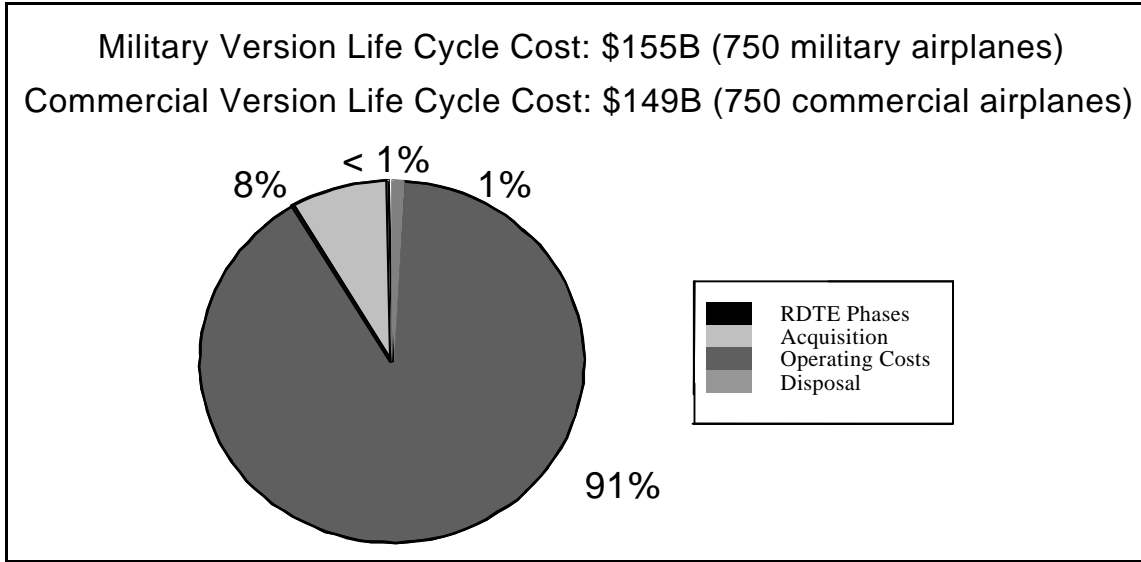


Figure 35: Life-Cycle Cost (LCC) Breakdown<sup>1</sup>

Table 29: Life-Cycle Cost (LCC) Breakdown<sup>1</sup>

LIFE CYCLE COST ELEMENT	MILITARY VERSION (in FY99 \$USBillion)	COMMERCIAL VERSION (in FY99 \$USBillion)
RDTE Cost:	0.7	0.6
Manufacturing & Acquisition Cost:	12.1	11.5
Operating Cost:	140.3	135.2
Disposal Cost:	1.5	1.5
<b>LIFE-CYCLE COST:</b>	<b>154.7</b>	<b>148.9</b>

#### 11.6 ASSESSMENT OF VERTICAL TAKEOFF COST

The mission requirements specified in the RFP were stringent enough to require the consideration of a vertical takeoff and landing (VTOL) capability, but not stringent enough to rule out super short takeoff and landing (SSTOL). This issue was of primary concern early in the design process, and was investigated thoroughly before final design selection. VTOL was not part of the final design, but remained an option for alternative configurations or missions.

This section discusses the cost impact for inclusion of the VTOL option. A summary for costs associated with the VTOL option is shown, along with more detailed discussion of key cost parameters that significantly impacted final design selection. Table 30 shows the numbers generated by the cost code<sup>1</sup> for both the VTOL option and the SSTOL option. Note that in every cost category used to choose the “better” design, the SSTOL design had lower costs than the VTOL design. The optimal Cardinal design presented in this section pushes the performance limits set out by the RFP—adding a vertical takeoff capability pushed these limits even further.

**Table 30: Assessment of Vertical Takeoff Option<sup>1</sup>**

CARDINAL COST METRICS	VERTICAL TAKE-OFF TILT-WING DESIGN		SHORT TAKEOFF FIXED-WING DESIGN	
	MILITARY VERSION (FY99)	COMMERCIAL VERSION (FY99)	MILITARY VERSION (FY99)	COMMERCIAL VERSION (FY99)
Direct Operating Cost:	\$9.06/nm	\$8.63/nm	\$7.03/nm	\$6.80/nm
Indirect Operating Cost:	\$1.81/nm	\$1.73/nm	\$1.41/nm	\$1.36/nm
Fuel Price:	\$1.20/gallon	\$1.20/gallon	\$1.20/gallon	\$1.20/gallon
Engine Price (per engine):	\$1.09 M	\$1.09 M	\$0.52 M	\$0.52 M
Airplane Estimated Price:	\$20.8 M	\$19.4 M	\$17.1 M	\$16.2 M
Airplane Market Price:	\$19.7 M	\$17.3 M	\$16.7 M	\$15.4 M
<b>LIFE CYCLE COST</b>	<b>\$200.6 B</b>	<b>\$189.3 B</b>	<b>\$154.7 B</b>	<b>\$148.9 B</b>

Section 2.2 presents a discussion of the three preliminary designs considered by the Cardinal team. Both VTOL and SSTOL were carefully analyzed. Using the optimization code<sup>1</sup> developed for the Cardinal endeavor, the VTOL option was rejected. The “objective function” for the Cardinal optimization was a minimization of life-cycle cost. While the tilt-wing design offers the added flexibility of vertical takeoff and landing, the significant cost impact cannot be ignored. If the customer so desires, the tilt-wing concept could be incorporated to allow for vertical takeoff at the expense of life-cycle cost.

#### 11.7 ACCURACY/FEASIBILITY OF ESTIMATE

The method used to estimate Cardinal costs was based on a statistical approach developed by Roskam.<sup>53</sup> This method is based on data from subsonic commercial aircraft. The Cardinal is designed as a dual-use, SSTOL airplane, and uses several new technologies. Unfortunately, this method does not fully account for these discrepancies. It would be reasonable to expect that Cardinal program costs would be significantly higher. An accurate cost estimation method for this type of aircraft has not yet been developed.<sup>43</sup> The Cardinal team was cognizant of the inaccuracy of the cost estimation, and used the Life-Cycle Cost calculation served as an “order-of-magnitude” result rather than an accurate representation for the actual cost. Despite the inaccuracy, the sensitivities to various parameters were very helpful and seemed a good way to characterize the feasibility of the Cardinal design. Details of this sensitivity analysis can be found in section 12.4.4. Table 31 shows costs comparable to those of the Cardinal—despite inaccuracy of the method, the final results seemed reasonable.

**Table 31: Existing Aircraft Cost Data**

Cost Element	Cardinal Design	Bell 609 <sup>64</sup> Tilt-Rotor	Beech 1900D	Embraer ERJ-145	Siaorsky <sup>57</sup> S-76C+	Canadair Challenger
Airplane Price <sup>61</sup> (USM)	\$17.1	\$8-10	\$4.8	\$15.5	\$5.9	\$20
Direct Operating Cost (USD)	\$7.03/nm	\$4.12/nm	NA	NA	\$4.37/nm	NA

## 12. DESIGN OPTIMIZATION

The design of the Cardinal is quite unconventional—the stringent constraints imposed on this SSTOL aircraft were not easy to meet<sup>2</sup>, requiring a large amount of analysis for each design area. Due the complexity of the design process for this aircraft, an independent team handled each of the major design categories. These “subsystem analyses” were then combined for collaborative optimization. Prior to writing the optimization code, a literature review was conducted to find methods for introducing collaborative optimization into the aircraft preliminary design process. While many optimization methods exist, tailoring those to preliminary aircraft design is some thing of an art—the Cardinal team built on the expertise of several aircraft design optimization experts to better define the scope of the optimization code (see references 14, 21, 23, 24, 26, 27, 29, 40, and 58).

The goal of this optimization was to make the best airplane design. For the Cardinal, several design variables (detailed in the following sections) were chosen to describe the best design. Each of these design variables describes airplane geometry, performance, or cost metrics which, when viewed together, describe the Cardinal airplane. At the start of this project, the team chose to investigate several different airplane designs: two SSTOL aircraft (a tilt-wing and a fixed-wing), and one VTOL aircraft (also using the tilt-wing configuration). All subsystem analyses were conducted for each of these aircraft, leading to initial designs that were ready for optimization. The optimization yielded results which allowed the designs to be compared in a quantitative way, thereby allowing selection of the best airplane design.

### 12.1 DESIGN VARIABLE SELECTION

One of the most challenging parts of collaborative optimization is selecting variables that accurately represent the entire design. While there are thousands of variables used to describe an airplane, not all of them have a significant impact on the overall design. To select variables that do have a significant impact, the Cardinal team began the subsystem analyses. Each analysis required specific inputs to yield outputs corresponding to the design constraints—these variables were selected for the optimization. This group of around 40 variables can be used to describe the geometry, performance, and cost of the Cardinal. Table 32 shows the design variables used in the Cardinal study.

Note that for the Cardinal study, fuselage geometry was fixed. The requirements imposed by the RFP<sup>2</sup> dictated a fixed maximum volume and a required cargo capacity. This left little room for alternate geometries.

The fuselage did not have an impact on final design selection since its parameters were so tightly constrained. A summary of the fuselage geometry can be found in section 6 and in reference 1.

**Table 32: Cardinal Design Variables**

DESIGN SECTION	VARIABLES
MISSION PROFILE	cruise altitude, cruise speed, range
WING GEOMETRY	$S_{ref}$ , span, taper ratio, thickness-to-chord ratio, sweep angle, wing location
EMPENNAGE GEOMETRY	$S_{ref}$ , span, taper ratio, thickness-to-chord ratio, sweep angle, tail location
LANDING GEAR GEOMETRY	distance <sub>nose-to-nose gear</sub> , distance <sub>nose-to-main gear</sub> , lateral position of main gear
PROPULSION	installed thrust/power, engine model (sfc, $T_{avail}$ vs. speed, $T_{avail}$ vs. altitude)
WEIGHTS	$W_{TO}$ , $W_{max}$ zero fuel, center-of-gravity locations

## 12.2 OPTIMIZATION METHODOLOGY

The purpose of constrained optimization is to transform a complex problem into much simpler subproblems that can be solved using iteration. Typically, the constrained problem is written as an unconstrained problem with penalty functions for constraints at, near, or beyond their limits. The constrained problem is then converged upon when the limit of a sequence of parameterized unconstrained optimizations is reached. There are numerous methods used to perform collaborative, constrained optimization. The Cardinal Team chose to use a Sequential Quadratic Programming (SQP) method.<sup>13</sup> This nonlinear method was implemented in an optimization code<sup>1</sup> written for the Cardinal project using the Matlab Optimization Toolbox.<sup>34</sup>

This section describes the set-up, execution, and results of the Cardinal design optimization. Each of these elements was central to the success of the routine. While the objective of the optimization code was to successfully find a mathematical optimum, the results from its execution were relied upon for final design selection.

### 12.2.1 DEFINING A WELL-POSED PROBLEM<sup>24</sup>

Early methods using the sequence of parameterized unconstrained optimizations are rather inefficient and have been replaced by methods which build upon the solution of the Kuhn-Tucker (KT) equations. These equations, and their solutions, represent necessary conditions for any constrained optimization problem. To satisfy the KT equations, the problem must be well-posed—such that at the solution point there will be cancellation of the gradients between the objective function and the active constraints.<sup>13</sup>

To pose the problem properly, the Cardinal design was represented by design variables, which could also be viewed as separate decisions to be made during optimization. The relevant measure of performance (life-cycle cost) was expressed as an objective function of these decision variables. Restrictions on the decision variables were then written as constraints, mathematical expressions relating the decision variable and its bound with inequalities and/or equations.

### **12.2.2 FLOW OF INFORMATION**

Of central importance to a successful optimization is selection of the overall flow of information. Prior to optimization, each subsystem was analyzed in terms of the design variables. Each subsystem function used some or all of the design variables to compute parameters relevant to that subsystem. These outputs were then used by other subsystems as inputs. The subsystem analyses, when combined in a sequence, yielded values for all design variables and constraints. The optimization code<sup>1</sup> then used this information to iterate on the design until reaching an optimal solution that satisfied all constraints.

Figure 36 shows a flow chart laid out to simplify the optimization procedure for the Cardinal. Note that the chart shows only feedforward—a concerted effort was made to eliminate feedback which would require iteration within iteration at the subsystem level, rather than overall design iteration at the systems level.

#### **12.2.2.1 INPUTS TO THE OPTIMIZER**

From Figure 36, the left-hand side shows the design variables. These parameters are the actual inputs to the optimizer. For the first iteration, initial guesses are made for each design variable. The initial guesses come from the independent subsystem analyses. Table 32, on page 64, shows a detailed list of decision variables used as inputs to the optimizer.

The variables can be broken into seven major categories: mission profile, fuselage geometry, wing geometry, empennage geometry, landing gear geometry, propulsion, and weights. The specific variables were chosen for several reasons. First, they each represent a fundamental quantity used in airplane design calculations. Second, they are used in multiple subsystem codes. Lastly, they represent constrained parameters that have large impacts on the final design.

## CARDINAL OPTIMIZATION FLOW CHART

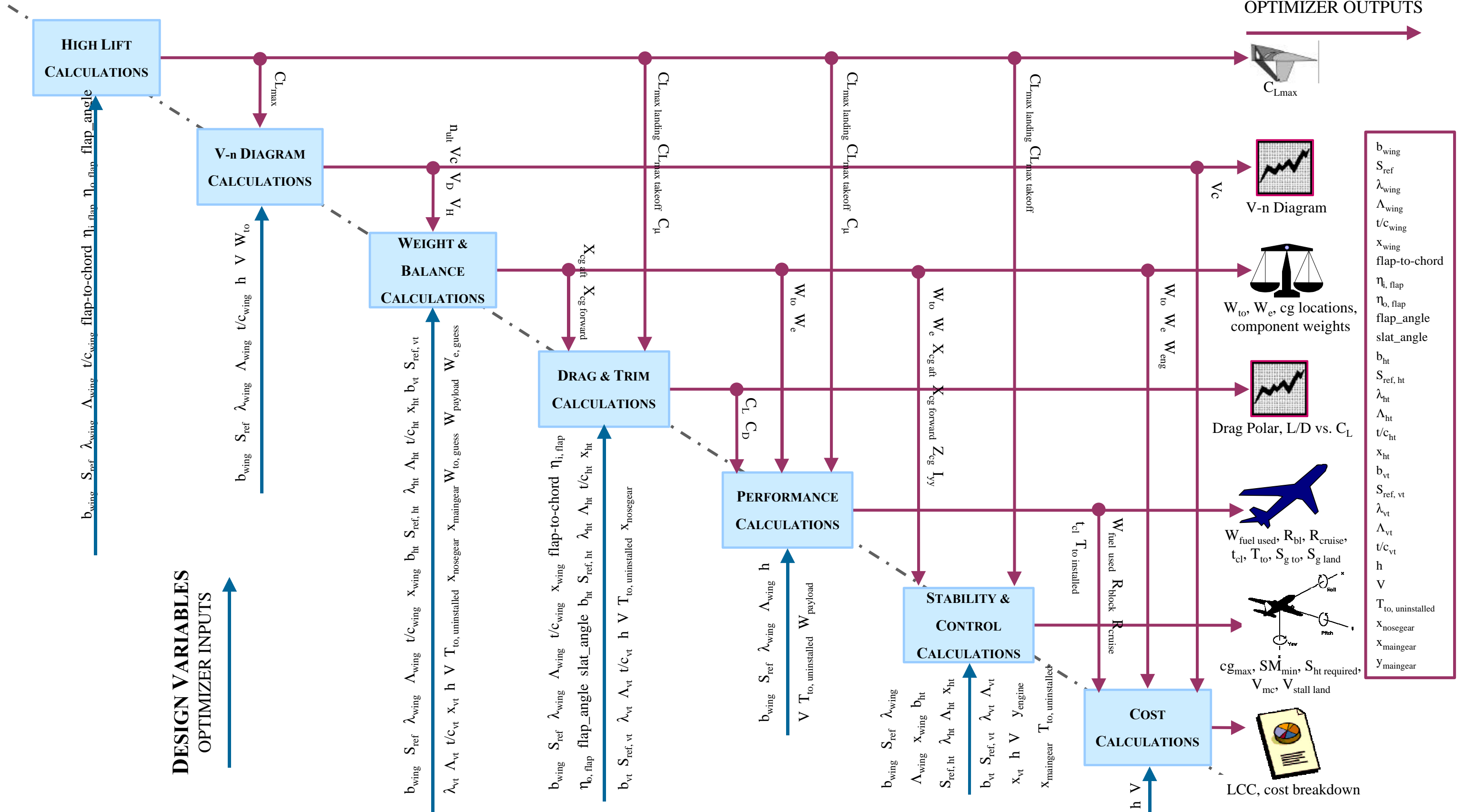
AIRPLANE DESIGN  
OPTIMIZER OUTPUTS

Figure 36: Cardinal Optimization Flow Chart

### 12.2.2.2 CONSTRAINTS

The optimization routine for the Cardinal project was highly constrained. These constraints were derived from several different areas. Some came directly from the Request for Proposal (RFP), others came from basic engineering guidelines for aircraft design, and still others came from Federal Aviation Regulations (FARs). None of the constraints were easy to achieve independent of all the others. Therefore, as a set of design requirements, it was desirable to use some type of optimization to capture the best design allowed in the small design space. Cardinal constraints can be summarized as follows:

**Table 33: Cardinal Mission Constraints<sup>1</sup>**

CONSTRAINT	$\leq, \geq$	BOUND
Volume	$\leq$	60 ft l x 29 ft w x 18.5 ft h
Takeoff ground roll	$\leq$	300 ft
Landing ground roll	$\leq$	400 ft
Cruise Range	$\geq$	1500 nm
Center-of-gravity excursion	$\leq$	25% mac
Static Margin	$\geq$	5 % mac
Takeoff Rotation, $S_{ht}$	$\geq$	$S_{ht, \text{required for rotation}}$
Tipover Angle	$\geq$	18 degrees
Turnover Angle	$\leq$	54 degrees
Fuselage Clearance Angle	$\geq$	10 degrees
Weight on Nose	$\geq$	8%
Minimum control speed	$\geq$	$1.2 * V_{\text{stall, landing}}$

### 12.2.2.3 OUTPUTS FROM THE OPTIMIZER

On the right-hand side of Figure 36, page 66, there is a block for the “airplane design.” This block consists of optimized design variables that meet all constraints and subsystem outputs (like charts, graphs, etc.) which are not captured solely with input design variables. Similar to the input variables, these outputs can be categorized into: mission profile, fuselage geometry, wing geometry, empennage geometry, landing gear geometry, propulsion, and weights.

In all previous sections of this proposal, data is presented for the Cardinal design. This data was generated using the outputs from the optimizer as inputs to the post-optimality running of the subsystem analyses. Each output parameter was chosen because it described an important element of the Cardinal final design (geometry, performance, etc.). As required for a completed proposal, each of these elements plays a roll in the presentation of the Cardinal.

### 12.2.3 CONSTRAINED OPTIMIZATION<sup>13</sup>

As discussed in section 12.2.1, there must be a cancellation of gradients between the objective function and the active constraints at the solution point. In order for this to occur, Lagrange Multipliers must be used to balance the equation. Many nonlinear algorithms are used to find the Lagrange Multipliers which will provide solutions to the KT equations. Methods where a quadratic programming sub-problem is solved at each major iteration are called Sequential Quadratic Programming (SQP) methods.

The basic idea in SQP is to use a nonlinear algorithm that is analogous to Newton's Method for unconstrained problems. At each major iteration, a quasi-Newton method is used to approximate the Hessian of the Lagrangian function. This approximation is used to generate a QP sub-problem. The sub-problem is solved in a conventional way—with an active set strategy<sup>23</sup> as described in reference 40. To end the major iteration, the solution to the sub-problem is used to find a direction for a line search procedure.<sup>40</sup> Major iterations continue until all constraints are met and the solution is sufficiently converged. In the optimization code,<sup>1</sup> a Matlab<sup>34</sup> function 'constr.m' was used to implement this algorithm.

### 12.3 BASELINE DESIGN OPTIONS

As noted at the start of this section, the Cardinal team considered three designs prior to optimization. Due to the strict requirements imposed on this aircraft, it was desirable to investigate several alternatives—parallel design and analysis were conducted to produce multiple feasible designs. This was not only to thoroughly explore the design space, but also to provide several points of reference for comparison during final design selection. Due to the highly unconventional nature of the Cardinal, the multiple design points provided a “sanity check” throughout the design process.

The objective function for the optimization was a minimization of Life-Cycle Cost (LCC). The three baseline designs were studied in both the military and commercial configurations, then optimized with respect to LCC. Table 34 shows data for metrics used to compare the designs. LCC was the chosen objective function, but Operating Cost, Airplane Estimated Price and Airplane Market Price were also used to validate the design choice. Note that fuel price was assumed constant for all design options.

**Table 34: Baseline Design Comparison Chart**

CARDINAL COST METRICS	VERTICAL TAKE-OFF TILT-WING DESIGN		SHORT TAKEOFF TILT-WING DESIGN		SHORT TAKEOFF FIXED-WING DESIGN	
	MILITARY VERSION (FY99)	COMMERCIAL VERSION (FY99)	MILITARY VERSION (FY99)	COMMERCIAL VERSION (FY99)	MILITARY VERSION (FY99)	COMMERCIAL VERSION (FY99)
Direct Operating Cost:	\$9.06/nm	\$8.63/nm	\$7.82/nm	\$7.41/nm	\$7.03/nm	\$6.80/nm
Indirect Operating Cost:	\$1.81/nm	\$1.73/nm	\$1.56/nm	\$1.48/nm	\$1.41/nm	\$1.36/nm
Fuel Price:	\$1.20/gallon	\$1.20/gallon	\$1.20/gallon	\$1.20/gallon	\$1.20/gallon	\$1.20/gallon
Engine Price (per engine):	\$1.09 M	\$1.09 M	\$0.81 M	\$0.81 M	\$0.52 M	\$0.52 M
Airplane Estimated Price:	\$20.8 M	\$19.4 M	\$18.0 M	\$16.8 M	\$17.1 M	\$16.2 M
Airplane Market Price:	\$19.7 M	\$17.3 M	\$17.3 M	\$15.3 M	\$16.7 M	\$15.4 M
<b>LIFE CYCLE COST</b>	<b>\$200.6 B</b>	<b>\$189.3 B</b>	<b>\$172.1 B</b>	<b>\$164.5 B</b>	<b>\$154.7 B</b>	<b>\$148.9 B</b>

## 12.4 OPTIMIZATION RESULTS<sup>1</sup>

The following sections contain a summary of actual values for the optimal design, and post-optimality analyses to highlight which parameters had the most significant impact on the objective function. Note that similar analyses were run for each Cardinal design configuration (see Table 34). The results presented here reflect only the final design—a fixed-wing SSTOL dual-use aircraft.

### 12.4.1 OPTIMIZED DESIGN

Following procedures outlined in section 12.2, design points generated by the subsystem analyses for each of the six options (see Table 34) were given as inputs to the optimizer. For all cases, the optimizer ran successfully (iteration numbers ranged from 196 to 324) and produced the “optimal design” for each configuration. After careful consideration of the cost metrics used to select the best design, the Cardinal team chose the SSTOL fixed-wing configuration. For clarity, the results presented here correspond to the military, SSTOL, fixed-wing version of the Cardinal. Similar results for each of the other configurations (including a full set of results for this version) can be obtained using the optimization code.<sup>1</sup>

Almost 40 design variables were varied during the optimization routine. While each variable did have an impact on the final design, not all were significant factors during the optimization. Table 35 shows a list of those design variables that most substantially impacted the optimization. The initial subsystem analyses yielded initial guesses not far from the optimized outputs. Of particular notice in Table 35 is the considerable change in Thrust. This large variation was due to the fact that the initial estimate of the maximum lift coefficient was rather conservative. The optimizer found that the lift coefficient would be much higher, resulting in the low thrust value. This result had a significant impact on life-cycle cost (see section 11), as the majority of LCC was due to fuel. Lower thrust meant lower LCC, an outcome that resulted in the final selection of this design.

**Table 35: Summary of Optimized Design (Military Version)**

FIXED-WING MILITARY VERSION		
DESIGN VARIABLE	INITIAL GUESS INPUT	OPTIMIZED OUTPUT
Wing Area	1035 ft <sup>2</sup>	1150 ft <sup>2</sup>
Wing Position	16.5 ft	15.0 ft
Horizontal Tail Area	225 ft <sup>2</sup>	190 ft <sup>2</sup>
Vertical Tail Area	275 ft <sup>2</sup>	208 ft <sup>2</sup>
Thrust	33000 lb	22875 lb
Takeoff Weight	46312 lb	46761 lb
Cruise Speed	350 ktas	350 ktas
Cruise Altitude	35000 ft	37000 ft

The design variables, while describing the configuration of the Cardinal, do not give a good representation of the performance metrics which make the aircraft desirable. During the optimization, the design variables were changed to better meet the constraints (see Table 33). Noting how the initial guess and the final design each met the constraints highlights the need for optimization—the values of the design variables did not change much during the optimization routine, but even the small changes resulted in a feasible design solution. Table 36 shows a summary of the change in constraint values from the initial guess to those from the optimal design point.

**Table 36: Summary of Optimized Constraint Values**

CONSTRAINT	≤, ≥	BOUND	INITIAL DESIGN	OPTIMAL DESIGN
Takeoff ground roll	≤	300 ft	184 ft	290 ft
Landing ground roll	≤	400 ft	347 ft	315 ft
Cruise Range	≥	1500 nm	960 nm	1500 nm

The initial design resulted in a non-feasible solution, as the range was less than the required 1500 nm. The takeoff ground roll for the initial design point, however, was easily met. This allowed for some combination of smaller wing area and lower thrust. The lower thrust required smaller engines which in turn lowered the weight and provided better cruise performance. As stated above, a significant portion of the life-cycle cost is due to propulsion (fuel and engines). The smaller engine has a large effect on LCC, so the trade between wing area

and engine size favors the smaller engine. The optimized result highlighted this fact—small engines and larger wings reduce LCC.

#### **12.4.2 GRADIENTS**

For the Cardinal, design optimization was conducted with the optimization code written during this investigation.<sup>1</sup> As discussed throughout this section, there were many factors that also contributed to the final design selection. Of primary importance was ensuring that the optimal design, as represented by the optimization calculation, was a reasonable one. A simple way to check the results is by analysis of the gradients. Gradients detail the trends of the constraints with changes in the design variables. These plots are especially useful for determining the accuracy of the optimization routine. If the gradients were continuous, the optimizer would find it possible to navigate the design space efficiently. With discontinuities in the gradients, however, the subproblems could return solutions that would lead to an improper search direction. In short, the optimizer would diverge instead of converging to an optimal solution.

Appendix B shows a few gradients for the range constraint. These gradients were of particular interest, as they limited the design space in two directions. Specifically, the range was only satisfied for cruise speed values very close to that chosen for the Cardinal design. While LCC increases with cruise speed, the range versus cruise speed gradient defined the optimum. The gradient of range versus cruise altitude was also quite interesting. From the gradient shown in Appendix B, it is obvious that cruise altitudes between 37,000 ft and 40,000 ft were the only ones acceptable with respect to the range constraint. The LCC versus cruise speed gradient, however, showed that LCC reached a minimum at an altitude of 32,000 ft. This altitude could not be that selected for the optimal design, as the range constraint required an altitude of 37,000 ft (the value selected for the Cardinal).

Gradients were plotted for each constraint as a function of each design variable. For brevity, all plots are not included. In general, the gradients for the Cardinal design showed expected trends. The constraints varied with the design variables as common sense dictated, and were continuous in nature. The gradient plots were an excellent tool for post-optimality analysis.

#### **12.4.3 CARPET PLOTS<sup>41</sup>**

The gradients discussed in section 12.4.2 were useful for noting the effect of one design variable on a single constraint. Although this data is quite important, data representing the coupling between parameters is

often more useful. Of particular interest are the interactions between a very stringent constraint and design-driving variables such as wing area, takeoff weight, or thrust. Carpet plots are used to display data depending on more than one variable in a clear, concise manner.

Figure 37 shows a carpet plot that aided in the optimization process. This plot shows the maximum takeoff weight that satisfies the 300 ft landing ground roll constraint for a given thrust and wing area. Using this plot, the Cardinal team could see the impact of wing area, weight, and thrust on the ground roll constraint. When selecting the final design, analyses such as the one discussed here were quite useful. While the optimizer gave a result that seemed reasonable, the carpet plots helped explain why this design was better than others subject to the same constraints.

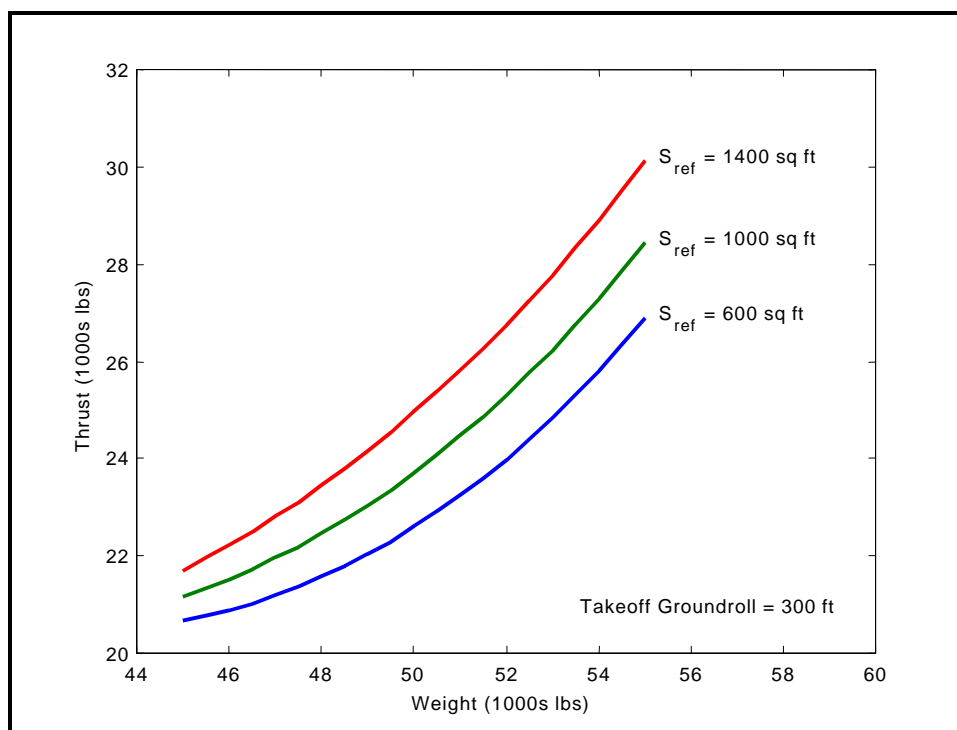


Figure 37: Carpet Plot for Takeoff Ground Roll Constraint

#### 12.4.4 SENSITIVITY ANALYSES

Collaborative optimization was an excellent way to find a design that met all constraints. The solution given by the optimizer was the optimum, but was not necessarily the best choice for the design. Post-optimality analysis showed which parameters were the most sensitive—those that could not change value without changing the optimal solution. Although the constraints for the Cardinal design were fixed by the RFP, the team felt it useful to show that by relaxing those parameters very slightly, the design would become lighter, less

costly, and more efficient. The following sections discuss a few of the most stringent design requirements, and what effect they had on the optimal design. Note that when the constraints are relaxed, the optimization produces an airplane design different from that of the optimal design given the original constraints. Details of each of these different designs can be found on the Cardinal web site.<sup>1</sup>

#### 12.4.4.1 TAKEOFF/LANDING DISTANCE

For this RFP,<sup>2</sup> the takeoff and landing distance requirements were the most difficult constraints to meet. The Cardinal optimal design was heavily influenced by the takeoff and landing distances—both were a major design driver. To analyze how significantly the takeoff and landing ground rolls impacted LCC, the constraints were relaxed by 100 ft. The LCC resulting from this constraint relaxation was \$130 B. For the optimal design with the original constraints, the LCC was \$154 B. A mere 100 ft of runway reduced the LCC by almost \$25 B. Figure 38 shows how LCC depends on takeoff ground roll (the most difficult of the two constraints to meet).

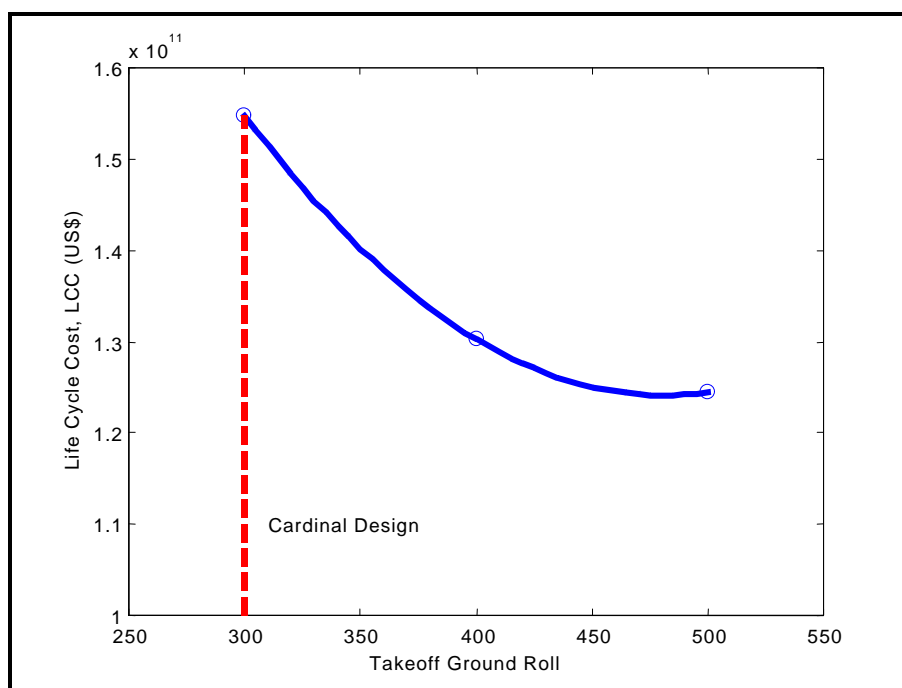


Figure 38: Life Cycle Cost vs. Takeoff Ground Roll

#### 12.4.4.2 RANGE

Range was also a mission specification that impacted the design significantly. A relaxation of the range constraint to 1000 nm reduced the LCC estimate to \$130 B. The Cardinal was designed for center-city to center-city travel. 1500 nm is obviously a much larger range, but 1000 nm seems an adequate distance for the

center-city to center-city objective. Similar to relaxation of the ground roll, a reduced range could improve the desirability of this airplane.

#### **12.4.4.3 PAYLOAD WEIGHT**

The Cardinal was designed as a dual-use aircraft. The military version required a cargo capacity that would support the transport of two F-14D engines (plus the containers used to house them during transport). The commercial version, however, needed to carry only 24 passengers—a much lower cargo weight than that of the military counterpart. In addition to the impact on cargo weight, the military version required a maximum airplane volume of 60 ft in length by 29 ft in width by 18.5 ft in height (stemming from aircraft carrier operations requirements). A commercial airplane would not be subject to these same volume constraints. With this in mind, an analysis of the fixed-wing design was conducted for a solely commercial (relaxed volume constraints and lower payload weight) version. As noted, the LCC for the optimal design given the original constraints was \$154B. For the optimal design considering the commercial constraints only, the LCC was \$126B. The military constraints have quite an impact on the LCC. Should the customer choose to operate this as a solely commercial aircraft, a \$28B reduction in LCC would likely far outweigh the cost of design modification.

#### **12.5 ACCURACY/FEASIBILITY OF “SOLUTION”**

Collaborative optimization was a powerful tool that aided in selection of the final Cardinal design. Mathematically, the optimization routine seemed quite reasonable—a conventional nonlinear SQP algorithm yielded the “best design” subject to constraints provided by the RFP<sup>2</sup>, FAR requirements, and the design team. The objective function, as stated throughout this section, was a minimization of life-cycle cost.

The design team was cognizant of the order of accuracy of the cost estimate (section 11), and took care not to place too much confidence in the Life-Cycle Cost (LCC) output. In terms of the optimization, LCC and other cost parameters were used as figures of merit to select the final design. For each version of the Cardinal, the same cost estimation method was used. While errors in the cost estimate would cancel when comparing two fixed-wing designs, they may not cancel when comparing the fixed-wing to the tilt-wing. The final design selection was based on several factors, not just the LCC. The LCC did, however, play a significant role.

The real worry was that there would be no way to tell if the cost discrepancies between the fixed-wing design and the tilt-wing design were due to actual cost parameters, or because the cost estimation model was not

accurate for both aircraft. In most situations, this would be a reason to discount the cost estimate as faulty, especially when the deciding factor for design selection was a mere 10% in LCC. For the Cardinal, however, the situation did not call for this course of action. The tilt-wing estimates were higher in every cost category—an expected result due to the significantly higher installed thrust. The tilt-wing was expected to yield higher cost, and it did. Therefore, the Cardinal team felt safe in choosing the fixed-wing design based on minimum LCC.

Another primary concern was the optimization technique itself. As is common with constrained optimization, the “optimal solution” for the Cardinal design pushed several of the constraints to their bounds. While this did meet the design specifications, it allowed no room for margin. In an actual design, margin would not only be desirable; it would be required to mitigate risk. Due to the academic nature of this proposal, the team chose to find the optimum solution, and perform post-optimality sensitivity analysis to investigate how the constraints drove the design. This technique has a major advantage; upon discussion with the customer, the sensitivity analyses could show how relaxing the constraints slightly would impact the design. The Cardinal team took advantage of this flexibility. Results of the sensitivity analyses can be found in section 12.4.2.

Overall, the Cardinal optimization technique seemed to work quite well. The AEP and DOC costs were compared with existing aircraft data and fell within a reasonable error bar (see Table 31). All performance constraints were met, and each of the gradients yielded results which were expected. Sequential Quadratic Programming (SQP) was an excellent choice for the Cardinal.

### 13. CONCLUSIONS AND RECOMMENDATIONS

The Cardinal fills the gap for a Super Short Takeoff and Landing aircraft capable of operating from river “barges” and providing center-city to center-city travel. The need of the U.S. Navy for a Carrier On-board Delivery (COD) aircraft to replace the C-2 Greyhound is also met. To aid in verification that all constraints and requirements were met a compliance matrix is provided (see Table 38) which lists the section and page numbers of all requested documentation. Performance of the Cardinal includes:

- Takeoff ground roll of 289 ft at maximum takeoff weight
- Landing ground roll of 273 ft at maximum landing weight
- Cruise speed of 350 knots with a range of up to 1500 nm with reserves
- Payload
  - 24 passengers and baggage for commercial version
  - 10,000 lb payload for military version
  - Capable of carrying two GE F110 engines for the F-14D
- Spot factor requirement of 60 feet by 29 feet for military version with wing folding and pivoting

Upper surface blowing (USB) and a tilt-wing configuration were considered to achieve the takeoff and landing ground roll requirements. Neither technology has been implemented on production aircraft, but both have been demonstrated in prototype and research aircraft. To assess which method was most cost effective to use a fixed-wing configuration with USB and a tilt-wing configuration were designed.

Wing and high lift design, propulsion selection and performance characterization, structural layout and design, drag polar buildups, stability and performance analysis, and cost estimation were performed for both designs. Automated design tools were written for each subsystem to aid in the analysis process and allow for timely design iteration. These automated design tools allowed the team to vary different design variables and the mission requirements to design an airplane that met the requirements and see how varying the requirements changed the design point. Communication between system groups was maintained using a web page containing the most current results for each iteration of the design and access to copies of the design codes. The web site may be viewed at <http://ape.stanford.edu/cardinal/> and provides additional information about the Cardinal designs.

Collaborative optimization was used to minimize Life Cycle Cost (LCC) for the fixed-wing design and a tilt-wing design. Table 37 summarizes the cost comparison for the two designs.

**Table 37: Summary of Cost Comparison Between Initial Designs**

COST METRIC	FIXED-WING	TILT-WING
Operating Cost	\$7.03/nm	\$7.82/nm
Acquisition Cost	\$17.1M	\$18.0 M
Life Cycle Cost	\$154.7B	\$172.1B

To understand how the design requirements affected the costs, several design studies were conducted. The cost associated with vertical takeoff using a tilt-wing aircraft was estimated to cost 16% more than the fixed-wing design with short takeoff and landing capabilities. Sensitivity analysis showed that increasing the takeoff ground roll requirement by 100-200 ft would decrease life cycle cost by 15-20%.

Although the technology used by the Cardinal has been demonstrated on research and prototype aircraft, it has not been implemented on production aircraft. This technology is also critical to the short takeoff and landing capabilities of the Cardinal. More detailed analysis will be necessary to ensure that the Cardinal will be able to meet its performance requirements. These might include windtunnel tests, small-scale radio control flight tests, or more detailed computational work.

The design of the Cardinal was selected over a competing tilt-wing design based on cost. The cost model used was based on conventional subsonic commercial aircraft and may not accurately estimate the cost. Although the cost trends resulting from changing the design are probably correct, the cost difference between the fixed-wing design and the tilt-wing design which was also studied may not be correct. Cost models for military aircraft or rotorcraft may be more applicable and the use of these should be investigated.

In the course of the post-optimization design the effect of the ground roll requirement on life cycle cost was investigated. An increase in takeoff ground roll from 300 ft to 400 ft decreased the life cycle cost by 20%. Increasing the ground roll requirement by 50-100 feet should be considered to reduce life cycle cost.

One of the driving factors in the design of the fuselage and the overall design was the 10,000 lb payload for the Cardinal and the need to accommodate two F-14D engines. A recent study found that engines are delivered to aircraft carriers by C-2 transport less than once a year.<sup>36</sup> If this is the case, the requirement to carry the engine payload and the costs to accommodate this requirement should be reassessed.

**Table 38: RFP Requirements Compliance Matrix**

RFP REQUIREMENT	COMPLIANCE SECTION	PAGE
• Creation of Automated Design Tools	2.2	3
• SSTOL Transport Aircraft Design for Commercial Use (24 passengers)	✓	✓
• SSTOL Carrier-On-Board Delivery Aircraft (Military Cargo)	✓	✓
• Cost Comparison of VTOL and SSTOL for the Same Mission	11.6	61
• Safety Issues—SSTOL vs. VTOL	2.3	6
• Assessment of Converting SSTOL Design to VTOL (Cost Justification)	11.6	61
• Risk Assessment, New Technology & Technology Readiness (Maturity)	2.2.1	5
• User/Passenger Preferences	2.3	6
• Adherence to Applicable Federal Aviation Regulations (FARs)	10	51
• Mission Profile:	✓	✓
✓ Standard Day Atmosphere, sea level plus 27° F	✓	✓
✓ Warm-Up and Taxi, 10 minutes	✓	✓
✓ Takeoff, Groundroll $\leq$ 300 ft, Full Passenger and Baggage Load	10.1	51
✓ Climb at Best Rate of Climb to Best Cruising Altitude	10.2	52
✓ Cruise at Best Speed (minimum 350 knots) for 1500 nm	10.3	54
✓ Descend to Sea Level (no credits for range)	✓	✓
✓ Land, Groundroll $\leq$ 400 ft, Domestic Fuel Reserves	10.1	51
✓ Taxi to Gate, 5 minutes	✓	✓
• Commercial Version Requirements:	✓	✓
✓ 24 Passengers Plus Baggage, 32 inch seat pitch, 200 lb each	4.1.3	15
✓ Overhead Stowage Capacity	4.1.3	15
• Military Version Requirements:	✓	✓
✓ Accommodation of Primary Cargo and/or Passengers	4.1.2	15
✓ Primary Cargo: two GE F110 engines (for F-14D) in shipping containers*	4.1.2	15
*[not stated in RFP, but included due to transportation requirements set by the engine manufacturer]		
✓ Maximum Cargo Weight: 10000 lb	4.1.2	15
✓ Spot Factor Requirement: 60 ft x 29 ft	4.2	17
✓ No Arresting Hooks or Catapult Devices to aid in Carrier Takeoff/Landing	10.1	51
• Describe Trade Studies and Justify Final Concept Selection:	✓	✓
✓ High-Lift Performance	4.2.2	19
✓ Propulsion Performance	5.3.1	30
✓ Performance Profiles for Takeoff & Landing	10.1	51
✓ Drag Polars for Takeoff & Landing	8.4	44
• Carpet Plots Used to Optimize Final Design	12.4.3	71
• Dimensioned 3-View General Arrangement Drawing	Figure 1	iv
• Inboard Profile for Commercial & Military Versions	Figure 22	34
• Primary Load-Bearing Structure (illustrated description)	Figure 22	34
• Rationale for Material Selection	6.1	33
• V-n Diagram	Figure 23	36
• Drag Build-up (takeoff, cruise, and landing configurations)	8.4	44
• Component Weight Breakdown	Table 13	39
• Center of Gravity Excursion	Figure 24	40
• Performance Estimates for All Flight and Loading Conditions	10	51
• Demonstrate Aircraft Stability for all Flight and Loading Conditions	9	47
• Fly-Away (Airplane Estimated Price, AEP) Cost for 750 Airplanes	11.5	60

## 14. REFERENCES

1. Cardinal Web Site, see appendix A for site map: <http://ape.stanford.edu/cardinal/>
2. American Institute of Aeronautics and Astronautics 1999 Graduate Team Aircraft Design Competition “RFP: Super STOL Carrier On-Board Delivery (COD) Aircraft.” Released 28 October, 1998.
3. Abbott, Ira H. and Albert E. Von Doenhoff. Theory of Wing Sections. New York: Dover Publications. June, 1959.
4. AIAA/United Technologies—Pratt & Whitney Individual Student Aircraft Design Competition. “Engine and Propellor Data Package.” American Institute of Aeronautics and Astronautics. 1989.
5. Anonymous. “NASA’s Quiet Short-haul Research Aircraft.” NASA Information Bulletin.
6. Anonymous. “Quiet Short-Haul Research Program.” Company Brochure. Boeing Commercial Airplane Company. Seattle, WA 98124.
7. Anonymous. “Tri-Service Evaluation of the Canadair CL-84 Tilt-Wing V/STOL Aircraft.” USAAVLABS Technical Report 67-84, November, 1967.
8. Anonymous. “XC-142A VSTOL Transport Category II Performance Evaluation.” Air Force Flight Test Center Technical Report No. 68-21. Edwards Air Force Base, CA. October 1968.
9. Bathke, Teal. “Questions Regarding the RFP.” E-mail to Robert Paczula. 10 January, 1999.
10. Bennett, W.S., Bond, E.Q., and Flinn, E.L. “XC-142A Performance Data Report.” Ling Temco-Vought (LTV) Report No. 2-53310/4R942. Dallas, TX. May 13, 1964.
11. Blanchard, B.S. Design and Manage to Life Cycle Cost. Portland, Oregon: M/A Press, 1978.
12. Boehm, Barry. A Spiral Development Model of Software Development and Enhancement. IEEE Computer vol. 21 #5. May, 1988.
13. Branch, Mary Ann and Andrew Grace. Optimization Toolbox. Natick, MA: The MathWorks, Inc., 1996.
14. Braun, R.D. and Kroo, I.M. "Development and Application of the Collaborative Optimization Architecture in a Multidisciplinary Design Environment." Multidisciplinary Design Optimization: State of the Art. Eds. N. Alexandrov and M.Y. Hussainin. Philadelphia, Society for Industrial and Applied Mathematics, 1995.
15. Chana, W.F., and Sullivan, T.M. “Download – The Tilt Rotor’s Downfall.” AIAA Paper 93-4814. 1993.
16. Cochrane, J.A., Riddle, D.W., and Youth, S. “Applications of Advanced Upper Surface Blowing Propulsive-Lift Technology.” Unpublished Paper.
17. Cochrane, J.A., Riddle, D.W., Stevens, V.C. “Selected Results from the Quiet Short-Haul Research Aircraft Flight Research Program.” Unpublished paper presented at AIAA/NASA Ames VSTOL Conference, Palo Alto, California, December 7-9, 1981.
18. Currey, N.S. Aircraft Landing Gear Design: Principles and Practices. Washington, D.C.: AIAA Education Series, 1988.
19. Eppel, J.C. “Quiet Short-Haul Research Aircraft Familiarization Document, Revision 1.” NASA Technical Memorandum 81298. September, 1981.

20. Fink, M.P. "Aerodynamic Data on Large Semispan Tilting Wing With 0.5-Diameter Chord, Single-Slotted Flap, and Single Propeller 0.08 Chord Below Wing." NASA Technical Note TN D-4030.
21. Fletcher, R. "Practical Methods of Optimization." Constrained Optimization (vol. 2). New York: John Wiley and Sons, 1980.
22. Gentry, C. L., Takallu, M.A., and Applin, Z.T. "Aerodynamic Characteristics of a Propeller-Powered High-Lift Semispan Wing." NASA Technical Memorandum 4541. April, 1994.
23. Gill, P.E., W. Murray, and M.H. Wright. Practical Optimization. London: Academic Press, 1981.
24. Hillier, Frederick and Gerald Lieberman. Introduction to Operations Research. New York: McGraw-Hill, 1995.
25. Jewell, Jamie. jamie.jewell@ae.ge.com. "F110-GE-400 Engine Shipping and Storage Container." Email to Ryan Vartanian. 12 February, 1999.
26. Kroo, I. "An Interactive System for Aircraft Design and Optimization." Proceedings of the AIAA Aerospace Design Conference (AIAA92-1190). February, 1992.
27. Kroo, I.M. "Decomposition and Collaborative Optimization for Large-Scale Aerospace Design Programs." Multidisciplinary Design Optimization: State of the Art. Eds. N. Alexandrov and M. Y. Hussaini. Philadelphia, Society for Industrial and Applied Mathematics, 1995.
28. Kroo, Ilan and Juan Alonso. AA241: Introduction to Aircraft Design: Synthesis and Analysis. Aero/Astro Course at Stanford University. Stanford, CA: 1999, <http://aero.stanford.edu/aa241/>
29. Kroo, I., Altus, S., Braun, B., Gage, P., and Sobieski, I. "Multidisciplinary Optimization Methods for Aircraft Preliminary Design." Proceedings of the 5th AIAA /USAF / NASA / ISSMO Symposium on Multidisciplinary Analysis and Optimization (AIAA 94-2543) September, 1994.
30. Lan, C.E. and Roskam, J., Airplane Aerodynamics and Performance, Roskam Aviation and Engineering Corporation, Ottawa, KS, 1980.
31. Lycoming Model No. ALF 502-D Turbofan Engine; Spec.No. 124.42, Lycoming Division, Stratford, Connecticut, Jan.1972
32. Maddalon, D.V. "Estimating Airline Operating Costs." CTOL Transport Technology (NASA N78-29046). 1978.
33. Mankins, John C. "Technology Readiness Levels: A White Paper." NASA Office of Space Access and Technology, Advanced Concepts Office. April 6, 1995.
34. MathWorks, Inc. Matlab version 5.3. Natick, MA: The MathWorks, Inc., 1999.
35. McCormick, Barnes. Aerodynamics of V/STOL Flight. London: Academic Press, 1967.
36. Norris, M.H. "A brief look at the legacy and future of the United States Navy's carrier-based support aircraft." Aircraft Design: An International Journal. June, 1998.
37. North, David M. "328 JET set to test 'Turboprop Aversion' Factor." Aviation Week and Space Technology, 29 June 1998: 52.
38. O'Rourke, M., and Rutherford, J. "Methods to Determine Limits to Tiltwing Conversion." AIAA Paper 91-3143. September, 1991.

39. Pegg, Robert J. "Summary of Flight-Test Results of the VZ-2 Tilt-Wing Aircraft." NASA Technical Note D-989. February, 1962.
40. Powell, M.J.D. "The Convergence of Variable Metric Methods for Nonlinearly Constrained Optimization Calculations." Nonlinear Programming 3. Eds. O.L. Mangasarian, R.R. Meyer, and S.M. Robinson. London, Academic Press, 1978.
41. Powers, Sidney A. sapowers@ix.netcom.com. "The Generation of Carpet Plots." Unpublished paper. Valencia, CA. 9 September, 1997.
42. Preston, J. and Scully, M. Personal Communication. NASA Ames Research Center. January – April, 1999.
43. Raymer, D.P. Aircraft Design: A Conceptual Approach. AIAA Education Series Washington, D.C.: American Institute of Aeronautics and Astronautics. 1989.
44. Riddle, D.W., Innis, R.C., Martin, J.L., and Cochrane, J.A. "Powered-Lift Takeoff Performance Characteristics Determined from Flight Test of the Quiet Short-Haul Research Aircraft (QSRA)." AIAA Paper 81-2409. November, 1981.
45. Riddle, D.W., Stevens, V.C., and Eppel, J.C. "Quiet Short-Haul Research Aircraft – A Summary of Flight Research Since 1981." SAE Paper 872315. December, 1987.
46. Roskam, J. Airplane Design Part I. Ottawa, KS: Roskam Aviation and Engineering Corporation, 1997.
47. Roskam, J. Airplane Design Part II. Ottawa, KS: Roskam Aviation and Engineering Corporation, 1989.
48. Roskam, J. Airplane Design Part III. Ottawa, KS: Roskam Aviation and Engineering Corporation, 1989.
49. Roskam, J. Airplane Design Part IV. Ottawa, KS: Roskam Aviation and Engineering Corporation, 1989.
50. Roskam, J. Airplane Design Part V. Ottawa, KS: Roskam Aviation and Engineering Corporation, 1989.
51. Roskam, J. Airplane Design Part VI. Ottawa, KS: Roskam Aviation and Engineering Corporation, 1990.
52. Roskam, J. Airplane Design Part VII. Ottawa, KS: Roskam Aviation and Engineering Corporation, 1991.
53. Roskam, J. Airplane Design Part VIII. Ottawa, KS: Roskam Aviation and Engineering Corporation, 1990.
54. Roskam, J., Airplane Flight Dynamics and Automatic Flight Controls, Part I, DARcorporation, Lawrence, KS, 1995.
55. Roskam, J., Airplane Flight Dynamics and Automatic Flight Controls, Part II, DARcorporation, Lawrence, KS, 1995.
56. Rutherford, J. and Bass, S. "Advanced Technology Tilt Wing Study." AIAA Paper 92-4237. August, 1992.
57. Sikorsky Web Site, <http://www.sikorsky.com/>
58. Sobieski, I. and Kroo, I. "Aircraft Design Using Collaborative Optimization." Proceedings of the 34th Aerospace Sciences Meeting and Exhibit (AIAA96-0715). Reno, NV. 15-18 January, 1996.
59. Sullivan, T.M. "The Canadair CL-84 Tilt Wing Design." AIAA Paper 93-3939. August, 1993.
60. Taylor, J.W.R. Jane's All the World's Aircraft 1969-70. London: Jane's Publishing Company, Ltd., 1969.

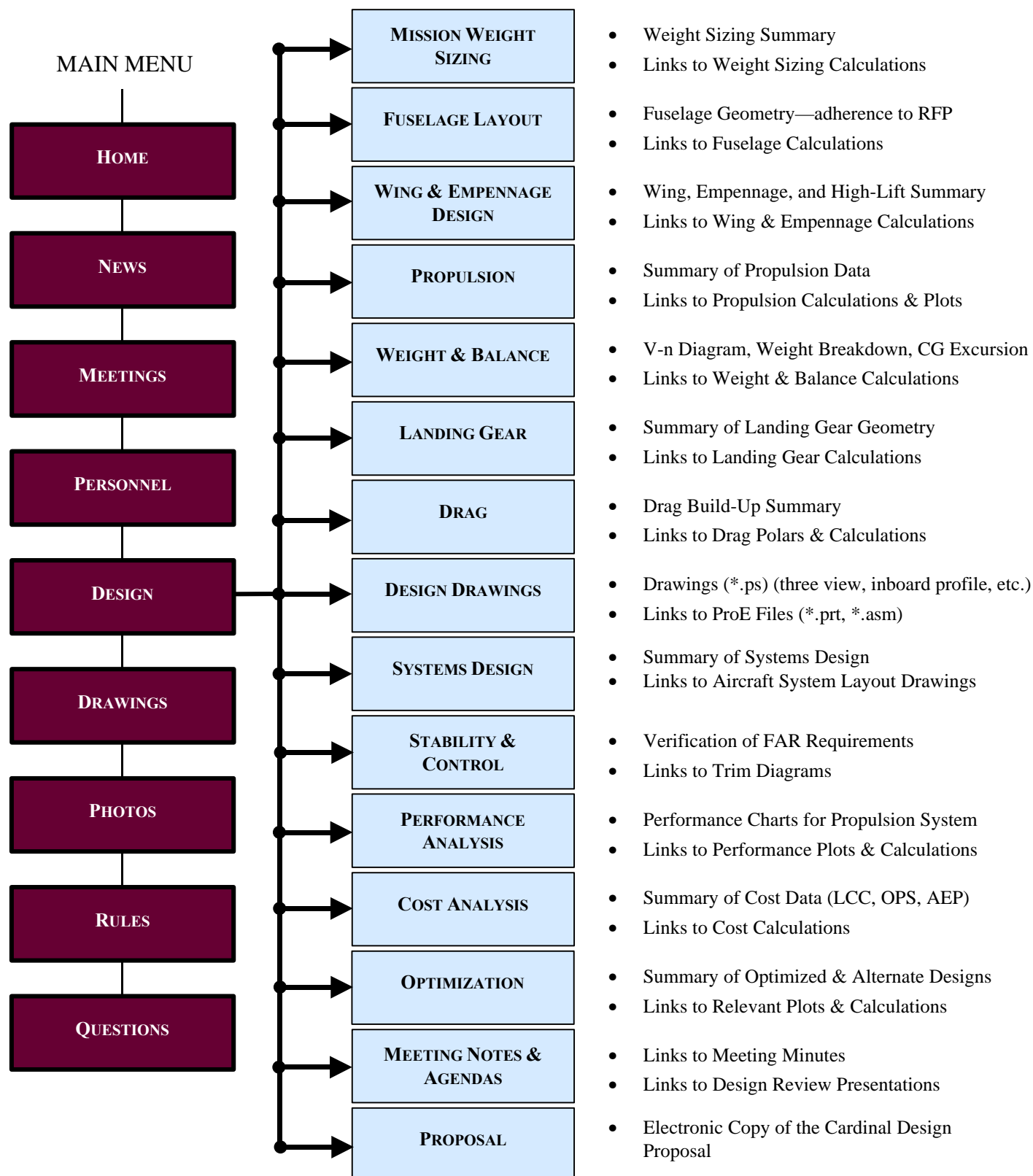
61. Taylor, J.W.R. Jane's All the World's Aircraft 1998-99. London: Jane's Publishing Company, Ltd., 1998.
62. Torenbeek, E. Synthesis of Subsonic Airplane Design. Hingham, Maine: Kluwer Boston Inc, 1982.
63. Wimpess, J.K., and Newberry, C.F. The YC-14 STOL Prototype : its design, development, and flight test : an engineer's personal view of an airplane development. Reston, Virginia: AIAA, 1998.
64. Wright, John. Jwright@bellhelicopter.textron.com. "Operating Cost." E-mail to Daniel Cornejo. 24 May, 1999

**APPENDIX A**  
**CARDINAL WEB SITE**  
SITE MAP

June 1, 1999

## CARDINAL WEB SITE

<http://ape.stanford.edu/cardinal/>



**APPENDIX B**  
**DESIGN OPTIMIZATION**  
GRADIENTS OF PARTICULAR INTEREST

June 1, 1999

## GRADIENTS OF PARTICULAR INTEREST

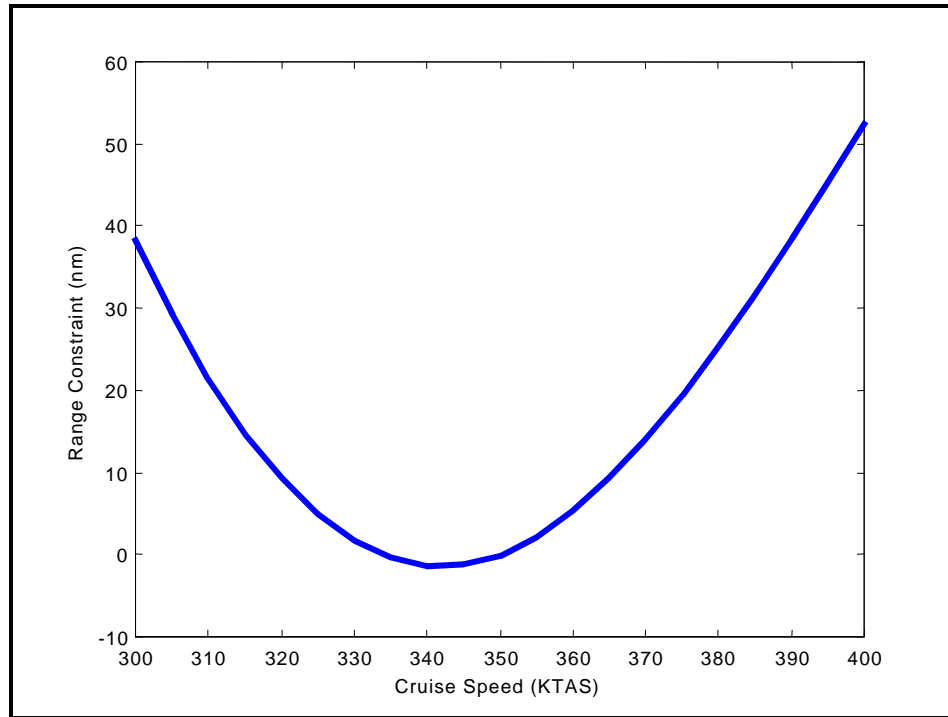


Figure 39: Range Constraint vs. Cruise Speed

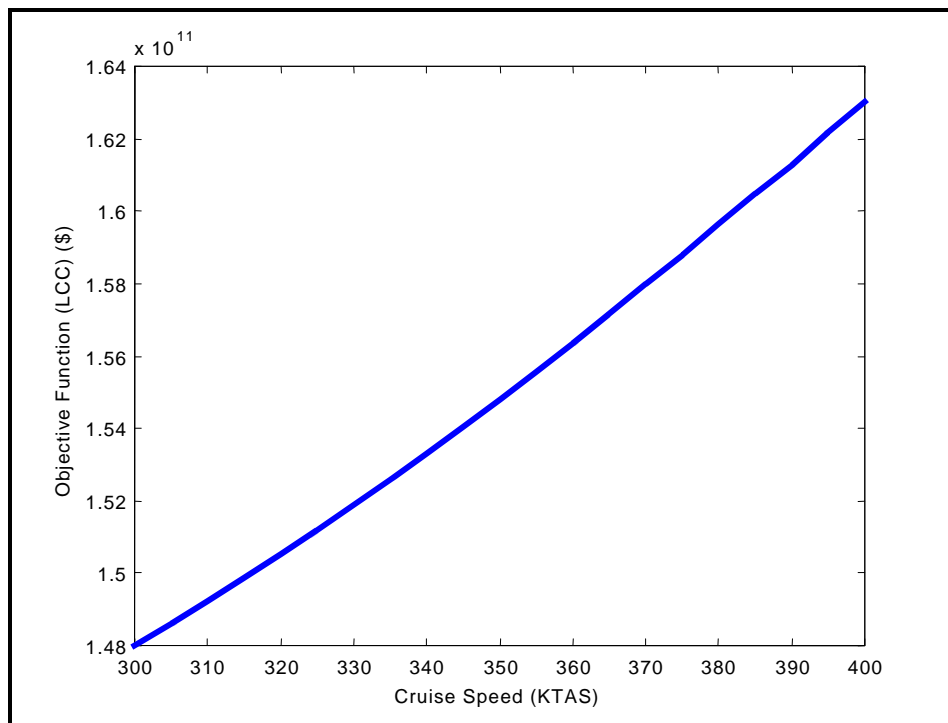


Figure 40: Life Cycle Cost vs. Cruise Speed

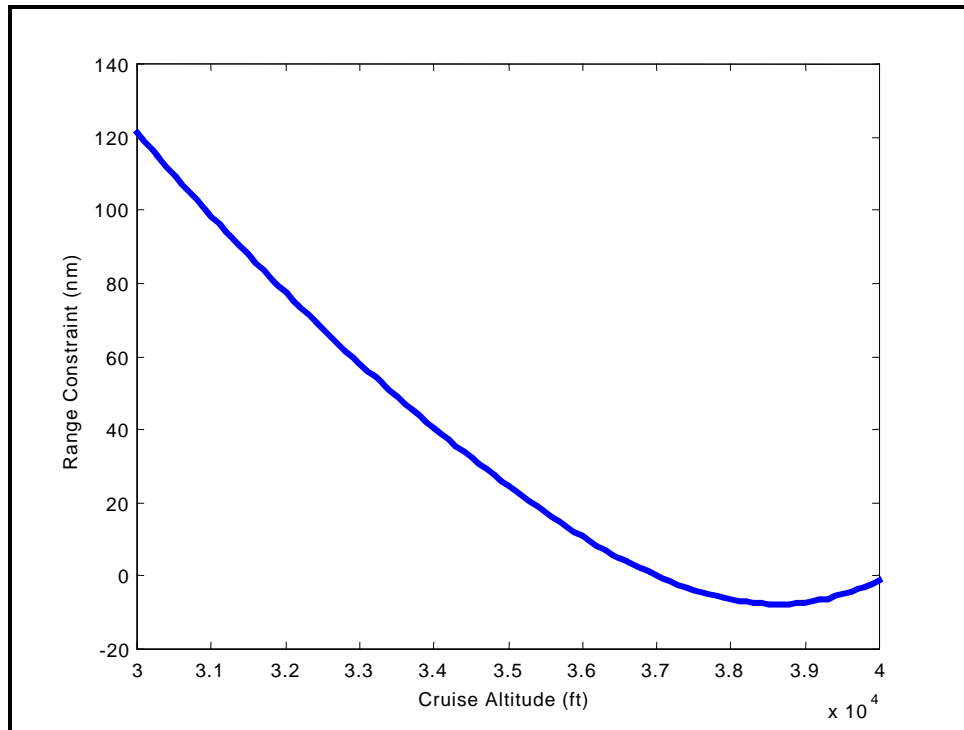


Figure 41: Range Constraint vs. Cruise Altitude

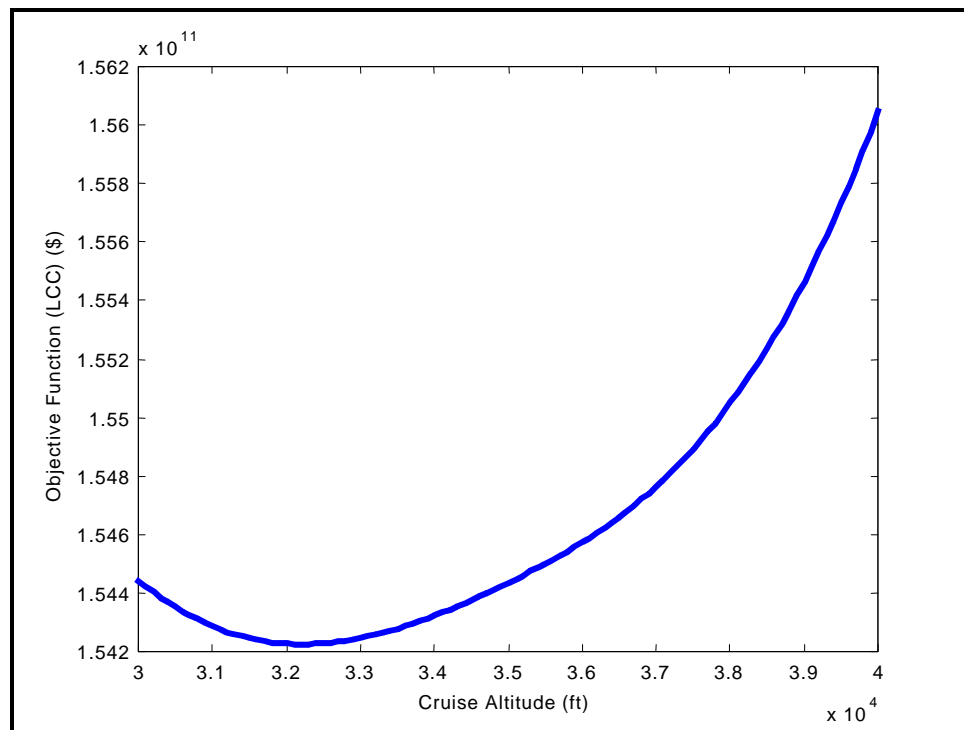


Figure 42: Life Cycle Cost vs. Cruise Altitude